POZNAN UNIVERSITY OF TECHNOLOGY

DOCTORAL THESIS

Radio resource management for C-V2X communication systems

Author:

Mgr inż. Saif Sabeeh

Supervisor:

Prof. dr hab. inż.

Krzysztof WESOŁOWSKI

Supporting Supervisor:

Dr inż. Paweł SROKA

A thesis submitted in fulfillment of the requirements for the degree of Doctor of Philosophy in Information and Communication Technology

Faculty of Computing and Telecommunications

Poznan University of Technology

November 2022

"Thanks a lot to my solid academic training at PUT, I can research and write on hundreds of topics related to wireless communication using the excellent experience I obtained during my doctorate research."

Saif Sabeeh

Abstract

Emerging wireless 5G and 6G technologies will support different applications, services, and use cases with extremely heterogeneous requirements. Examples of these requirements result from the main classes of 5G services such as enhanced Mobile Broadband (eMBB), Ultra-Reliable and Low-Latency Communications (URLLC), and massive Machine-Type Communications (mMTC). They include, among others, drive automation and Cellular-Vehicle-to-Everything (C-V2X) services. The increasing number of services that use wireless communications creates new challenges that need to be investigated. Several technologies share the same radio spectrum when implementing various services. In order to support these different services and their requirements, resource allocation and spectrum management play a critical role in the commercial and technical success of these applications.

This dissertation considers the scheduling and allocation of radio resources for C-V2X technologies to support highly reliable and error-free transmission. It investigates two modes of transmission of C-V2X communications in centralized and decentralized resource allocation in two technologies of air interfaces. Long Term Evolution (LTE) and New Radio (NR) are used to support sidelink C-V2X communications. The half-duplex, hidden terminal, and packet/radio resource collision errors are problems in decentralized resource allocation of LTE-V2X Mode 4 and NR V2X Mode 1. The signalling cost, limitation of resources, resource re-selection latency, and spectrum partitioning among cellular infrastructure in a network are problems in centralized resource allocation of LTE-V2X Mode 3 and NR V2X Mode 2. Therefore, all these problems are investigated in this dissertation.

We propose new resource scheduling algorithms to improve decentralized resource allocation management. These algorithms work by predicting the moment of the next free resources. They show excellent performance in terms of packet reception ratio and packet collision ratio. The high channel load in a network is another challenge investigated in this dissertation when the number of resources is limited (the channel frequencies are evenly divided between the vehicles) and the autonomous resource allocation is applied. We propose a new algorithm that works by adjusting the transmission parameters (that is, the modulation and coding scheme) to vary the number of vehicles currently served.

Another new algorithm is proposed to reduce congestion control problems in autonomous resource allocation. The 3GPP C-V2X standard does not solve this problem and depends on the solutions proposed in IEEE 802.11 technology. The proposed algorithm is based on the channel busy ratio to estimate channel load in the network. Thus, based on the value of this parameter, the algorithm can determine the values of the transmission parameters for subsequent transmission.

Another significant problem overlooked by the 3GPP C-V2X standard is the distribution of radio resources among the elements of cellular infrastructure in a highway scenario. Considering the sidelink overlapping coverage area of the vehicles' broadcast is essential in a centralized resource allocation of C-V2X. With this aim, we propose new spectrum partitioning techniques to avoid these overlaps.

The last problem investigated in this dissertation is the latency of resource allocation for the centralized resource allocation algorithm of NR V2X. We propose a new scheduling of radio resources managed by the centrally controlled cellular infrastructure. The proposed scheduling works by dividing the periodical time intervals of the vehicles' broadcasting between the roadside unit in the network to avoid creating an overlapped broadcasting area.

Streszczenie

Powstające technologie piątej i szóstej generacji 5G i 6G będą zapewniać realizację różnych aplikacji, usług i obejmować przypadki zastosowań o bardzo zróżnicowanych wymaganiach. Przykłady tych wymagań wynikają z głównych klas usług 5G takich jak: szerokopasmowy, wzbogacony dostęp mobilny (eMBB), ultra niezawodna komunikacja o niskich opóźnieniach (URLLC) i masowa komunikacja między maszynami i urządzeniami (mMTC). Przykłady te obejmują miedzy innymi autonomiczne kierowanie pojazdani i usługi wykorzystania komunikacji komórkowej w komunikacji pomiędzy pojazdami i wszystkimi elementami struktury telekomunikacyjnej (C-V2X). Wzrastająca liczba usług stosujących komunikację bezprzewodową stwarza nowe wyzwania, które wymagają badań. Różne technologie współdzielą pasmo radiowe w realizacji różnych usług. Aby umożliwić realizację różnych usług i związanych z nimi wymagań, niezbędne jest odpowiednie zarządzanie zasobami i widmem, które spełnia istotną rolę w zapewnieniu komercyjnych i technicznych sukcesów tych usług.

W niniejszej dysertacji rozważane są alokacja i planowanie zasobów w technologiach V2X, aby zapewnić wysoce niezawodną i bezbłędną transmisję. Przedstawione są w niej wyniki badań dwóch trybów transmisji w komunikacji C-V2X w przypadku scentralizowanej i zdecentralizowanej alokacji zasobów dla dwóch technologii dostępu radiowego. Systemy LTE oraz NR (New Radio) są zastosowane do wspierania transmisji komunikacji C-V2X w łączach bezpośrednich (sidelinks). W systemie LTE-V2X w trybie 4 oraz w systemie NR V2X w trybie 1 problemami są transmisja półdupleksowa, zjawisko terminala ukrytego oraz błędy wynikające z kolizji pakietów i rozdziału zasobów. Z kolei w scentralizowanej alokacji zasobów w systemie LTE-V2X w trybie 3

oraz w systemie NR V2X w trybie 2 problemami są koszty sygnalizacji, ograniczenia ilościowe zasobów, opóźnienia w ponownym wyborze zasobów oraz podział widma częstotliwości. Z tych więc powodów problemy te stały się przedmiotem badań w tej dysertacji.

W rozprawie zaproponowano więc nowe algorytmy szeregowania zasobów, aby poprawić zarządzanie alokacją zasobów w trybie zdecentralizowanym. Algorytmy te działają dokonując predykcji chwil, w których wystąppią nowe wolne zasoby. Charakteryzują się doskonałą jakością działania mierzoną stopą odebranych pakietow i stopą kolizji pakietów. Kolejnym wyzwaniem badanym w tej rozprawie jest problem dużego obciążenia sieci, gdy liczba dostępnych zasobów jest ograniczona a jest zastosowana zasada autonomicznej alokacji zasobów. Dlatego w rozprawie zaproponowano nowy algorytm, który działa przez dopasowanie parametrów transmisyjnych (tj. schematu modulacji i kodowania kanałowego), aby zmienić liczbę aktualnie obsługiwanych terminali/pojazdów.

Inny nowy algorytm zaproponowany w tej rozprawie ma za zadanie redukcję problemu sterowania przeciążeniem w autonomicznej alokacji zasobów. Standard 3GPP C-V2X nie rozwiązuje tego problemu i stosuje rozwiązania użyte w technologii IEEE 802.11. Zaproponowany algorytm bazuje na stopniu zajętości kanału, aby estymować obciążenie kanałów w sieci, Tak więc, biorąc pod uwagę wartość tego parametru, algorytm może zadecydować o wartościach parametrów dla kolejnych transmisji.

Kolejny znaczący problem niedostrzeżony w standardzie 3GPP C-V2X to dystrybucja zasobów radiowych między elementy infrastruktury komórkowej w scenariuszu komunikacji z pojazdami i między bnimi na autostradzie. Rozważanie nakładania się obszarów pokrycia w transmisji bezpośredniej wiadomości rozsiewczych wysyłanych przez pojazdy jest kluczowym zagadnieniem w scentralizowanej alokacji zasobów w systemie C-V2X. W tym celu w rozprawie proponujemy nowe techniki podziału widma, aby uniknąć nakładania się tych obszarów pokrycia.

Ostatnim problemem badanym w rozprawie jest opóźnienie w alokacji zasobów w systemie scentralizowanej alokacji w systemach NR V2X. Zaproponowano nowe szeregowanie zasobów radiowych zarządzane przez centralnie sterowaną infrastrukturę komórkową. Proponowane szeregowanie działa na zasadzie podziału okresowych odstępów czasowych w rozsiewaniu wiadomości do pojazdów pomiędzy jednostki infrastruktury drogowej w sieci w celu unikania tworzenia obszarów nakładania się pokrycia.

Acknowledgements

This dissertation could not have been completed without the support and assistance of many people. First, I would like to sincerely thank my supervisor, Prof. dr. hab. inż. Krzysztof WESOŁOWSKI, for his endless support, patience, motivation, tremendous knowledge, and for giving me space to think and create ideas. It is a great honor to be his doctorate student. I appreciate his efforts to make my doctorate study a productive and stimulating experience.

Furthermore, I would like to thank to the staff members of the Institute of Radiocommunications for their exceptional support and helpful advice. I would like to extend my sincere thanks to Dr. Anna PAWLACZYK for her uniqueness, honesty, sincerity, greatness and love for helping others, which I found from her while studying at PUT.

Finally, my deepest gratitude goes to my parents for their blessings and prayers and to my family (my wife, Dr. Thura Tariq, my lovely daughter Jana, and my twins Musa and Asser) for their support and wishes.

Thanks to all.

Contents

List of Figures

List of Tables

List of Abbreviations

3GPP	**Third Generation Partnership Project**
5GAA	**5G Automotive Association**
5GC	**5G Core**
ACK	**Acknowledgement**
AF	**Application Function**
AMF	**Access and Mobility Management Function**
BS	**Base Station**
BSM	**Basic Safety Message**
BWP	**Bandwidth Part**
CAM	**Cooperative Awareness Message**
CBR	**Channel Busy Ratio**
CDM	**Code Division Multiplexing**
CG	**Configured Grant**
CP	**Cyclic Prefix**
CQI	**Channel Quality Indicator**
CR	**Channel Occupancy Ratio**
CRlimit	**Maximum Channel Occupancy Ratio**
CSI	**Channel State Information**
D2D	**Device-to-Device (Communications)**
DCC	**Decentralized Congestion Control**
DCI	**Downlink Control Information**
DG	**Dynamic Grant**
DL	**Downlink**
DMRS	**Demodulation Reference Signal**
DSRC	**Dedicated Short Range Communications**

eNB	**Evolved Node B (LTE Base Station)**
EPC	**Evolved Packet Core**
ETSI	**European Telecommunications Standardization Institute**
eV2X	**Enhanced Vehicle-to-Everything**
FCC	**Federal Communications Commission**
FDM	**Frequency Division Multiplexing**
FEC	**Forward Error Correction**
FR1	**Frequency Range 1**
FR2	**Frequency Range 2**
gNB	**Next generation Node B (NR Base Station)**
HARQ	**Hybrid Automatic Repeat Request**
ITS	**Intelligent Transportation Systems**
LTE	**Long-Term Evolution**
MAC	**Medium Access Control**
MBMS	**Multimedia Broadcast Multicast Services**
MBS	**Multicast Broadcast Services**
MCS	**Modulation and Coding Scheme**
NACK	**Negative Acknowledgement**
NEF	**Network Exposure Function**
NR	**New Radio**
OFDM	**Orthogonal Frequency Division Multiplexing**
PBCH	**Physical Broadcast Channel**
PDCCH	**Physical Downlink Control Channel**
PDSCH	**Physical Downlink Shared Channel**
PRB	**Physical Resource Block**
ProSe	**Proximity Service**
PSBCH	**Physical Sidelink Broadcast Channel**
PSCCH	**Physical Sidelink Control Channel**
PSFCH	**Physical Sidelink Feedback Channel**
P**SSCH**	**Physical Sidelink Shared Channel**
PUCCH	**Physical Uplink Control Channel**

PUSCH	**Physical Uplink Shared Channel**
QoS	**Quality of Service**
RAN	**Radio Access Network**
RB	**Resource Block**
RF	**Radio Frequency**
RP	**Resource Pool**
RRC	**Radio Resource Control**
RSRP	**Reference Signal Received Power**
RSRQ	**Reference Signal Received Quality**
RSSI	**Received Signal Strength Indicator**
RSU	**Road Side Unit**
SC-FDMA	**Single-Carrier Frequency Division Multiple Access**
SCI	**Sidelink Control Information**
SCS	**Subcarrier Spacing**
SF	**Subframe**
SL	**Sidelink**
SPS	**Semi-Persistent Scheduling**
SB-PSS	**Sensing Based Semi-Persistent Scheduling**
SR	**Scheduling Request**
TB	**Transport Block**
TDD	**Time Division Duplex**
TPC	**Transmit Power control**
TTI	**Transmission Time Interval**
UL	**Uplink**
URLLC	**Ultra-Reliable Low Latency Communication**
V2I	**Vehicle-to-Infrastructure**
V2N	**Vehicle-to-Network**
V2P	**Vehicle-to-Pedestrian**
V2R	**Vehicle-to-RSU**
V2V	**Vehicle-to-Vehicle**
V2X	**Vehicle-to-Everything**

Chapter 1

Introduction

Over the past forty years, the world has seen four generations of mobile communications (see Fig. 1.1).

The first generation of mobile communications, which emerged around 1980, was based on analogue transmission, and technology at the time led in the USA to the standardization of the Advanced Mobile Telephone System (AMPS). AMPS in North America and Nordic Mobile Telephony (NMT) in Scandinavian countries were jointly developed by government-controlled public telephone network operators. In some other countries, the Total Access Communications System (TACS) similar to AMPS was used. Although the first generation of mobile communication technology at that time was limited to providing only voice services, this was the first time that ordinary people could use a cell phone.

In the second generation (2G) of mobile communications, which appeared at the beginning of the 1990s, the first digital transmission through wireless links was applied. Although the main objective was voice service with more

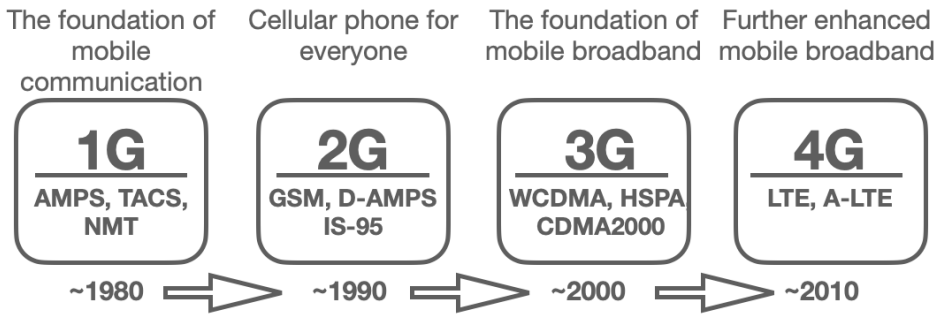

FIGURE 1.1: The different generations of mobile communication.

users, digital transmission enabled 2G mobile communication systems to offer limited data services. Initially, 2G operated applying several technologies, such as the Global System for Mobile Communication (GSM), jointly developed by several European countries, Digital AMPS (D-AMPS), offered primarily in the US, and Personal Digital Cellular (PDC) only used in Japan.

Within the development of 2G technologies, Code Division Multiple Access (CDMA) was also introduced on the basis of the IS-95 standard. Over time, GSM expanded from Europe to other regions with solutions that fully support 2G technologies. Primarily, this expansion occurred because of the success of GSM. Furthermore, 2G systems prompted the change of cellular devices to be more sophisticated and relatively more diminutive than they used to be before, and to be a necessary part and essential communication tool in the life of most of the world population. Even today, GSM technologies are used in many areas around the world for some services. In some cases, GSM is the only technology available for cellular communications, despite the subsequent introduction of 3G and 4G technologies.

Following the success of 2G technology based mainly on GSM, 3G technology was introduced. Its operation relies on the CDMA multiple access method. Two main types of systems were developed: UMTS (Universal Mobile Telecommunication System) and cdma2000. Although initially offering voice services in the channel switching mode, UMTS versions standardized by 3GPP (The Third Generation Partnership Project) were substantially extended offering high speed data transmission in downlink and uplink (HSPA) in the packet switching mode.

Up to that level of development, cellular communication technologies were established on the basis of the Frequency Division Duplex (FDD) concept. 3G also witnessed the first introduction of mobile communication in unpaired spectrum applied by China-developed TD-SCDMA technology based on Time Division Duplex (TDD). 3GPP also standardized the Time Division Duplex (TDD) version of UMTS for unpaired spectrum ranges; however, its FDD version dominates.

In recent years, we have been in the era of the fourth generation (4G) of mobile communications, represented by LTE technology and its extensions. LTE followed the HSPA steps to provide greater efficiency, a better mobile broadband experience, and greater capacity in terms of the higher data rates achievable for end users. These higher data rates are obtained on the basis of Orthogonal Frequency Division Multiplexing (OFDM) transmission to enable wider transmission bandwidths and better developed multi-antenna technologies. Furthermore, while 3G allowed for cellular communication in the unpaired spectrum employing a specific radio access technology (TD-SCDMA) or TDD version of UMTS, LTE supports both FDD and TDD operations in both paired and unpaired portions of the spectrum within one standard for radio access technology. LTE is an example of the convergence of the world into a single global mobile communication technology applied by all mobile network operators and applicable to both paired and non-paired spectra. The subsequent development of LTE also expanded the operation of mobile telecommunication networks to unlicensed bands.

1.1 The Fifth-Generation (5G/NR) Technologies

Discussions about the fifth generation (5G) of communications began around 2012. 5G has been designed in a much broader context, referring to particular wireless access technology and the wide content of new services and benefits that cellular communications will enable.

Meanwhile, the number of devices connected to mobile networks in 2018 exceeded 5 billion. This number is expected to increase to 5.9 billion by 2025, covering about 70% of the world population. Furthermore, technologies that will be launched in the future, such as 4K, 8K, 3D video, 360° video for sport broadcasts, augmented reality, and virtual reality for games, will increase the volume of data that will generate high traffic in mobile networks. At the same time, the development of technologies introduced over the past few years, such as automated driving, intelligent grids, and massive sensor deployment,

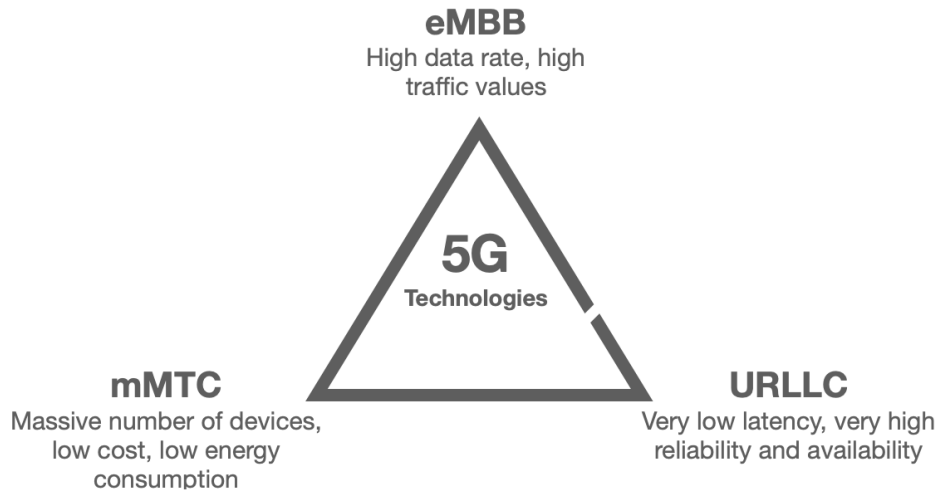

FIGURE 1.2: High level 5G use case classification.

continues to meet the need for a highly configurable and flexible Radio Access Network (RAN). In addition, emerging services the world is looking forward to seeing soon, such as the delivery by drones, consumer robots, and self-driving cars, as well as applications for smart homes, cities, and buildings, are creating the so-called Internet of Things (IoT) world [66].

As a result, 5G technologies must offer high flexibility enabling a service-based approach. There are three main categories of services and system types in 5G communications (see Fig. 1.2): enhanced Mobile BroadBand (eMBB), Ultra-Reliable Low-Latency Communication (URLLC), and massive Machine-Type Communications (mMTC). Radio resource management plays an increasingly crucial role in enabling a customizable QoS that also requires the support of the adaptable Physical Layer (PHY) [67].

1.2 Vehicular Communication

Direct Vehicle-to-Vehicle (V2V) communication can help reduce accidents by providing the driver with up-to-date local and emergency information. To this end, periodic and event-driven notifications are transmitted. All vehicles send periodic messages to inform neighbors of their current status, such as

position, speed, direction, and acceleration. Additionally, event-driven messages are transmitted when an emergency event has occurred. Conveying such safety-critical messages requires low latency and high reliability of vehicular communication. Therefore, the efficiency of safety applications depends on the establishment of a reliable communication system [5].

The current conventional solution for V2X communications is based on the IEEE 802.11p standard or communication over cellular networks (C-V2X, that is, V2X based on LTE systems (LTE-V2X) and V2X based on 5G New Radio systems (NR-V2X)). The V2V based on the IEEE 802.11p standard has an established physical layer (PHY) analogous to regular 802.11 with a 10 MHz channel, and the Medium Access Control (MAC) layer is similar to Carrier Sense Multiple Access (CSMA) [24]. As mentioned above, the physical layer of C-V2X can be based on the Long-Term Evolution (LTE-V2X) cellular standard or the 5th Generation New Radio air interface (5G NR-V2X).

Vehicles operating according to the LTE-V2X standard broadcast awareness messages to surrounding nodes. Unlike LTE-V2X, vehicles with 5G NR-V2X use unicast, multicast, and broadcast to notify the surrounding nodes of their driving parameters and emergency cases.

C-V2X is designed in two modes of communication: with and without cellular communication support for vehicles located within and outside the coverage area, respectively. C-V2X is complementary to Device-to-Device (D2D) communication defined in 3GPP standards. C-V2X and D2D communications work simultaneously by sharing two basic spectrum approaches [30]:

1. **Spectrum underlay**, the radio spectrum of D2D communications reuses parts of the spectrum used by cellular transmitters.

2. **Spectrum overlay**, where momentary empty radio resources of the spectrum are utilized.

The critical challenge in both cases is to mitigate packet collisions and interference that occur. However, more sophisticated techniques such as interference cancelation, interference coordination, and radio resource scheduling

are needed to improve communication performance.

Radio resource allocations and scheduling severely limit a typical C-V2X communication system using cellular communication. Vehicles located within cellular coverage and supported by cellular infrastructure suffer from high signaling costs between vehicles and cellular networks with higher transmission reliability. Meanwhile, vehicles in areas lacking cellular network coverage depend on the sensing process to obtain the appropriate radio resources for transmission [53].

1.3 Research Objectives and Contributions

Even though cellular-based V2X communications have recently gained a lot of attention, there are many challenges before the cellular system can be widely used for vehicular communications. Structure of the physical layer, synchronization, multicast broadcast mobile services (MBMS), radio resource selection and (re)allocations, and security issues are the main challenges for cellular V2X communications. The current physical layer structure for cellular communication cannot handle vehicles' high carrier frequency and high mobility due to Doppler effects, so a new physical layer architecture is needed for cellular V2X communication. Likewise, the high speed of vehicles can cause frequent modifications in the channel characteristics and may cause synchronization problems between vehicles and the cellular base station. To support a wide range of vehicular communication applications, this dissertation investigates the scheduling of radio resources and the allocation of centralized and autonomous vehicle resources to support sidelink vehicular communication. To realize our problem statements of improving the concepts of technologies proposed earlier, the main research objectives and improvements have been specified below. They are the following.

1. Proving that the widely assumed fact that the selection of radio resources for the autonomous allocation of resources (without cellular network support) in vehicular communication depends entirely on the sensing

process is incorrect. This fact causes many problems, such as resource collisions and hidden nodes. However, motivated by the above, **the author of this dissertation proposes a new selection of radio resources to fix the problem of the sensing process and increase the reliability of the broadcast of awareness messages.**

2. Supporting the selection and allocation of radio resources for vehicle sidelink communication when these vehicles are in high mobility and outside the cellular coverage area. Therefore, many errors occur when the number of nodes in the broadcast area changes rapidly over time, causing the loss of radio resources reserved for sidelink communication (reserved by vehicles) and creating confusion in the sensing process. To solve this resource selection problem, **we propose a method for fast reselecting resources when a loss of reserved radio resources is detected.**

3. One of the main challenges in vehicular communication is the limitation of radio resources in areas of high vehicular density. Many series of errors are detected when the number of vehicles is greater than the number of radio resources in a coverage area. To solve this problem, **we propose a method that can adaptively provide the radio resource according to the number of vehicles in the sidelink coverage area of a vehicle.**

4. Vehicles with autonomous resource allocation need an accurate and reliable radio congestion controller, especially when the channel is heavily loaded. However, the radio resource of a broadcast coverage area of awareness messages transmitted by a vehicle should not conflict with another transmission in the same coverage area. To manage this challenge, **we propose a new adjustment o f resource congestion control to be used in resource allocation.**

5. The cellular infrastructure supports vehicles within its coverage area with centralized C-V2X resource allocation to periodically broadcast awareness messages. The distribution of resources among these cellular infrastructures (that is, gNB, small cells, etc.) needs a strategic method

to avoid the overlap of the coverage areas of the vehicles' transmission. Overlapped coverage areas can cause hidden nodes and collisions. For this reason, **we propose a manner to distribute the spectrum between cellular infrastructures along a highway.**

6. Another important challenge to investigate is the time required for sidelink resource reselection in centralized resource allocation in the cellular infrastructure. Because resource reselection time is a critical issue in vehicular communication, it is crucial to ensure that the reselection time is short enough for reliable self-driving of vehicles.

Concerning the statement of the above problems and objectives, the following thesis is formulated.

Thanks to the methods proposed in this dissertation such as specific autonomous resource allocation, tracking radio resources, planning the accessible resources, adaptive modulation and coding scheme and balancing the physical parameters according to the channel load level, the performance of C-V2X communication systems may be substantially improved, e.g. in terms of packet reception ratio and collision ratio.

1.4 Organization of the Work

The outline of this dissertation is as follows.

Chapter 1 introduces the background of cellular-vehicular communication and then defines the motivations, research objectives and main contributions to be included in this thesis.

Chapter 2 presents the background on vehicular communication and the first proposed solutions, methods, and techniques that have been standardized by the IEEE or 3GPP standardization bodies. Furthermore, this chapter presents comprehensive studies and comparisons between the methods and techniques used in vehicular communication.

Chapter 3 describes two proposed radio resource scheduling and allocation algorithms for the C-V2X sidelink with autonomous resource allocation. The first proposal uses a new resource scheduling algorithm to increase the packet reception ratio and decrease the packet collision ratio. We compare the performance of the system using the proposed algorithm with that of the standard algorithm. Moreover, the second proposal improves on the earlier work of the first proposal. This improvement increases transmission reliability for high vehicular density and high mobility networks.

Chapter 4 investigates the drawbacks in autonomous resource allocation in C-V2X when the number of vehicles in a given area is greater than the number of radio resources. In this chapter, we propose an algorithm to adjust transmission parameters to be more compatible with the number of vehicles operating within the network.

Chapter 5 investigates radio congestion control when the given channel is heavily loaded by vehicle terminals in a given area. Based on the calculation of the channel busy ratio, we propose an algorithm to adjust the channel load by varying the values of the transmission parameters.

In **Chapter 6**, the problem of overlap of broadcast coverage is considered when radio resources are allocated and managed centrally. Spectrum repartitioning is essential when vehicles transmit awareness messages to surrounding nodes. We propose and test a new spectrum partitioning technique for more reliable transmission.

Chapter 7 investigates the latency of resource allocation in centralized NR V2X. It presents a new resource partitioning technique among roadside units supervised by a cellular base station, called the partial time reuse technique in a highway scenario.

Finally, **Chapter 8** summarizes the dissertation and provides potential guidance for future research.

Chapter 2

Background in Vehicular Communications

In this chapter, the state-of-the-art within the field of this dissertation is discussed. This chapter is divided into four main sections. The first section provides an overview of the general concept of Cellular Vehicle-to-Everything (C-V2X) communication. The second section presents the architecture of C-V2X. The main challenges are discussed in the third section. Furthermore, the C-V2X radio resource allocation algorithms are identified in the fourth section.

2.1 General Concept of Vehicular Communications

The US Federal Communications Commission (FCC) in 1999 specified 75 MHz of bandwidth in the 5.9 GHz frequency band (5.850–5.925 GHz) for the case of intelligent transportation services for vehicular communication [1]. Vehicular communication aims to provide road safety, passenger infotainment, comfortable services, automated driving, a green environment, and vehicle traffic optimization [2]. Over the past two decades, this topic has attracted considerable attention from researchers in promoting vehicular communications as one of the hottest topics in future mobile communication technologies [3]. 3GPP in Rel. 14 (and redefined in Rel. 15) defined Cellular Vehicle-to-Everything

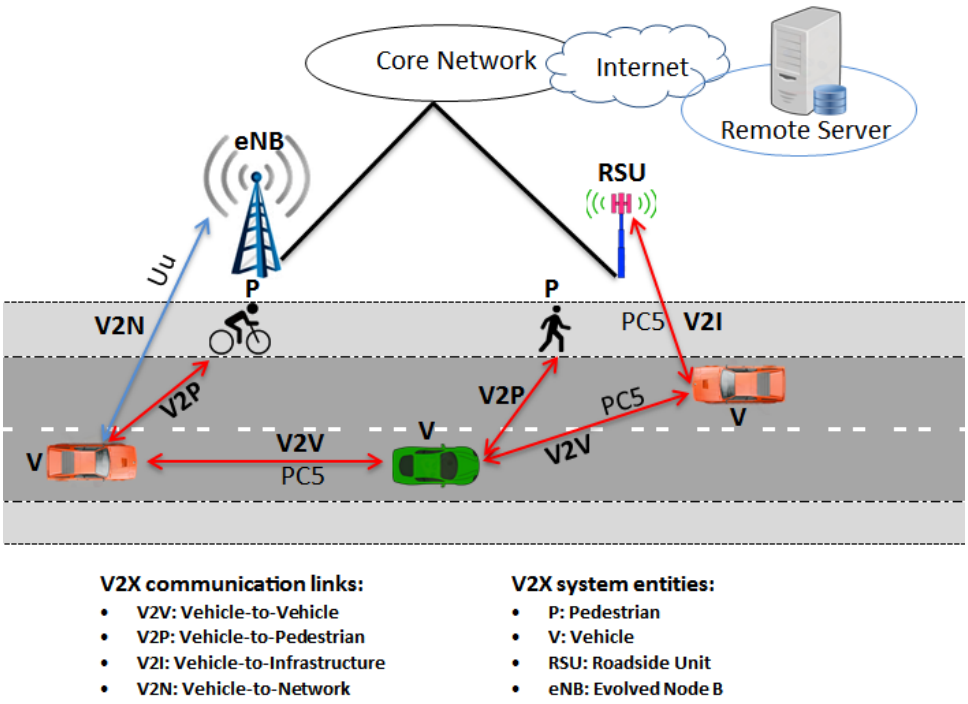

FIGURE 2.1: Description of Cellular-V2X entities.

Communication (C-V2X) by adding new features to the cellular system [4]. C-V2X communication is integrated with the cellular network using LTE or 5G systems to support the exchange of information between Vehicle-to-Vehicle (V2V), Vehicle-to-Infrastructure (V2I), Vehicle-to-Network (V2N) and Vehicle-to-Pedestrian (V2P) that can be composed as follows:

- **Vehicle-to-Vehicle communication (V2V):**
  It performs direct communications between nearby vehicles. This direct communication enables the exchange of information related to the application layer (e.g., location, speed, acceleration, deceleration, vehicle type and movement direction) with surrounding vehicles in broadcast, multicast, or unicast transmission. When cars are located within the cellular coverage area, the cellular infrastructure (i.e., eNB in the case of LTE or gNB in the case of 5G technology) will support V2X communication. Otherwise, each vehicle will depend on itself to communicate with the others in the same network [5].

- **Vehicles-to-Infrastructure communication (V2I):**
  V2I enables the wireless exchange of information between vehicles and infrastructure such as traffic lights, lane markings, Roadside Units (RSUs), and cellular base stations. The intelligent transportation system (ITS) uses V2I communication as an environmental advisory to enable safety applications in various road issues such as traffic congestion, construction sites, road curves, parking places, and speed limits. In the C-V2X communication, V2I supports the radio resource management of V2V communications [6].

- **Vehicle-to-Network communication (V2N):**
  V2N is the communication of the vehicle with the cellular infrastructure to exchange data such as information related to traffic updates and media streaming. One of the most popular services of V2N is Google Maps, which uses navigation functions and synchronizes vehicles with smartphones. Like V2I, in C-V2X communication, the cellular infrastructure can play a crucial role in supporting the resource management of V2X communication [7].

- **Vehicle-to-Pedestrian communication (V2P):**
  V2P communication performs data exchange between vehicles and pedestrians within proximity communication. The pedestrians in V2P represent people on the sidewalks. V2P can predict accidents based on the speed, position, acceleration, and deceleration of vehicles directly linked to pedestrians. Therefore, the V2P communication will warn pedestrians and drivers of approaching vehicles in the appropriate situations and times [8].

2.2 DSRC Based on IEEE 802.11p Standard

Drawing on research in the field of Mobile Ad-hoc NETworks (MANETs), Vehicular Ad-hoc NETworks (VANETs) concentrated considerable attention of

many research groups focused on supporting V2X communication [9]. In general, researchers' discussions focused on the use of Dedicated Short-Range Communications (DSRC) based on the IEEE 802.11p standard in VANET communication [10]. The IEEE 1609 family of standards known as Wireless Access in Vehicular Environments (WAVE) has supplemented the definitions of this standard, such as architecture, management framework, security issues, and physical access methods for wireless vehicular networks [5]. DSRC offers direct communication links between vehicles on the road using DSRC devices such as On-Board Units (OBUs) and infrastructural Road-Side Units (RSUs) [12]. DSRC technology provides several advantages for V2X communication, such as low vehicle-to-vehicle latency, low cost, and manageable structure when centralized control is lacking [13].

Nevertheless, this technology failed in several situations, including the degradation of the service in congested environments, security issues, and difficulty in coping with non-line-of-sight communication. However, some of these failures may be mitigated by a robust RSU infrastructure, but it is not yet clear which side is responsible for the construction and maintenance costs [14]. DSRC took considerable time in the investigations and examinations by the European Telecommunications Standards Institute (ETSI)

IEEE 802.11p supplemented the IEEE 802.11 Wi-Fi standard in the physical and Medium Access Control (MAC) communication layer. Submitted to IEEE for addition to the standards in 2010 by IEEE 802.11 Task Group p [15], the 11p amendment made several changes to the IEEE 802.11 standard to accommodate inter-vehicular communications. These modifications are primarily related to the control functions of the 802.11 MAC layer and service operations required to maintain connectivity in a dynamic environment when there is no connection with the traditional Basic Service Set (BSS) of the IEEE 802.11 network. The 802.11 standards did not contain a discussion on the spectrum ranges of DSRC communication. However, in the standards, it is considered

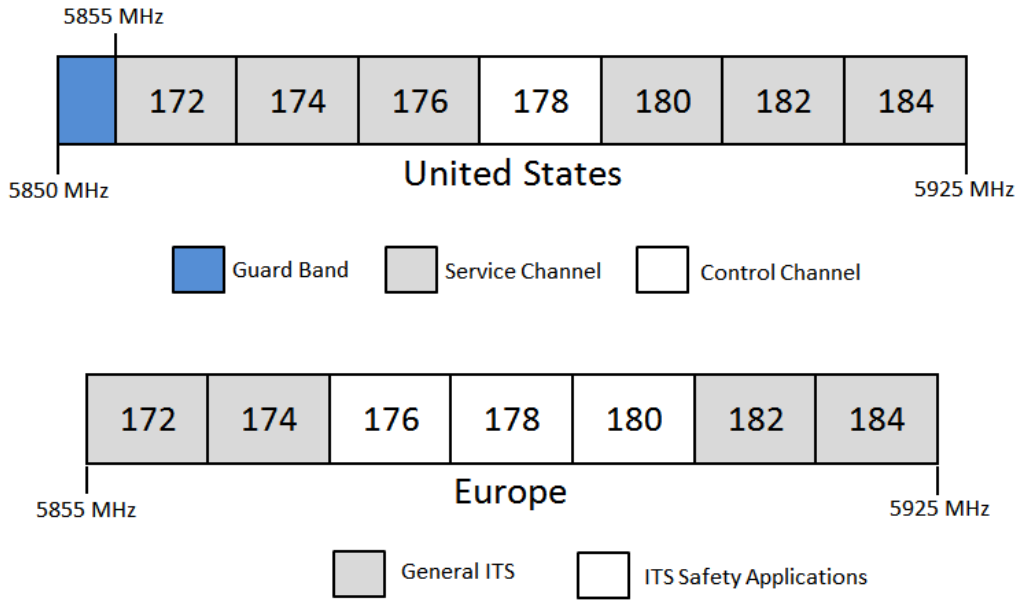

FIGURE 2.2: DSRC frequency bands.

how the communication technique takes place over different types of channels [16]. Meanwhile, the VANET spectrum range was defined by various regional institutes. European ITS-G5 specifies 70 MHz (5855 - 5925 MHz) for vehicular communication and 30 MHz (5875 - 5905 MHz) for traffic safety applications. On the other hand, the Federal Communication Commission (FCC) of the United States reserved 75 MHz (5850 - 5925 MHz) of the 5.9 GHz band [17]. The 5885 - 5895 MHz channel band is used as a traffic control channel band for vehicle safety, and the 5915 - 5925 MHz channel band is used for public safety communication [18] (see Fig. 2.2).

As mentioned above, the IEEE 802.11p supplement of the IEEE 1609 family is collectively called WAVE. The 1609 standards describe interfaces and features for the physical and MAC layers defined by 802.11 [19].

In IEEE 802.11p, the MAC layer procedure is equivalent to the Enhanced Distributed Channel Access (EDCA) of IEEE 802.11e. The ECDA holds the feedback mechanisms represented by the ACK and the Request-To-Send/ Request-To-Clear (RTS/CTS) process. Furthermore, it adds the ability to utilize a transmission opportunity (TXOP). In other words, different Access Categories (ACs) can be used depending on message priority (that is, AC0 has the lowest

message priority and AC3 has the highest message importance) [20].

At the MAC layer, the Distributed Coordination Function (DCF), known as Carrier Sense Multiple Access with Collision Avoidance (CSMA/CA) of IEEE 802.11, is adopted as the primary access method of IEEE 802.11p. The carrier sensing process is essential to ensure that a vehicle that wants to transmit the message recognizes that the medium is free. When a car senses the frequency channel as idle, it will start transmitting signals. Otherwise, a car will defer its transmission when another vehicle uses the frequency channel (busy channel). The channel is busy when the vehicle detects a Clear Channel Assessment (CCA) greater than the established threshold. The CCA is higher than the receiver's sensitivity (or sensing power threshold). When the busy channel period ends, vehicles must wait for a backoff time named the contention period [21]. The CSMA/CA introduces considerable overhead, especially when applying a high modulation order and a small packet size. Furthermore, packet/resource collision appears as a severe communication problem when Channel Occupancy (CO) increases in time by 50–60% [22].

When analyzing the MAC layer, it is essential to mention the most critical phenomena, such as hidden nodes and the frame capture effect. These phenomena usually reduce the performance of IEEE 802.11p vehicular communications [23]. Typically, the hidden node problem is the main reason for the performance degradation within vehicular connectivity. One can check the hidden nodes by comparing two control mechanisms of access, Carrier-Sense Multiple Access (CSMA) and Self-organized Time Division Multiple Access (STDMA). Both methods show that hidden node detection did not significantly improve or affect the system performance of both MAC protocols. However, synchronized transmitted packets in the TDMA protocol offered a higher probability of packet reception [24]. Frame capture (sometimes called capture echo phenomenon) appears as a side effect in IEEE 802.11 chipsets when dealing with frame collisions. Frame capture is affected by the arrival times of many transmitted frames and the respective signal-to-interference plus noise ratio.

TABLE 2.1: Basic OFDM parameters concerning channel bandwidth based on IEEE 802.11a.

Parameters	20 MHz Bandwidth	10 MHz Bandwidth	5 MHz Bandwidth
Bit rate (Mbit/s)	6, 9, 12, 18, 24, 36, 48, 54	3, 4.5, 6, 9, 12, 18, 24, 27	1.5, 2.25, 3, 4.5, 6, 9, 12, 13.5
Modulation mode	BPSK, QPSK, 16QAM, 64QAM	BPSK, QPSK, 16QAM, 64QAM	BPSK, QPSK, 16QAM, 64QAM
Code rate	1/2, 2/3, 3/4	1/2, 2/3, 3/4	1/2, 2/3, 3/4
Number of sub-carriers	52	52	52
Symbol duration	4 µs	8 µs	16 µs
Guard time	0.8 µs	1.6 µs	3.2 µs
FFT period	3.2 µs	6.4 µs	12.8 µs
Preamble duration	16 µs	32 µs	64 µs
Sub-carrier spacing	312.5 kHz	156.25 kHz	78.125 kHz

The receiver might receive a frame according to one correctly instead of dropping them and wasting both [25].

In the physical layer, IEEE 802.11p has made many changes to IEEE 802.11a to be more appropriate for high mobility vehicles. One of the most significant changes in physical parameters is an operating frequency of 5.9 GHz instead of 5 GHz. Moreover, IEEE 802.11a supports 5, 10, and 20 MHz bandwidth channels, while IEEE 802.11p employs a 10 MHz bandwidth channel. IEEE 802.11a functions follow full-clocked mode with 20 MHz bandwidth when operating a shortened clock/sampling rate, while IEEE 802.11p runs the half-clocked mode when the bandwidth is 10 MHz. The Fast Fourier transform (FFT) size in IEEE 802.11p is 64, and the number of subcarriers is 52 (4 subcarriers used to carry the pilots and 48 subcarriers used to hold the data). Table 2.1 presents the parameters related to the channel bandwidth of applied orthogonal frequency division multiplexing (OFDM) technique [26].

As observed above, IEEE 802.11p has inherited the physical layer of IEEE 802.11 by using OFDM as a modulation technique. However, there are two crucial variations in the specifications of both sides of communication to support IEEE 802.11p for vehicular communications. Significant rejections are represented in these variations to the spectrum mask and adjacent and non-adjacent channels. These terms require challenges because the cross-channel

TABLE 2.2: The main differences between IEEE 802.11a and IEEE 802.11p.

Parameters	IEEE 802.11a	IEEE 802.11p
Sample rate	20 MHz	10 MHz
Number of FFT points	64	64
Number of subcarriers	52	52
Number of data subcarriers	48	48
Number of pilot subcarriers	4	4
OFDM symbol period	$T_{Symbols}$ = 80 sampling periods = 4 µs	8 µs
Cyclic prefix	16 sampling periods = 0.8 µs	1.6 µs
FFT symbol period	64 sampling periods = 3.2 µs	6.4 µs
Modulation scheme	BPSK, QPSK, 16QAM, 64QAM	BPSK, QPSK, 16QAM, 64QAM
Coding scheme	1/2 industry convolutional	1/2
Available data rate	6, 9, 12, 18, 24, 36, 48, 54 Mbps	3, 4.5, 6, 9, 12, 18, 24, 27 Mbps

interference meddles with the transmitted signals, especially when the transmitter and receiver frequencies are close to each other or the distance between transmitter and receiver is ten times higher than the interference power and receiver source.

Table 2.2 represents the main similarities and differences between the IEEE 802.11a and IEEE 802.11p standards [27].

2.3 Vehicular Communication Using Cellular Support

3GPP in Rel. 12 [28] introduced Device-to-Device (D2D) communication as an innovation to enable direct connection between nearby cellular devices to increase connectivity in the cellular environment. D2D communication utilized a new LTE-based interface called PC5. Furthermore, the Uu interface has been introduced as a necessary interface to consider the cellular network in uplink/downlink communication in two kinds of cellular connectivity: full and partial one. Full cellular connectivity refers to direct data exchange between devices within the coverage area [29]. Partial cellular connectivity refers to the direct exchange of data between devices within and outside the coverage

TABLE 2.3: The timeline and 3GPP releases related to cellular V2X communication.

3GPP Release year	Technology	Features
Rel. 12 and 13 / 2014	ProSe	D2D communication over PC5
Rel. 14 / 2017	LTE-V2X	High mobility support. Mode 3 and Mode 4. Broadcast only.
Rel. 15 / 2018	PC5 improvement	Up to 64-QAM Modulation. Carrier aggregation. Selection window size reduction. Radio resources sharing between Mode 3 and Mode 4.
Rel. 16 / 2020	5G-V2X	Uni-cast, multi-cast support. Feedback channel. New modes 1 and 2. Adaptive DMRS. Adaptive traffic prioritization. mmWave.
Rel. 17 / 2022	End-to-end enhancements	Beyond VUE. Relay support. Improved group management and communication.

area. Furthermore, if the D2D communication takes place under infrastructure supervision, it is called that it works in Mode 1. Meanwhile, if the D2D transmission is placed outside of the infrastructure supervision, it works in Mode 2 [30]. Cellular V2X communication is based on the concept of D2D communication. The Cellular V2X communication timeline according to 3GPP standards is summarized in Table 2.3.

These considerations are included in the LTE enhancements and the fifth generation (5G) New Radio (NR), which contains the latest improvements in vehicular communication [31].

In Release 14 [32], 3GPP announced new advanced LTE features to support V2X, enabling SideLink (SL) communication between vehicles and the nodes surrounding them (e.g., other vehicles) in a high mobility network. The new features are defined in two modes: Mode 3 and Mode 4. Mode 3 requires infrastructure support using centralized resource allocation, and Mode 4 determines operation without infrastructure support using autonomous resource allocation.

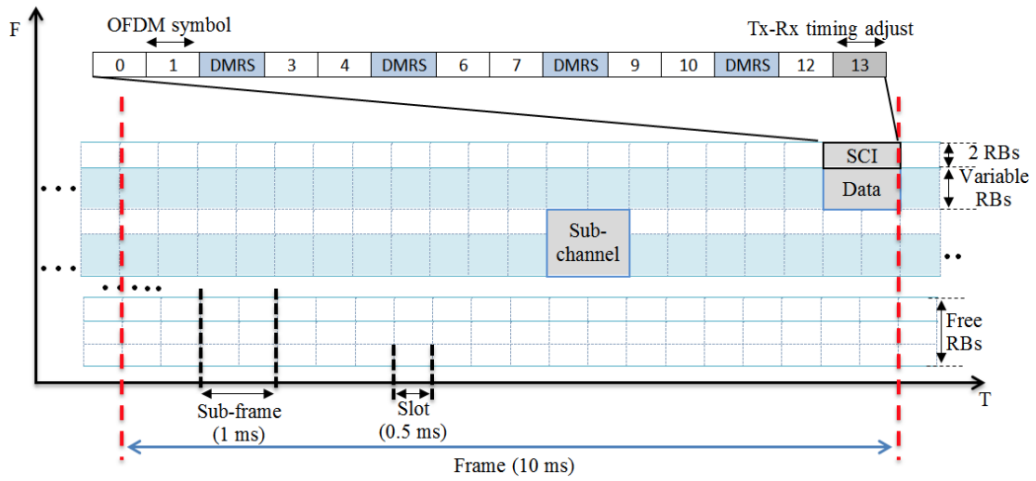

FIGURE 2.3: C-V2X resource grid description in time and frequency domains.

In the standard [33] modifications are added to the physical layer arrangements to manage the Doppler effect at high mobility speed. The number of DeModulation Reference Signals (DMRS) in one subframe is increased from two in Device-to-Device (D2D) to four in C-V2X communication.

The Cooperative Awareness Message (CAM) was suggested by ETSI for all vehicles to periodically broadcast notifications to their surrounding vehicles about speed, direction of movement, type, acceleration, and deceleration. IEEE defines this message as a Basic Safety Message (BSM) or a Beacon [5].

To support 10 MHz and 20 MHz bandwidth channels, 3GPP standardized the uplink LTE communication technique [35]. Single-Carrier Frequency Division Multiple Access (SC-FDMA) is a time-frequency multiplexing technique that is applied in the channel by dividing it into several subchannels. Each subchannel comprises a group of resource blocks (180 kHz each) as the smallest frequency unit that carries information. Furthermore, each resource block consists of 12 subcarriers spaced by 15 kHz on the frequency axis. The subframe (two slots, 0.5 ms each) is the shortest time unit of a duration of 1 ms in the time domain. The subchannel consists of several resource blocks whose number varies according to the amount of data and the MCS used. Each vehicle in the network uses one subchannel to periodically broadcast a CAM message [36].

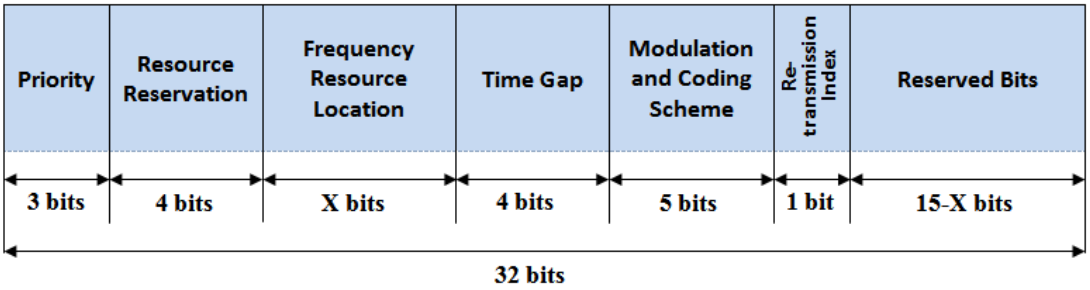

FIGURE 2.4: SCI content [37].

The CAM message consists of two parts of information placed in two physical channels. The first part is placed in two resource blocks in each subchannel, transmitted by a physical channel called the Physical Sidelink Control Channel (PSCCH). The PSCCH carries 32 bits of Sidelink Control Information (SCI format 1) to help the receiver decode the second part (see Fig. 2.4) [37]. The 32 bits of SCI are divided into several parts that are summarized as follows:

- **MCS:** Five bits are indicated by higher layers to carry information related to the MCS of the second part of the CAM message.
- **Priority:** The vehicle establishes this three-bit field according to the highest priority of several priorities indicated by the upper layers corresponding to the transport block.
- **Time Gap:** The vehicle in four bits in this field establishes a period between initial transmission and retransmission.
- **Resource Reservation:** This field is four-bit long and is used only in autonomous resource allocation to announce selected resources based on sensing decisions (to be used in future transmission).
- **Frequency Resource Location:** This X bit field indicates the resource locations of the initial transmission.
- **Retransmission Index:** It is a bit that denotes the first transmission or retransmission of Physical Downlink Shared Channel (PDSCH).
- **Reserved Bits:** zero-valued bits of length $15 - X$.

The Transport Block (TB) represents the second part of the CAM message containing the information broadcast through the Physical SideLink Shared Channel (PSSCH). The second part of the CAM message has a changeable number of resource blocks that carry vehicle information, such as speed, direction, acceleration, and deceleration [38].

Furthermore, Cellular-V2X communication can broadcast parts of the CAM message in adjacent or non-adjacent transmission configurations (see Fig. **??**). In the adjacent configuration, both the PSCCH and the PSSCH are transmitted adjacently to each other in the frequency domain in the same subframe. However, in non-adjacent transmission, both physical channels, PSCCH and PSSCH, are transmitted in the same subframe in a non-adjacent manner [39].

Each subframe consists of 14 OFDM symbols with a standard cyclic prefix. Due to the high mobility and density of vehicles on the road, 3GPP has increased the number of symbols carrying DeModulation Reference Signals (DMRSs) in each subframe, especially for vehicles that move fast at a speed greater than 250 kmph. Furthermore, to better track the channel at high vehicle speeds, an OFDM symbol has been added at the end of the subframe as the Tx-Rx turn-around symbol [40].

2.3.1 LTE-V2X Requirements

This section introduces the technical requirements that LTE-V2X technology should meet, which are summarized in the following list [41]:

1. **Low communication latency:** Communication latency refers to the time between the moment of packet generation at the source and the time of its receipt at the receiver. Communication latency is a critical factor in ensuring safe driving. For example, collision warning includes warning announcements to/from vehicles in dangerous conditions. The collision warning message requires a latency between 10 and 100 ms. On the other hand, driving autonomous vehicles requires low latency in the exchange

of information between vehicles and vehicles with the network to adapt to traffic and road conditions.

2. **High reliability:** It is the level of acceptable packet loss at the application layer. The packet is considered lost if the latency exceeds the maximum acceptable end-to-end latency.

3. **Support for high mobility:** The LTE-V2X supports communication in high-mobility vehicles (kmph) to avoid Doppler effects at high speed. One of the main improvements in LTE to support V2X is, as already mentioned, increasing the modulation reference signals from two symbols in D2D communication to four in V2X communication in one subframe.

4. **Support for high vehicle density:** If the number of vehicles in a network (vehicles/km^2) is high, then V2V systems operating according to IEEE 802.11p face a serious problem. Unlike IEEE 802.11p, LTE-V2X supports several subchannels within a subframe, where each vehicle can transmit its packet in a subchannel. This feature enables more vehicles to utilize subchannels at the same time.

5. **High data traffic:** A high data traffic is expected in vehicular communication, especially in urban and highway scenarios. The urban scenario triggers high signaling costs to transfer information to vehicles. Highway scenarios can include fast traffic, requiring environmental vision; therefore, more information must be sent to the car.

6. **Wide communication range:** It refers to the maximum distance between the transmitter and the receiver for radio transmission that achieves acceptable reliability in the application layer. Several factors can affect this distance, that is, the speed of the vehicle, the MCS used and the transmission power. Flexibility in using these factors is essential to reach the desired range.

7. **High data rate:** The high rate of data transfer in a time unit is essential to support several applications and to open new horizons to create new

applications in the future. Several new services in C-V2X have been demanded in the last few years, for example, the Internet of vehicles that required bandwidth higher than 100 Mbit/s.

2.3.2 Use Cases of LTE-V2X

Cellular-V2X use cases focus on increasing the safety of self-driving vehicles, improving situational awareness and travel comfort, and reducing traffic congestion. ETSI described the technical service requirements and critical functions in the ITS. These requirements and functionalities typically use periodic and non-periodic warning messages to increase environmental awareness. CAM is used as periodic broadcast messages for vehicle-to-vehicle communication with a repetition rate not exceeding 100 ms. However, an event-driven decentralized environmental notification message (DENM) is defined as a periodic broadcast message with the same repetition rate. ETSI also described the use cases of cellular V2X in its release of the standard [42]. Table 2.4 shows the most critical communication use cases.

TABLE 2.4: Performance requirements in examples of V2X use cases.

Cellular - V2X use cases specified by 3GPP TR 22.885 [12]			
Use case	**Latency**	**Reliability**	**Message size**
Emergency vehicle warning	100 ms	99%	50-300 Bytes
Queue warning	100 ms	99%	50-400 Bytes
Forward collision warning	-	99% to 99.99%	50-300 Bytes
Vulnerable road user safety	60 ms	95%	1600 Bytes
5G V2X use cases specified by 3GPP TR 22.886 [14]			
Lane merge (cooperative maneuver)	30 ms	99.99%	1200-16000 Bytes
Cooperative collision avoidance	10 ms	99.99%	2000 Bytes
Vehicle platooning	10 ms	99.99%	50-1200 Bytes
Collective perception of environment	3-50 ms	99% to 99.99%	1600 Bytes

2.3.3 Comparison of IEEE 802.11p Based DSRC and LTE V2X Communications

In this subsection, two types of comparison between DSRC based on IEEE 802.11p and C-V2X communications are discussed. The definitions of these comparisons are based on performance assessment and technical characteristics [43].

- **Comparison of performance appraisal**

  This item discusses the comparison of IEEE 802.11p with C-V2X from a performance point of view as follows:

  1. The wide deployment of LTE, high data rate, Quality of Service (QoS) support, and ubiquitous coverage area cause the development of C-V2X to gain more attention to be applied.
  2. Upgrades to the LTE system infrastructure play an essential role and are an excellent opportunity to support vehicular communication. The C-V2X features in the LTE system added some critical keys to the eNB and the Core Network to enable C-V2X applications.
  3. An eNB supervises resource allocation when vehicles are located within the coverage area to prevent overlap in used resources. When vehicles are outside cell coverage, vehicles will depend on the sensing process to schedule the free resource autonomously. Unlike C-V2X, resource collisions are unavoidable in DSRC, especially in congestion areas.
  4. Two air interfaces support C-V2X communication. The first air interface is Sidelink between vehicles to exchange information only between them. The second air interface is between vehicles and the infrastructure to support uplink and downlink exchange information between vehicles and the network.

5. Cellular communication supports broadcast messages from multiple cells simultaneously using evolved Multimedia Broadcast Multicast Services (eMBMS). This feature is handy in automated vehicles to share knowledge about the road and emergencies.
6. Vehicle communication using LTE supports multiplexing in the frequency domain, unlike DSRC, where only one vehicle can transmit information simultaneously on the given channel. This benefit makes the exchange of information between vehicles more efficient in areas of high-density vehicles.
7. LTE has a better sensitivity for weak received signals compared to DSRC. This means that vehicles that use LTE have a more efficient decoding of weak signals. Furthermore, LTE uses turbo code to ensure a better coding gain than the convolutional code used by DSRC.
8. The performance of the link in V2X based on LTE shows an efficient behavior to avoid hidden nodes. However, the IEEE 802.11p link shows a performance degradation caused by hidden nodes that remains unsolved.

- **Comparison of technical features** This comparison aims to show the differences in parameters between 802.11p and C-V2X that are summarized in Table 2.5.

2.4 V2X in 5G NR Systems in Recent 3GPP Standards

3GPP in Release 16 announced a newly developed C-V2X standard based on the 5G NR (New Radio) air interface [45]. The precursor to the scientific work on Rel. 16 NR V2X was the Study Item (SI) established under Rel. 15. SI developed the evaluation methodology and ideas for both LTE and NR V2X, which are essential to evaluate and weigh many proposals in the 5G NR V2X standard [46]. Next, 3GPP established an SI and a Work Item (WI) to announce the

TABLE 2.5: Basic OFDM parameters for DSRC and LTE-V2X [41].

Features	**DSRC based IEEE 802.11p**	**LTE-V2X**
Frequency band	5.86 - 5.92 GHz	450 MHz - 4.99 GHz
Modulation	OFDM	SC-FDMA
Channel access mechanism	CSMA/CA	S-SPS, SPS
Retransmission mechanism	No HARQ	HARQ
Synchronization requirements	Asynchronous	Synchronous
Resource multiplexing	TDM only	FDM and TDM
Channel coding scheme	Convolution code	Turbo code
Data rate	Up to 27 Mb/s	Up to 1 Gb/s
Capacity utlilization	Medium	High
Coverage is	Intermittent	Ubiquitous
Mobility support	Up to 60 km/hr	Up to 350 km/hr
Quality-of-Service support	EDCA	QCI and bearer selection
Broadcast/ multi-cast support	Native broadcast	Through eMBMS

first 5G NR V2X communication standard in Release 16. SI on the radio interface was approved until March 2019, and then the WI was officially deduced in December 2019 [47]. WI has shown the first 5G NR V2X assumptions and specification sets in the 3GPP Technical Specifications (TS). The timeline to improve cellular V2X focusing on the developments of the Radio Access Network (RAN) is shown in Table 2.3.

The 5G NR in Release 15 was developed without including the features of SL. Rel. 16 was the first standard to include SL features in 5G NR V2X communication, making Rel. 16 NR V2X SL is the basis for future improvements and expansions for V2X applications [48]. It is vital to mention that the NR V2X SL was developed to supplement the LTE V2X SL communication. Furthermore, NR V2X SL aims to support use cases and applications that could not be successful in LTE V2X [49].

2.4.1 Overview of 5G NR V2X System Architecture over PC5 and Uu Interfaces

Cellular V2X supports two types of communication interface. The PC5 interface is operated on NR and LTE to support SL V2X communication and Uu

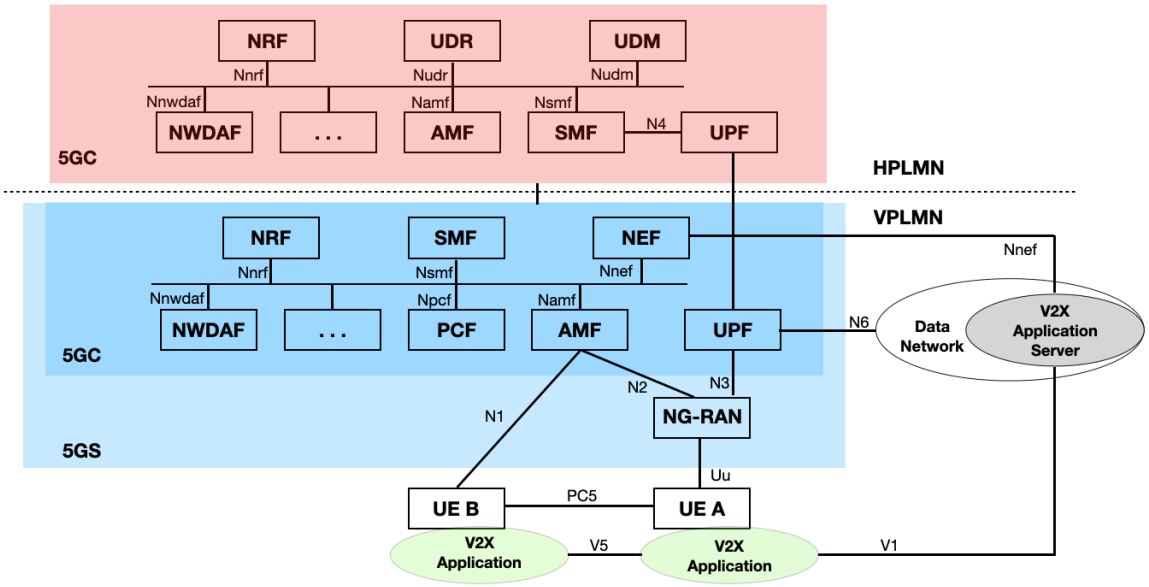

FIGURE 2.5: 5G system architecture for V2X communication over PC5 and Uu – local breakout scenario (roaming case) [53].

for uplink/downlink communication with the cellular infrastructure [50]. According to Release 16, the Uu interface supports unicast communication. It is essential to note that Uu in LTE can be used for broadcast in download through Multimedia Broadcast Multicast Services (MBMS) [51].

The high-level view of the PC5 and Uu interfaces and the roaming architecture with a local breakout of the 5G V2X communication system is described in Fig. 2.5. The system generally consists of the Home Public Land Mobile Network (HPLMN) and the visiting PLMN (VPLMN). The HPLMN identifies the PLMN in which the subscribers' profiles are grasped. In other words, HPMN is the home network that provides service to subscribers. The Home Public Land Mobile Network (HPLMN) identifies the Public Land Mobile Network (PLMN) in which subscribers' profiles are held. When a user roams to other networks, it will receive collaboration approval information from the HPLMN to provide the necessary parameters for V2X services to the VPLMN. The Session Management Function (SMF) in HPLMN is responsible for establishing, altering, or releasing a session for all User Plane Functions (UPFs) that are engaged in a Protocol Data Unit (PDU) session under the VPLMN command.

However, PC5 in V2X communication supports roaming and inter-PLMN operations, which are critical to reduce latency. In this case, the PC5 configuration must be compatible with the particular geographical area [52].

The Next Generation Radio Access Network (NG-RAN) and the 5G Core Network (5GC) represent the main 5G system domains in the 5G Core (5GC) network. Many Network Functions (NF) are involved in the 5GC, such as Policy Control Function (PCF), Access and Mobility Management Function (AMF), Session Management Function (SMF), Unified Data Repository (UDR), Unified Data Management (UDM), Network Repository Function (NRF), Network Data Analytic Function (NWDAF), Network Exposure Function (NEF), and User Plane Functions (UPF). All network functions in the 5GC Control domain except UPF use interfaces according to their services to support their interactions (e.g., Nnef, Nnwdaf, Npcf, etc.). Furthermore, network functions within the 5GC control domain allow other approved network functions to access their services [53].

Fig. 2.5 also shows the application layer interfaces to exchange information and configuration parameters between vehicles through the V5 interface and the vehicle application layer with the V2X Application Server (AS) through V1. According to the specification, there are no new NF interfaces in the 5G system architecture. Instead, the extension of existing NFs with V2X-related functions is found [54].

2.4.2 5G NR V2X Use Cases

In the 3GPP technical reports [50] and [56] the objective, use cases, and requirements of the NR V2X are described. Ranging from 0 to 5, 3GPP further classifies various degrees of automation following the society of automotive engineers, where zero means no automation and one means full automation. Typically, higher levels of automation lead to a higher number of NR V2X requirements. In general, use cases are summarized in the following groups [57]:

1. **Vehicles Platooning:** This group involves use cases for dynamic forms and the supervision of combinations of vehicles in platoons. Vehicles in a platoon exchange messages periodically to warrant the conventional functioning of the platoon. In the platoon, the distance between vehicles depends on the QoS available.

2. **Advanced Driving:** This group covers the ability to drive partially or fully automated vehicles. The vehicles in this group share the data collected from their local sensors with the vehicles that circle in proximity. Additionally, vehicles on the network share their intention to drive to manage their trajectories or maneuvers, preventing road accidents and improving traffic efficiency.

3. **Extended Sensors:** By supporting the exchange of data obtained by the sensors of the surrounding vehicles, RSUs, pedestrian cell phones, and V2X application servers, vehicles can create a vision of the environment higher than the vehicle sensor capability.

4. **Remote Driving:** This group allows remote driving in a teleoperation manner. This group aims to help travelers who cannot drive themselves or their vehicles are in dangerous environments (such as construction areas).

2.4.3 3GPP Requirements

The key requirements of the 5G NR V2X services based on Rel. 14 [58] and Rel. 15 [59] are the following:

1. **Payload:** It indicates the amount of data generated in the application layer and required for a specific service.

2. **Tx rate:** It indicates the number of messages transmitted in a given time unit.

3. **Maximum end-to-end latency:** It refers to the maximum acceptable time between message generation in the application layer of a transmitter and message receiving in the application layer of the receiver.

4. **Reliability:** It refers to the probability of correctly receiving messages to the total number of messages transmitted in a specified maximum allowed end to end latency.

5. **Data rate:** It represents the amount of data that must be transmitted from the transmitter side in a specific time unit. Other requirements, such as the amount of data in each message, the maximum allowed latency, and the transmission reliability, affect the data rate.

6. **Required communication range:** It refers to the minimum and maximum communication distance between the transmitter and the desired receiver, allowing the required amount of data, the maximum latency, and the data rate.

2.4.4 Physical Layer Design for 5G NR V2X SL

Based on Rel. 15 Uu scheme and reuse of some of the Rel. 14 LTE V2X notions of 3GPP, the physical layer NR V2X SL is structured with additional procedures to introduce a physical layer support of groupcast transmissions.

This subsection looks at three crucial parts related to the physical layer. These parts include the structures for NR V2X SL, channels and signals, and procedures.

1. ***Numerology***

   The NR V2X SL in Rel. 16 operates at frequencies similar to Rel. 15 NR Uu [47] [61] in the following frequency ranges [62] [63]:

   - Frequency Range 1 (FR1): 410 MHz – 7.125 GHz.
   - Frequency Range 2 (FR2): 24.25 GHz – 52.6 GHz.

Generally, NR V2X SL employs orthogonal frequency division multiplexing (OFDM). The NR V2X SL organizes the spectrum in radio frames of 10 ms length. In addition, each frame of 10 ms is a collection of subframes of 1 ms each. The SubCarrier Spacing (SCS) and the number of slots in each subframe are adaptable in NR V2X to support various requirements. Scalable OFDM numerology is considered to adjust resource usage based on the amount and type of data that need to be transmitted. Furthermore, each OFDM numerology is characterized by an SCS and a cyclic prefix (CP). NR V2X defines the subcarrier spacing multiples based on 15 kHz for the OFDM waveform [61]. Scalable SCS is given by 2^{μ}x15kHz where 2^{μ} represents the scalable factor of SCS. The SCS scalability factor μ in NR V2X can be equal to 0, 1, 2 or 3, so the SCS is equal to 15 kHz, 30 kHz, 60 kHz, or 120 kHz, respectively. FR1 supports 15 kHz, 30 kHz and 60 kHz subcarrier distance, and FR2 supports 60 kHz and 120 kHz distance. The high-level SCS increases the robustness of the OFDM waveform against deterioration of the signals caused by several problems, such as Doppler effect, device noise, and thermal noise, which are apparent in FR2 [64].

In the time domain of NR V2X SL, the duration of the time slot is also specified by the scalability factor μ through the expression 2^{μ}. In other words, the largest SCS of 120 kHz has the shortest time slot duration, equal to 0.125 ms. Moreover, as in Rel. 15 NR Uu, two lengths of CP of the OFDM signal are supported. The standard (normal) CP supports all SCS configurations except the 60 kHz one, supported with extended CP. However, with standard CP, when the SCS increases from 15 to 60 kHz, the time slot duration decreases from 1 ms to 0.25 ms, getting the CP shorter than enough to handle the channel effects and delay spread. For this reason, Rel. 15 NR Uu extended the CP when an SCS equals 60 kHz, which has the same duration as when the SCS equals 15 kHz [**?**] and [66]. The number of symbols in each time slot is equal to 14 or 12 OFDM symbols, depending on the length of the CP, respectively.

As an essential point, the bandwidth in NR V2X SL depends on the subcarrier spacing applied. As a general numerology design guideline, the selection of the SCS scalability factor is based on several factors, such as the frequency of the carrier, the condition of the radio channel, requirements (e.g., latency) and hardware complexity. The additional vital point is to mention and contrast Rel. 15 NR Uu is the fact that the smallest time unit in NR V2X is a time slot. The mini slot can be scheduled as part of the OFDM symbols (does not support SL scheduling) to support ultra-reliable low-latency communication (URLLC) [67].

2. ***Sidelink Bandwidth Parts***

In 5G NR V2X Uu, the maximum bandwidth when FR1 is applied is 200 MHz, while it is 400 MHz when FR2 is used [68]. Furthermore, cellular infrastructure such as gNBs can manage such wide bandwidths. The considerable bandwidth may require higher power consumption in the vehicle than a lower bandwidth due to radio frequency and baseband signal processing. The 3GPP in Rel. 15 introduced the concept of bandwidth partitioning (BWP) for 5G NR. This concept helps to support those UEs that cannot manage large bandwidths due to processing limitations or high transmission power consumption. In BWP, there are contiguous fragments of bandwidth within the channel bandwidth that have the same numerology. In other words, with the BWP concept, the channel can be subdivided and used for various purposes. Each BWP in the channel has a specific numerology order. Each BWP is configured with a different signal characteristic, allowing more flexibility and efficient utilization of the spectrum and more acceptable power consumption. BWP also supports SL NR V2X, where an SL BWP uses a contiguous fragment of carrier bandwidth [69]. SL BWP operates on the carrier frequency for transmissions and receptions of sidelink communication and uses the same numerology. Thus, all necessary signals, such as sidelink synchronization, reference, and control signals, are transmitted in the same SL

BWP (that is, the vehicle does not anticipate receiving or transmitting packets in another numerology). Twelve sequential subcarriers with the same subcarrier spacing form the popular RB in the SL BWP configuration [70].

3. ***Resource Pools***

An essential factor in SL communication is the meaning and purpose of SL resource pools. The upper layers in each UE using NR V2X can configure to use one or more resource pools to be applied for transmission and reception packets via PSCCH or/and PSSCH. The concept of a resource pool is associated with the allocation of resources for NR V2X Modes 1 and 2 [71]. The SL resource pool consists of several contiguous subchannels of fixed size. Furthermore, each subchannel consists of several contiguous RBs (pre-)configured by the Radio Resource Control (RRC) layer. The standard supports the size of the subchannel for a given bandwidth, that is, N = 10, 15, 20, 25, 50, 75 and 100 RBs per subchannel. The available resources in the time domain (i.e., slot) for SL are specified by repeating the preconfigured SL bitmap and identified by a precise size. The RCC in the higher layer specifies the resource pool parameter, sl-TimeResource, and describes the bitmap size to be in values 10, 11, 12, ..., 160 [72].

In the ITS spectrum, all OFDM symbols are used for SL when available slots with fixed and pre-configured SL transmission/reception are applied. Two pre-configured RRC parameters indexed in the first symbol and a set of subsequent symbols in a time slot are available for sidelink [70], [71], and [74].

For example, Fig. 2.6 clarifies the configuration of the 5G NR V2X time/frequency resource pool by applying the TDD technique when the given bandwidth equals 10 MHz and using numerology 1 (the subcarrier spacing equals 30 kHz)). There are two subchannels in each time slot (each subchannel contains 10 RBs). The TDD configuration is represented by

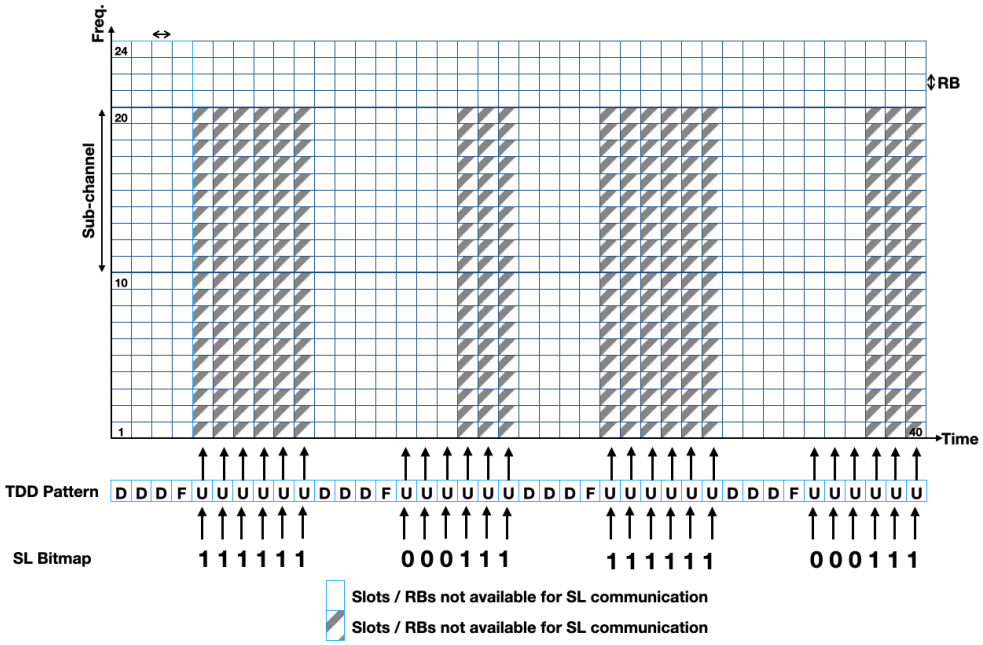

FIGURE 2.6: Definition of SL resource pool for 5G NR V2X when applying TDD technique. Example with 2 subchannels of 10 RBs each, using TDD configuration of [D D D F U U U U U U] and SL bitmap pattern of [1 1 1 1 1 1 0 0 0 1 1 1].

[DDDFUUUUUU] (three time slots for the downlink, one slot for flexibility, and six time slots for the uplink), which defines a sidelink bitmap of [111111000111].

As shown in Fig. 2.6, the TDD configuration is found repeatedly in the time domain of the configured SL bitmap. Each bitmap index uses the uplink slots (U) periodically, demonstrating the available time slots for SL communication. The SL resource pool consists of a number of adjacent subchannels in the frequency domain.

Fig. 2.6 represents 5G NR V2X Mode 2 when the UEs are located in the cellular coverage area. We present green and blue slots / RBs for the resources available for SL communication and the resources not available for SL communication [76].

4. ***Physical layer channels and signals***

In this part of the text, the physical channels and signals of 5G NR V2X are discussed and compared (see [77] and [78]).

(a) *Physical Sidelink Control Channel (PSCCH)*: is the physical channel that carries the sidelink control information.

(b) *Physical Sidelink Shared Channel (PSSCH)*: is the physical channel responsible for carrying the data payload in the sidelink with other control information.

(c) *Physical Sidelink Broadcast Channel (PSBCH)*: is the physical channel responsible for carrying the synchronization information of sidelink communication within the sidelink synchronization signal block (S-SSB).

(d) *Physical Sidelink Feedback Channel (PSFCH)*: is the physical channel that carries the feedback from the receiver to the transmitter related to the successful or failed packets received.

Furthermore, four signals are contained in (or associated with) the physical channels. These signals are specified for NR V2X and are classified as follows [79]:

(a) *DeModulation Reference Signal (DMRS)*: the transmitter generates it to help the receiver decode the data that are sent through physical channels, ie, PSCCH, PSSCH, PSBCH.

(b) *Sidelink Primary Synchronization Signal (S-PSS) and Sidelink Secondary Synchronization Signal (S-SSS)*: generated by the transmitter and used by a receiver to synchronize the signals with the transmitter. S-PSS and S-SSS are sent within a Sidelink Synchronization Signal Block (S-SSB).

(c) *Sidelink Channel State Information Reference Signal (SL CSI-RS)*: The receiver uses SL CSI-RS for measuring information related to the channel state information (CSI) and for feedback to the transmitter. The transmitter adjusts the transmission parameters according to the CSI feedback information from the receiver. Furthermore, the SL CSI-RS is located within a slot of the PSSCH channel.

(d) *Sidelink Phase-Tracking Reference Signal (SL PT-RS)*: is employed to reduce the influence of phase noise (particularly at higher frequencies) resulting from inaccuracies of the oscillator. Furthermore, SL PT-RS is transmitted within a slot of the PSSCH channel.

As a compression between LTE V2X and NR V2X, LTE V2X uses only broadcast to transmit information between vehicles without any feedback. However, NR V2X can broadcast, groupcast, and unicast using sidelink transmissions. Unlike LTE V2X, there are two stages of SCI in NR V2X. In NR V2X, the first stage of the SCI is transmitted on the physical sidelink control channel PSCCH, and the second stage is transmitted on the physical sidelink shared channel PSSCH.

The division of SCI into two stages qualifies other nodes that are not receivers (in groupcast and unicast) to receive and decode only the first stage of SCI for the radio resource sensing objective. However, the additional control information required in the receivers is provided using the second stage of SCI.

NR V2X improves feedback acknowledgment in unicast and groupcast communications to increase the reliability of sidelink transmissions. Transmission feedback is formulated using the Hybrid Automatic Repeat Request (HARQ).

Receivers can send the sidelink HARQ feedback in two options when applied groupcast communication. In the first option, HARQ feedback can be sent when the distance between the transmitter and the receiver is less than the maximum communication range. In the second option of sending HARQ feedback, all receivers send feedback to the transmitter over PSFCH as a reaction when applying unicast transmission or PSSCH when applying groupcast transmission.

In unicast transmission, NR V2X supports CSI reporting. The transmitter sends a CSI request and the receiver returns the CSI within the PSSCH [80].

2.4.5 Resource Allocation for 5G NR V2X SL

As mentioned above, Mode 1 and Mode 2 are the two modes defined in NR V2X SL communications using the V2X PC5 interface. Like Modes 3 and 4 in LTE-V2X work to support broadcasting of SL messages, Modes 1 and 2 in NR V2X work similarly to broadcast, groupcast and unicast SL messages [46].

5G NR V2X Mode 1 Resource Allocation

In this mode, the gNB selects and manages the radio resources for SL communications using the NR Uu interface between the UEs and the gNB. In this case, the UEs must be located within the network coverage area. Two resource scheduling methods are named for NR V2X Mode 1, namely, Dynamic Grant (DG) and Configured Grant (CG). DG needs to send a Scheduling Request (SR) to the gNB using PUCCH to transmit every TB (and possible retransmissions or HARQ). gNB replies to the UEs with the DCI via the PDCCH. The DCI refers to the recommended resource addresses for TB transmission and two possible retransmissions. The UE declares these addresses to the surrounding nodes using the first-stage SCI. However, UEs that use Mode 2 will be informed which subchannels are reserved for UEs operating in Mode 1 [69].

Due to the delay that can be increased due to DC, Mode 1 comprises the CG scheduling to decrease delays by pre-allocating subchannels for SL communication. With CG, the gNB can allocate a set of subchannels for a group of TB transmissions. UE needs to send supporting information to gNB to illustrate the expected SL traffic and periodicity of TBs, the maximum size of the TB, and the QoS information. The gNB uses this information to configure, assemble, and allocate a CG to the UE that satisfies the requirements of SL traffic. The allocation of resources points to the time slot(s) and frequency(s) periodically allocated to the UE in a CG. The maximum number of SL resource allocations that can be assigned is three during each period of the CG. During each CG period, the UE can transmit only one new TB [67].

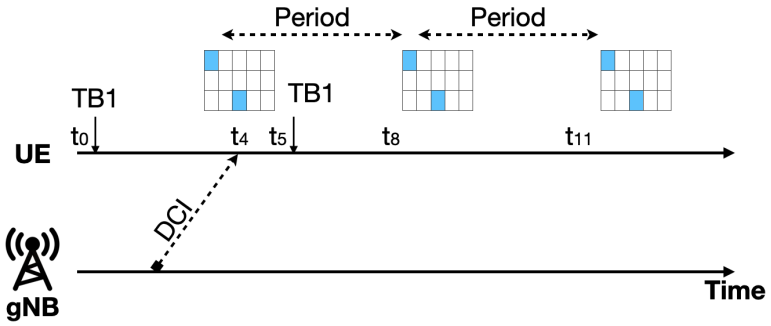

(A) 5G NR V2X Mode 1, Configured Grant (CG) scheme.

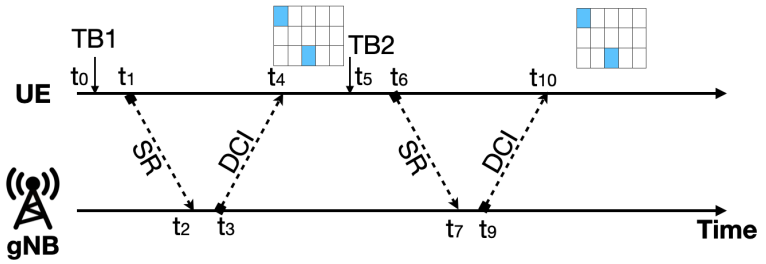

(B) 5G NR V2X Mode 1, Dynamic Grant (DG) scheme.

FIGURE 2.7: Mechanisms for the allocation of resources of Mode 1 of 5G NR V2X.

Fig. 2.7a shows an example of how resource utilization and scheduling are done when the CG scheme is applied. The UE does not need to send a resource request to the gNB, but waits for grants from it [53].

It is assumed that the UE may receive the CG granted resource at $t4$ (see Fig. 2.7a). This CG consists of a set of resources that will be periodically assigned to the UE at $t4$, $t8$, and $t11$. The time period is based on the interval between TBs indicated by the UE in the UE assistance information provided by the UE. To transmit TB1 and TB2, UE uses the reserved subchannels at $t4$ and $t8$, respectively. The CG scheme reduces the time it takes to transfer two TBs compared to the DG. However, the DG scheme can use the resource more efficiently when handling aperiodic traffic because the resource is allocated only when it is needed to forward the TB.

The case of the DG scheme is shown in Fig. 2.7b, an SR resource request is sent at $t1$ from UE to gNB. At $t3$, gNB responds with a DCI that points to the address of the resource that must be used at $t4$ to transmit TB2. The UE will repeat this operation at $t5$ by sending SR to gNB to transmit the next TB.

Three MCS tables are defined in Mode 1 that are used to select the appropriate MCS of each TB. gNB can support an UE to select one or more MCSs, or an MCS can be selected autonomously by the UE. The gNB can also configure an UE to employ one to three of the MCS tables. In this case, the UE can autonomously choose the modulation and coding from the configured table. UE points to the specified MCS and MCS tables for data transport in the first stage SCI [85].

5G NR V2X Mode 2 Resource Allocation

Similar to Mode 4 in LTE-V2X, vehicles in 5G NR V2X Mode 2 can autonomously (re)select and manage the SL resources needed for one or several transmissions from the preconfigured resource pool. The resource pool was pre-configured by gNB for the UEs located outside the cellular coverage area or operating without cellular infrastructure support.

Mode 2 can work by employing a dynamic scheme (DS) or semi-persistent scheduling scheme (SPSS), respectively. Like the DG, the DS allocates resources for one transmission and reserves resources for TB retransmissions. The reserved resource is an appointed resource that a UE reserves for incoming transmission by declaring it to surrounding UEs via the first stage of SCI. When SPSS is used, selections and reservations can be obtained for several TB transmissions [86].

It is essential to mention that the SPSS scheme can be activated or deactivated in a resource pool by preconfiguration. Mode 2 operates in the way of assigning resources for DS and SPSS. The DS is used to assign one resource to one TB. On the contrary, SPSS assigns resources for several consecutive TBs using Reselection Counter (RC). The time between the radio resources assigned for RC of TB transmissions using SPSS is known as the Resource Reservation Interval (RRI). The allowed values of RRI are 0, [1: 99], 100, 200, 300, 400 500, 600, 700, 800, 900, 1000 ms. It is essential to note that NR V2X Mode 2 provides greater flexibility to handle the necessities and features for various V2X applications by accepting the integer RRI values between 1 and 99, while LTE

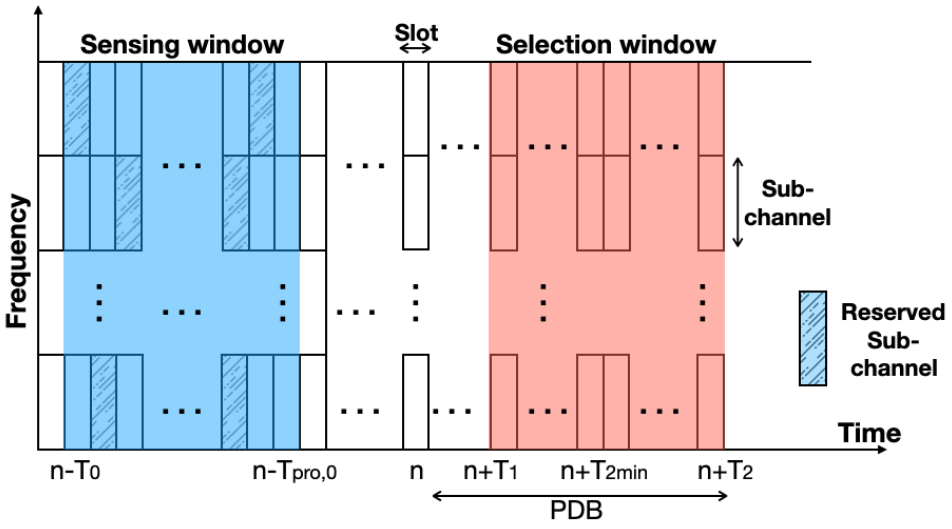

FIGURE 2.8: Sensing and selection windows in SL communication of 5G NR V2X Mode 2, when $PDB = T2$.

V2X Mode 4 supports RRI with the following values: 0, 20, 50, 100, 200, 300, 400, 500, 600, 700, 800, 900, 1000 ms. The UE can choose the RRI based on the current traffic. The established RRI also defines the RC randomly placed in an interval depending on the established RRI. If $RRI \geq 100$ ms, the RC is set at random within [5, 15]. If RRI<100 ms, the RC is set randomly within [5*S, 15*S] where S=100/max(20, RRI) (Section 5.22.1 in [87]).

UE can trigger resource selection in two cases: when a new TB is created and needs a radio resource for transmission and when the reserved resource does not handle the created TB.

For both SL resource selection schemes, the resource selection procedure can be presented in the following steps.

The UE should define the selection window of candidate resources for TB transmission. The resource candidates should be within the range of slots $[n + T1, n + T2]$, where n is the resource (re-)allocation request time slot. T1 represents the time slots required by an UE for the examination and selection of candidate resources for transmission. $T1$ is defined as equal to or smaller than the value $Tpro, 1$. $Tpro, 1$ equals 3, 5, 9 or 17 time slots for an SCS equal to 30 of 15, 30, 60 or 120 kHz, respectively. The value $T2$ is left to the implementation of UE to select within the range $T2min \leq T2 \leq PDB$, where PDB

indicates the Packet Delay Budget (in time slots). PDB is the highest latency within which the UE should transmit TB. PDB is set by the application that generates the packet. The value of $T2min$ is set according to the priority of the packet and the applied numerology. The value of $T2min$ should be included in the range within $\{1, 5, 10, 20\} \cdot 2\mu$ slots. Thus, the value of $T2min$ will be equivalent to $\{1, 5, 10, 20\}$ ms. Consequently, the minimum achievable latency of NR V2X Mode 2 is reduced to 1 ms compared to 10 ms in LTE V2X Mode 4 [67].

The UE must identify the addresses of candidate resources within the selected window. The time slot and adjacent subchannels L_{PSSCH} in the range $[1 : max(L_{PSSCH})]$ (where $max(L_{PSSCH})$ indicates the total number of subchannels in a single time slot) indicate in frequency these addresses of candidate resources.

The number $max(L_{PSSCH})$ varies depending on changes in traffic load (when congestion control mechanisms are needed). In the time between two consecutive UE transmissions, the UE senses the SL resources to recognize free or busy subchannels. The interval of the sensing window is ranging as in the previous step between time slots $[n - T0, n - Tpro, 0]$. $Tpro, 0$ is the time needed to find busy and free resources, which depends on applied numerology when a single time slot for the carrier spacing is 15 or 30 kHz and equal to two or four time slots when the carrier spacing is 60 or 120 kHz, respectively.

In the sensing operation, the UE decodes the first stage of the SCIs received from the surrounding UEs and determines their RSRP. The UE keeps the information on the monitored resources (the decoded first stage of SCI and the determination of RSRP) to decide which candidate resources in the selection window will be recommended when a new resource is needed [70].

Mode 2 defines two steps of resource selection processes for both selection schemes.

First, the candidate resources are identified within the selection window period. Candidate resources were indicated as reserved resources by a previous SCI in that slot or in the corresponding slot, and candidate resources that

feature a measured RSRP higher than the established threshold are excluded from the candidate resource list. The list of the remaining candidate resources from the resources in the selection window should be equal to or greater than X% of the total number of candidate resources in the selection window to move to the next step of resource selection. The RRC can configure the value of X to be set to 20, 35, or 50%. In case the required X-value is not achieved, the RSRP threshold is increased by 3 dB, and the last process is repeated.

Second, the UE can start the resource selection process to transmit and retransmit a packet using the list of identified candidate resources by randomly picking up the resource address from the remaining candidate resources. Additionally, the Resource Reservation Interval (RRI) is defined to exclude the address of resources from the candidate list based on previous SL measurements in slots. UEs transmit RRI in first-stage SCI. The first stage SCI carries the length of the time interval between two consecutive packet transmissions. UE that processes resource selection will use periodicity and assume periodic transmission during Q periods. This assumption allows for the identification and excluding of improper candidate resources in the list of resources in the selection window.

2.5 Summary

In this chapter, we have presented the background in vehicular communication in several parts. The first part presents an in-depth explanation of the concept of vehicular communication. In the second part, the ideas, parameters, and features of dedicated short-range communications based on the IEEE 802.11p standard are shown. IEEE 802.11p is the first standard that enables the exchange of information between vehicles on the road. The version of Cellular-Vehicle-to-Everything (C-V2V or LTE-V2X) standardized within 3GPP Releases 14 and 15 using the uplink LTE transmission method is characterized in the third part of this chapter with its concept, timelines, use cases, and features. Furthermore, this part includes a comparison between the LTE-V2X and IEEE

802.11p standards. Details of the New Radio air V2X interface (NR V2X), such as an overview, concepts, requirements, use cases, and resource allocation algorithms, are included in the last part of this chapter.

In the author's opinion, the general introduction on V2X communications presented in this chapter is a good basis for the main topics of this dissertation related to radio resource management that improves the reliability of V2X transmission as compared with the current solutions.

Chapter 3

Autonomous Resource Allocation for C-V2X Communications

3.1 Motivation

In this chapter, autonomous selection of resources for the C-V2X of LTE Mode 4 is considered. The Sensing-based Semi-Persistent Scheduling (S-SPS) method faces several serious problems, like half-duplex errors, hidden terminal errors, and packet/radio resource collision errors. C-V2X Mode 4 is a type of transmission in which decentralized resource allocation occurs when the cellular infrastructure is absent. Each vehicle is individually responsible for selecting and reselecting the resources for broadcasting. The S-SPS method is less reliable than the selection of resources in Mode 3, especially when the number of vehicles in the network is high, causing conflicts in resource usage between them.

S-SPS depends on the sensing process to assign free resources to the network vehicular transceivers. Still, this method fails to handle the packet /resource collision that appears when more than one vehicle selects the same resource allocation at the same time within the awareness range and when the number of resources is restricted in the awareness range.

This chapter is based on the articles [91] and [92] published previously by the author.

3.2 Challenges and Contributions

The challenges of the research work reported in this chapter can be summarized as follows.

- The present C-V2X Mode 4 relies on the history of sensed signals to make a list of free resources. Then each vehicle that generates its list decides which resources should be used when re-selection is needed, making the resources more limited in usage.
- The S-SPS method needs at least 20% of free resources in the sensed window to select the appropriate resource. This condition is not applicable when the number of vehicles is high (that is, when the number of vehicles is greater than 80% of resources in a CAM interval).
- Transmission with autonomous resource selection is blind, in the sense that the transmitter does not know whether the packet is correctly decoded or not. Therefore, this kind of communication needs to be more reliable.

Motivated by the above facts, a system-level simulation was first implemented to study the performance of the S-SPS, and then the author proposed a new algorithm called estimation and reservation resource allocation (ERRA) algorithm. The ERRA algorithm aims to improve system performance by decreasing the packet/resource collision ratio and increasing the packet reception ratio. Generally, the idea is that each vehicle lists all resource locations of the received packets with the same Random Counter (RC). In this way, each terminal can estimate which resource location will be accessible in the next resource selection to reserve and track it. Additionally, the vehicle that reserves this resource for the next broadcast will announce it to the surrounding terminals. The vehicle does not need to depend on the sensing process, which improves resource utilization.

Furthermore, the extension of ERRA (E-ERRA) also introduced in this chapter aims to solve the problem of the lost reserved resources when the vehicle

with pre-allocated resources has just left or appeared in the broadcast range before the reselection process. E-ERRA defines an alternative list of resources to use when this problem occurs. E-ERRA has proven to be a promising way to support efficient and reliable vehicular communications by choosing and announcing the next allocation of resources. The decrease in collision ratio (CR) and increase in packet reception ratio (PRR) shown in this chapter indicate that ERRA and E-ERRA perform substantially better than S-SPS in reliable broadcasting and resource allocation for vehicle transceivers operating in C-V2X Mode 4.

During the last few years, several researchers have studied and evaluated the performance of C-V2X Mode 4. Its system-level evaluation is described in [93], in which the packet reception ratio related to the distance between a transmitter and a receiver is investigated. Furthermore, the authors of [94] have published a valuable investigation and a comprehensive study on transmission errors in Mode 4. They have noticed such errors due to half-duplex, propagation, and packet collisions. The authors of [94] proposed that collision can occur depending on the performance of the link level and the distance between the transmitter and the receiver. To improve the collision avoidance algorithm, the authors assumed in [95] that the scheduling assignment and data packets are transmitted in different subframes for a single vehicle. Data packets are received according to the decoded scheduling assignment that indicates the positions of the vehicles. In [96] the physical layer performance of multiple access is studied in the case of a large number of vehicles. In [97], the number of neighbors in the awareness range and the packet reception ratio with the distance between transmitters and receivers are investigated. In [98] the S-SPS resource allocation algorithm is evaluated in terms of PRR as a function of the number of available subchannels.

3.3 Assumptions and Background

According to 3GPP, SC-FDMA is applied to support vehicular communication by representing radio resources in the time-frequency domain [99]. In the time domain, a subframe (two slots, 0.5 ms each) is defined as the minimum period for several groups of Resource Blocks (RBs). RBs occupy the 180 kHz band, and they are the smallest units of LTE resources. Each group of RBs constitutes a subchannel. The number of subchannels in one subframe should correspond to the number of bits in a CAM message and the selected modulation and coding scheme (MCS) [33], [100]. The number of subchannels η in one subframe is determined by the formula:

$$\eta = \left\lfloor \frac{RB_{TRB\_sf}}{RB_{SCH}} \right\rfloor \tag{3.1}$$

where RB_{TRB_sf} is the total number of resource blocks in a given frequency band, and the number of RBs in one subchannel is denoted by RB_{SCH}.

The maximum number of vehicles V_{Total} that can broadcast CAM messages without interference in the broadcast range for a given period of CAM messages T_{step} is determined by the expression:

$$V_{Total} = T_{step} \cdot \eta \tag{3.2}$$

Each vehicle transmits one CAM message in one cycle period and is to be received by all surrounding vehicles located in the broadcast range. Denote the transmit power of the broadcast vehicle V_i by $P_{tx,i,dB}$ [dB]. The path loss at distance $Dist$ can be written as $PL_{dB}(Dist)$ [dB], and the attenuation caused by obstacles is represented by shadowing SH [dB]. The power $P_{r,g,dB}$ of the signal received in vehicle V_g can then be formulated as follows:

$$P_{r,g,dB} = P_{tx,i,dB} - (PL_{dB}(Dist) + SH) \tag{3.3}$$

If we assume that there are N vehicles in the broadcast range of vehicle V_i, and

U vehicles are outside the range, then the signal-to-interference plus noise ratio γ_g at receiver V_g should be greater than the minimum signal-to-interference plus noise ratio γ_{min}, that is,

$$\gamma_{min} < \gamma_g = \frac{P_{r,g}}{\sum\limits_{x \in N \setminus i} P_{r,x} + \sum\limits_{y \in U} P_{r,y} + N_0} \tag{3.4}$$

where N_0 is the noise power on the receiver side, $P_{r,x}$ denotes the power of the interference signal originating from the xth transmitter placed in the transmission range of vehicle V_g. This interference generated by the vehicles that broadcast CAM messages using the same resources has the power (in dB):

$$P_{r,x,dB} = P_{tx,x,dB} - (PL_{dB}(Dist_{coll}) + SH) \tag{3.5}$$
$$\text{where } Dist_{max} \geq Dist_{coll}$$

The power in (3.5) is related to the signals that occupy the resources in which the collision has occurred and the distance $Dist_{coll}$ between the broadcaster and the receivers is less than the maximum broadcast range $Dist_{max}$ for vehicle V_g. Furthermore, let $P_{r,y}$ denote all powers of interfering signals from vehicles located outside the V_g broadcast range $Dist_{Interf}$.

$$P_{r,y,dB} = P_{tx,y,dB} - (PL_{dB}(Dist_{Interf}) + SH) \tag{3.6}$$
$$\text{where } Dist_{max} < Dist_{Interf}$$

and y ($y \in U$) is the index of these interfering signals.

3.4 Sensing-based Semi-Persistent Scheduling (S-SPS)

In C-V2X Mode 4, each vehicle is responsible for managing the available radio resources to broadcast its current status. The RC counter is decremented by one in each broadcast. In addition, when the RC reaches zero, a decision is

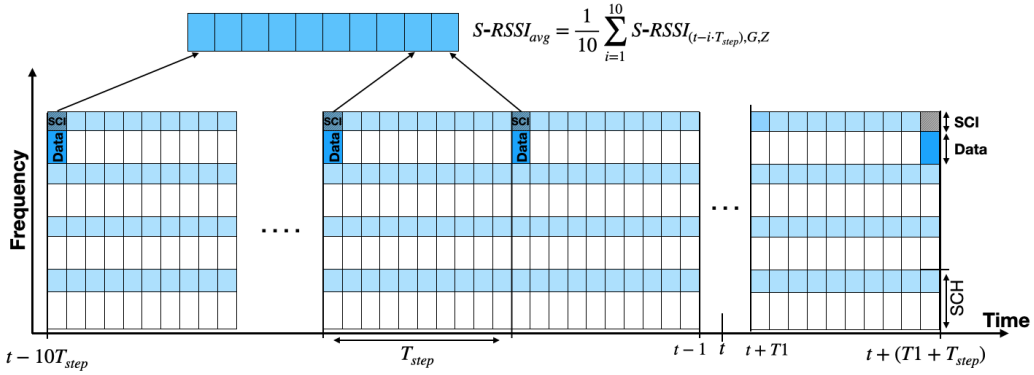

FIGURE 3.1: Single sub-frame resource candidate in the sensing procedure (SCI and transport block are coordinated in the adjacent subchannel).

needed about the selection of a new resource location with probability $1-p$ or keeping the same resource location with probability p. Furthermore, RC is generated in a specific range of integers depending on the periodicity interval of the CAM message, as follows. When the duration of the CAM cycle is equal to 100 ms, the RC range is selected from the interval [5, 15]. When the CAM cycle duration is equal to 50 ms, the RC range is selected from the interval [10, 30]. However, when the CAM cycle duration is 20 ms, the RC range is between 25 and 75.

The goal of S-SPS is to find future resources to be used in the next reselection process depending on the sensing process in the physical layer [101]. The sensed signals are reported to the higher layer for monitoring. The MAC layer asks the lower layers to send a sensing report when the last RC packet is sent in the subframe t. In addition, the physical layer extracts the resource locations of subchannel candidates in sensing windows that are saved in its buffer. The size of a sensing window is equal to the periodicity of the CAM messages (allowed latency). The saved sensing windows can be defined as $[t-1, t-10T_{step}]$ where T_{step} is the sensing window (see Fig. 3.1). Furthermore, 3GPP has proposed the $T1$ period in [101] as the reselection time process, $T1$ can take any value below the duration of four subframes.

The SPS process can be described in the following steps.

1. The link layer should monitor all subframes in the interval $[t-1, t-10T_{step}]$, where $t-1$ is the last received sidelink subframe.

2. In this step two lists should be created: $List_A$, which contains all subframe candidates that could be used in the next broadcast process, and an empty list $List_B$.

3. All candidates from $List_A$ that have Reference Signal Received Power (RSRP) higher than the established threshold should be excluded.

4. The number of remaining candidates should be greater than or equal to 20% of all candidates in $List_A$, otherwise Step 3 must be repeated with an increase in the threshold by 3 dB.

5. The remaining candidates with the average Sidelink-Received Signal Strength Indicator (S-RSSI) of the subchannels for the last $10T_{step}$ should be moved to the created list $List_B$. The average S-RSSI ($S\text{-}RSSI_{avg}$) can be calculated as follows:

$$S\text{-}RSSI_{avg} = \frac{1}{10}\sum_{i=1}^{10} S\text{-}RSSI_{(t-i\cdot T_{step}),G,Z} \tag{3.7}$$

   where G and Z indicate the subframe index and the subchannel index in the resource grid, respectively.

6. $List_B$ should be reported to the higher layers.

The main drawbacks of the S-SPS method are possible resource collisions when more than one RC counter of the vehicles being in the same broadcast range reaches zero and the same resource allocation is chosen. Some errors can also be the result of negligence in observing vehicles entering or exiting the coverage area.

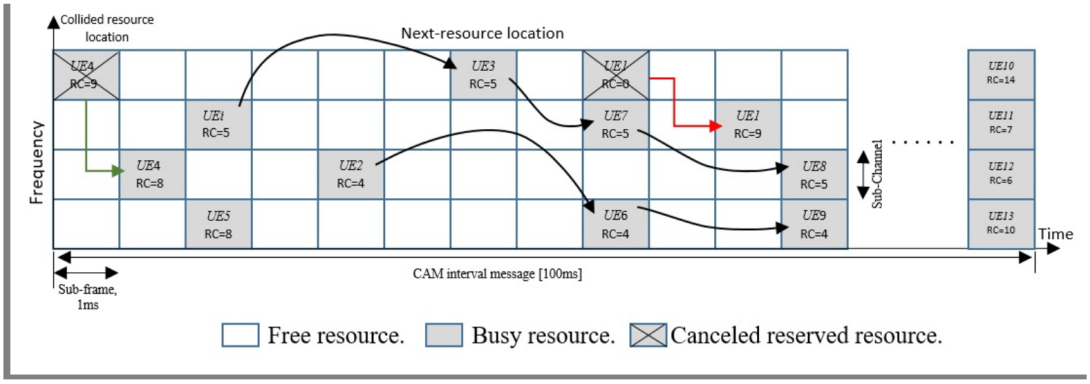

FIGURE 3.2: C-V2X Mode 4 ERRA scheduling.

3.5 ERRA Resource Allocation Algorithm

Despite the random selection of resources picked out from the lowest S-RSSI list, the S-SPS method fails to solve the problems that arise when more than one vehicle chooses the same sub-channel at the same time. It also fails when other vehicles have entered the awareness range with the same assigned resources. Consequently, miscarriages can appear (i.e., packet collisions, hidden terminal effects). The proposed algorithms handle these failures precisely.

The ERRA works in the following steps:

1. The UEi user equipment continuously analyzes the packets and takes notes of the decoded sidelink control information (SCI) received from the nodes contained in the awareness range.

2. Then, UEi keeps all packet locations that have the same RC value in the created $List_A$.

3. The estimated location of the resource is evoked from $List_A$ when RC_i reaches 5 and then UEi announces it as the next location of the resource, as shown in Fig. 3.2 (UEi, UE3, UE7, UE8).

4. The UEi constantly checks the predefined next location to ensure that it will be available in the next re-selection (see UE2 in Fig. 3.2).

5. When RC_i reaches zero, the next location of the resource selected by UEi is used for broadcast, and the new RC is generated (see UE1 in Fig. 3.2).

As mentioned before, a small extension for SCI (about two bytes) is needed to obtain a more reliable transmission and announce the next resource location when it is required, the RC, and the collision location if it exists. The proposed algorithm does not depend on the sensing method, and thus decreases packet collisions due to resource selection. In this section, we suggest that the RC does not generate in an entirely random way like S-SPS. The new RC should be compatible with other RC packet values broadcast in the same subframe (check UE10, UE11, UE12, and UE13 in Fig. 3.2). As a result, we avoid vehicles that broadcast on the same subframe to reserve the location of the same resource for the next reselected location. The availability of the next location or the current location of the UE*i* resources can change, either when a new UE enters the neighborhood with the exact location of the UE*i* resource (which is declared next location) or with the current location of the UE*i* resource. Thus, it results in packet collision (see UE4 in Fig. 3.2). The UEs disapprove and indicate to all other UEs colliding resource locations by extending the SCI data. This way, vehicles know when there is a collision in broadcasting.

3.5.1 Simulation Parameters and Environment

Using the MATLAB® platform, the system-level simulator was developed to compare the performance of the ERRA and S-SPS resource allocation/scheduling methods for C- V2X Mode 4. Matlab was integrated with the open source traffic Simulation Platform of Urban Mobility (SUMO) [102] to generate a more realistic environment for vehicles of different speeds and positions. Three simulation scenarios on motorways were investigated to obtain different values at different vehicle densities. The main parameters of the simulations for S-SPS and ERRA are the same, according to [48], as shown in Table 3.1. The parameters of the SUMO scenarios are summarized in Table 3.2. The positions started with different gaps between the UEs in each lane and constant acceleration and deceleration. The length of this gap was established according to the speed, as shown in Table 3.2. These models reflect realistic traffic patterns as vehicles overrun each other. These models can adequately model the potential packet

collision that could be increased when high vehicle densities are observed. The WINNER+B1 model was assumed to be a propagation model [103].

TABLE 3.1: System parameters.

Parameters	Values	Parameters	Values
Carrier Freq.	5.9 GHz	Bandwidth	10 MHz
PRB/sub-channel	12	S-CH/S-FR	4 S-CH
Tx. power	23 dBm	Awareness range	700 m
Shadowing	Log-normal	Std. dev.	3/LOS, 4/NLOS
MSC	QPSK. Turbo 1/2	Simulation time	6 sec.
Time step	100 ms	No. lanes	6
Packet size	190 byte	Tx, Rx, Antenna	1
Road length	2000 m	Tx, Vehicle speed	70,100, and 140 km/h

3.5.2 System Performance

The simulation was performed in 100-ms time steps for which the positions of all vehicles were calculated. For example, each vehicle calculates the performance of all messages received that are transmitted by other vehicles in the CAM interval. The Packet Reception Ratio (PRR) was adopted to calculate transmission reliability. The PRR for a signal receiver was calculated as follows.

$$PRR = \frac{CAM_{success}}{CAM_{total}} \tag{3.8}$$

where $CAM_{success}$ and CAM_{total} are the numbers of correctly decoded packets on the receiver side and the total number of CAM messages transmitted during the CAM interval within the awareness range, respectively. The packet

TABLE 3.2: Scenarios.

Parameters	Scenario 1	Scenario 2	Scenario 3
Min-Gap when 70, 100, and 140 km/h	35, 50.5, and 72 m	26, 38.6, and 54 m	15, 24.7, and 34.8 m
No. of vehicles in the network	253	235	550
Max. no. of vehicles in the awareness range	165	227	320

collision ratio can be obtained by the following expression:

$$CR = \frac{RS_{collided}}{RS_{total}} \tag{3.9}$$

where $RS_{collided}$, RS_{total} are the numbers of packets collided and the total number of packets during the CAM interval in the range of awareness, respectively.

3.5.3 Simulation Results and Discussion

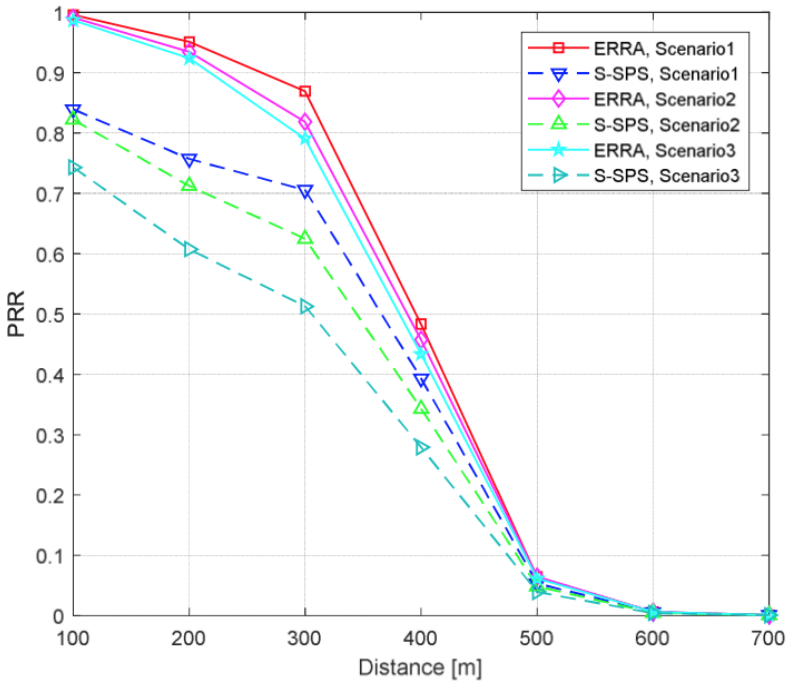

FIGURE 3.3: Packet reception ratio (PRR) of the S-SPS and ERRA for three scenarios (Table 3.2) in NLOS.

In Fig. 3.3, the packet reception ratios are drawn for Non-Line-of-Sight (NLOS) links as a function of the distance between transmitters and receivers for three scenarios (Table 3.2). They are examined for the standard method of C-V2X Mode 4 - S-SPS and ERRA. The performances of S-SPS and the proposed ERRA method show big differences. The PRR with ERRA is higher than for S-SPS by 18% and 19% for Scenarios 1 and 2, respectively, and approximately 25% in Scenario 3. In Fig. 3.4, the PRR for the Line-of-Sight (LOS) links shows better performance. The difference between the S-SPS method and

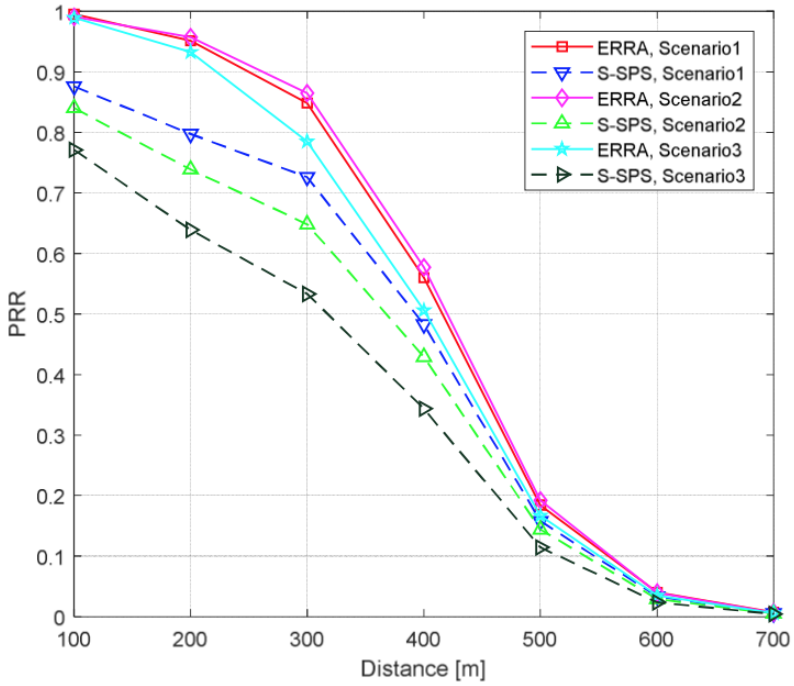

FIGURE 3.4: Packet reception ratio (PRR) of the S-SPS and ERRA for three scenarios (Table 3.2) in LOS.

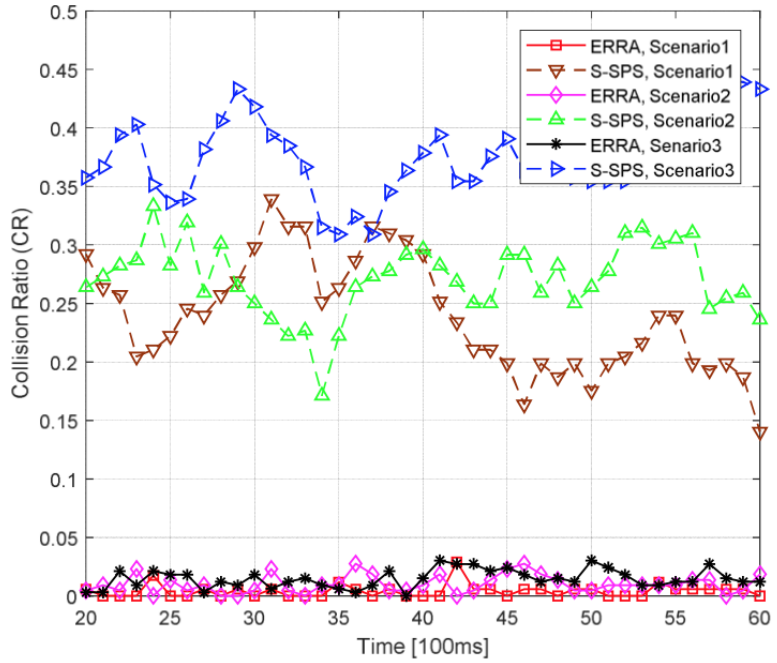

FIGURE 3.5: Collision ratio (CR) of the S-SPS and ERRA for three scenarios (Table 3.2) in NLOS.

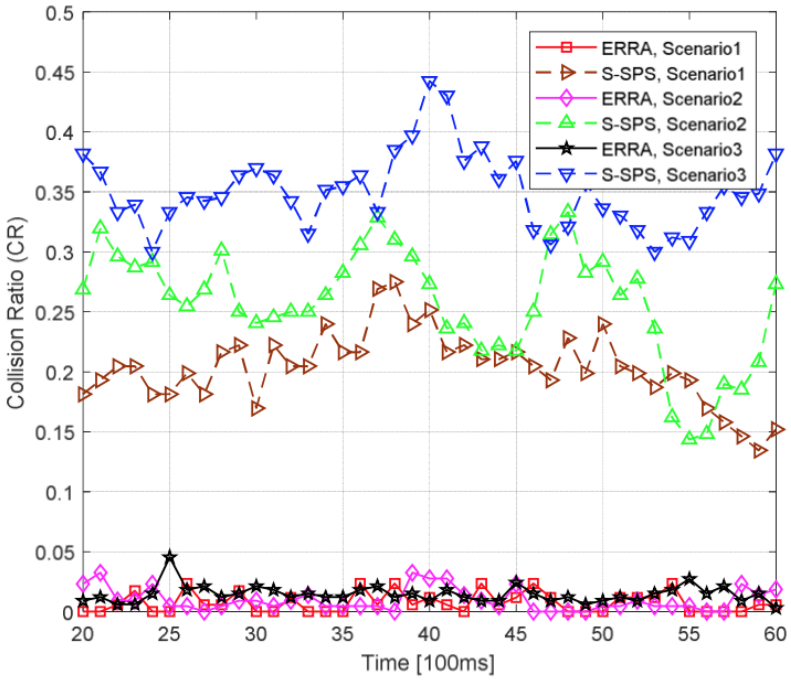

FIGURE 3.6: Collision ratio (CR) of the S-SPS and ERRA for three scenarios (Table 3.2) in LOS.

ERRA is rather constant up to 500 m, to become identical for both algorithms in 700 m. One can observe in Fig. 3.3 that for NLOS, the difference becomes negligible at 600 m.

In Figs. 3.5 and 3.6, exciting results of the collision ratio are shown. The results of CR for S-SPS are affected by the number of vehicles in the network. In Scenario 3, vehicles using S-SPS experience a higher packet collision ratio because the number of surrounding vehicles increases. For example, in the first scenario, the number of cars in the network is smaller than in the second. In each consecutive scenario, the number of vehicles has increased in the awareness range. This means that the probability of congestion with resource allocation has increased, and thus the reservation of resources will be more difficult.

Moreover, the collision ratio is significantly lower, and the performance is more stable with the proposed algorithm than with S-SPS. The CR for ERRA in LOS and NLOS is very low and more stable during vehicle travel time. Moreover, the collision ratio in ERRA is nearly zero in all scenarios.

3.6 Extended-ERRA (E-ERRA) Resource Allocation Algorithm

In this part of the chapter, we show the extension of ERRA aimed at solving the problem of losing reserved resources, which could arise when new vehicles enter the coverage area. These vehicles can broadcast the CAM messages by applying the resources used by other vehicles in the same area. The E-ERRA algorithm is characterized by creating a list of backup resource locations to use when needed. This constitutes the main extension of the ERRA algorithm. The steps of the E-ERRA process can be formulated as follows.

1. The link layer of vehicle V_x is responsible for monitoring signals in the last CAM interval $[t-1,\ t-T_{step}]$. The moment $t-1$ is the time of the last received subframe and T_{step} is the CAM interval.

2. The set $List_A$ is initialized by filling it with all subchannel candidates. The set $List_B$ is initialized as an empty set.

3. In this step, all candidates in $List_A$ that meet the following conditions listed below should be excluded from it:

   (a) The locations of the resource of the packets received from vehicles located in the awareness range that do not have the same value as the RC of V_x.

   (b) All candidates in a subframe that have an RSRP higher than the established threshold.

   (c) All candidates that have been reserved by other vehicles (if $P_{resv} = 1$, the location of the resource is reserved by another vehicle; otherwise, it is not).

   (d) All candidates indicated by other vehicles as collided resources.

   Note: All the remaining candidates in $List_A$ have RC values equal to the RC of V_x (RC_x).

4. All candidates in $List_A$ (in Step 2) that meet the conditions listed in Step 3 except condition a) have been collected in $List_B$.

5. The remaining candidates in $List_A$ should be organized as a FIFO queue according to the time of packet arrival.

6. When RC_x decreases and reaches a content equal to five, the first location of the resource in the queue will be fetched and announced as the location of the resource reserved in the next subframe and subchannel, and will be used in the next selection. The vehicle that uses the reserved location will activate the reservation bit ($P_{resv} = 1$) in the next broadcasting cycle.

7. Vehicle V_x should continuously check the availability of the next resource location until RC_x drops to zero. If the availability of the next resource location is decreased for any reason, the reserved resource location must be replaced by a resource location with the lowest S-RSSI in $List_B$ and should be announced again as the next resource allocation reselection. This way we avoid a conflict of resources used by new vehicles which have entered the awareness area and a vehicle checked out of the awareness range with reserved resources.

8. The next location of the resource shall be used when RC_x reaches zero and a new content of RC is generated. It is important to mention that the new range of RC should exclude all RC values of received packets in the same subframe to avoid additional resource allocation collisions.

3.6.1 System Level Simulation

The system-level simulation was developed to compare the performance of the E-ERRA and S-SPS algorithms. The MATLAB platform has been used to test both algorithms again, with the assumption of Poisson distribution applied to map the vehicles on the highway road. The Poisson distribution is parameterized by a single value, known as the rate parameter λ. In our case, λ is defined

as the ensemble average of the number of vehicles in a fixed length of the highway within a given time interval. Thus, a random variable that represents the number of vehicles in a given interval has the mean value λ. In the report [48], the average distance ρ between vehicles in a lane with vehicles moving at a fixed speed can be determined by

$$\rho = 2.5\,\text{sec} \cdot \frac{V_{kmph}}{3600} \cdot \alpha \tag{3.10}$$

where V_{kmph} is the absolute value of the vehicle speed. To ensure more flexibility in controlling the average distance between vehicles, we apply the scalar coefficient α selected from the interval $[0.2, 1]$. We call it the density factor. Furthermore, for fixed highway length $d_{highway}$, the Poisson distribution parameter λ can be found as [104]:

$$\lambda = \frac{d_{highway}}{\rho} \tag{3.11}$$

A random number that varies according to the Poisson distribution with the parameter λ determines the number of vehicles that are randomly distributed along the lane.

The main simulation parameters for both E-ERRA and S-SPS are the same and are shown in Table 3.3. In three lanes, different vehicle speeds are observed in each direction. The same vehicle density α is assumed. This model can adequately monitor the possibility of packet collision, which could increase when high vehicle densities occur. The WINNER+B1 model was assumed to be a radio propagation model [103].

3.6.2 System Performance

PRR and CR system performance is found using equations 3.8 and 3.9, respectively. Furthermore, the difference in packet collision ratios (D-CR) between

TABLE 3.3: Main settings.

Common parameters and settings	**Values**
Carrier frequency	5.9 GHz
Bandwidth	10 MHz
MCS	QPSK. Turbo 1/2
No. of subchannels per subframe	4
No. of PRB in each subchannels	12
Road length $\times$ road width (in each lane)	2000 m $\times$ 4 m
No. of lanes in each direction	3
Max. distance of the awareness range	700 m
Vehicle density factor	variable
Subframe duration	1 ms
Shadowing	Log-normal
Standard deviation	3
Absolute vehicle speed	70, 100, 140 kmph
Antenna gain at the receiver side	3 dB
Loss exponent	4
Noise power over 10 MHz	-95 dBm
Periodicity of CAM message	100 ms
Simulation time	100000 ms
CAM packet size	190 bytes

E-ERRA and S-SPS in the same broadcast range is computed as follows:

$$D\text{-}CR = CR_{S\text{-}SPS} - CR_{E\text{-}ERRA} \tag{3.12}$$

where $RS_{collided}$, and RS_{total} are the numbers of packets collided and the total number of packets during the CAM interval in the range of awareness, respectively, for each of the scheduling algorithms. *Average-CR* can be formulated as:

$$Average\text{-}CR = \frac{1}{Q}\sum_{i=1}^{Q} CR_{total,i} \tag{3.13}$$

where Q and $CR_{total,i}$ are the number of time steps in the simulation time and the total number of resource collisions in the ith time step T_{step}, $(i = 1, ..., Q)$;, respectively. Q can be found using the following expression:

$$Q = \frac{\text{Simulation time}}{T_{steps}} \tag{3.14}$$

3.6.3 Simulation Results and Discussion

In this subsection, we will show some simulation results to evaluate and compare the system-level performance of the proposed E-ERRA and S-SPS algorithms. Fig. 3.7 presents the packet reception ratios for the E-ERRA algorithm as a function of the distance between the transmitters and the receivers for the vehicle density factor α $[0.2, 0.3, ..., 1]$. The proposed E-ERRA algorithm shows very promising performance results with high stability at different vehicle densities in the packet reception ratio compared to the S-SPS performance shown in Fig. 3.8.

In Fig. 3.9, each step represents the average collision ratio for a specific vehicle density factor ρ. It can be observed in Fig. 3.9 that vehicle density substantially influences the performance of the S-SPS algorithm, whereas for the proposed E-ERRA algorithm the performance is much better and almost constant for the entire range of density factor ρ. In Fig. 3.10, the difference in collision ratios between the E-ERRA and S-SPS algorithms has been shown for some of the vehicle densities tested during the simulation time. This figure also indicates that the superiority of E-ERRA over S-SPS depends on vehicle density but remains meaningful.

3.7 Summary

In this chapter, the estimation and reservation of the resource allocation algorithm has been proposed to improve the performance of C-V2X Mode 4, and the performance results are compared with the S-SPS algorithm standardized by 3GPP. Both methods were simulated using Matlab that was integrated with SUMO package. Simulation was carried out for three scenarios for a more realistic environment of the traffic densities of vehicles. The simulations showed significant performance differences in PRR and CR between S-SPS and the proposed algorithm. The impressive result is that the collision ratio for the proposed algorithm is much lower than that for S-SPS. It is nearly zero and is stable. Packet collisions are also stable for different vehicle traffic densities.

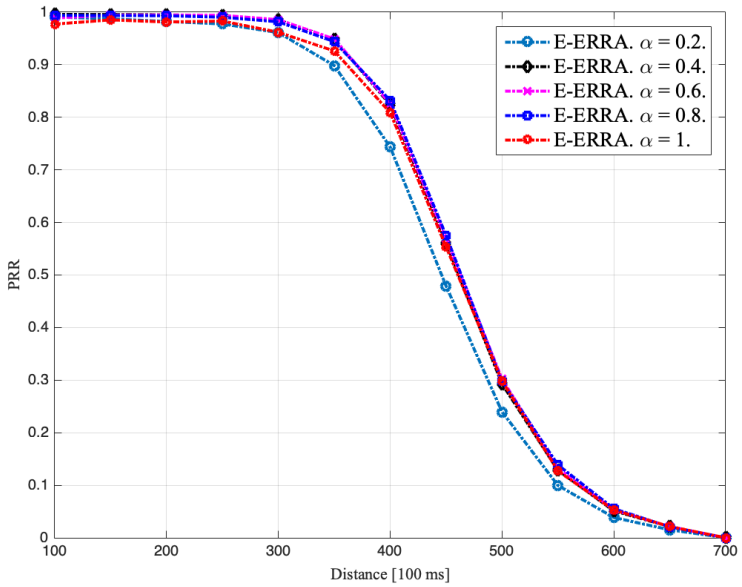

FIGURE 3.7: The packet reception ratio of E-ERRA algorithm vs. distance.

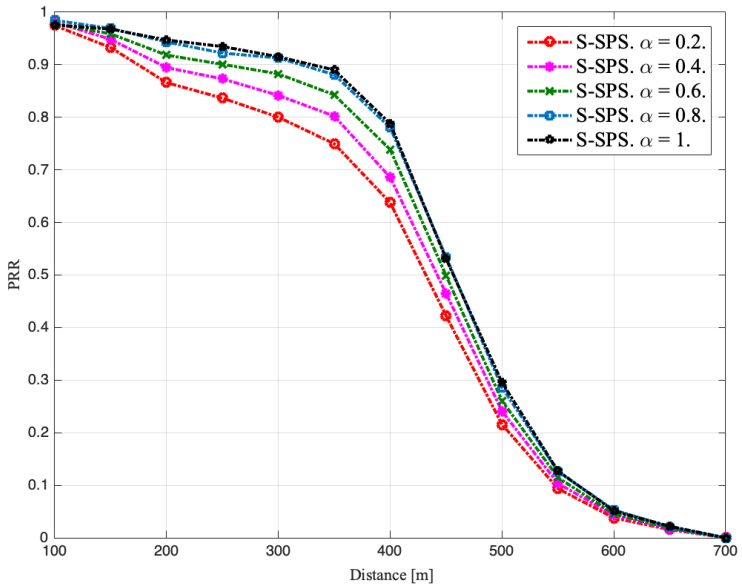

FIGURE 3.8: The packet reception ratio of S-SPS algorithm vs. distance.

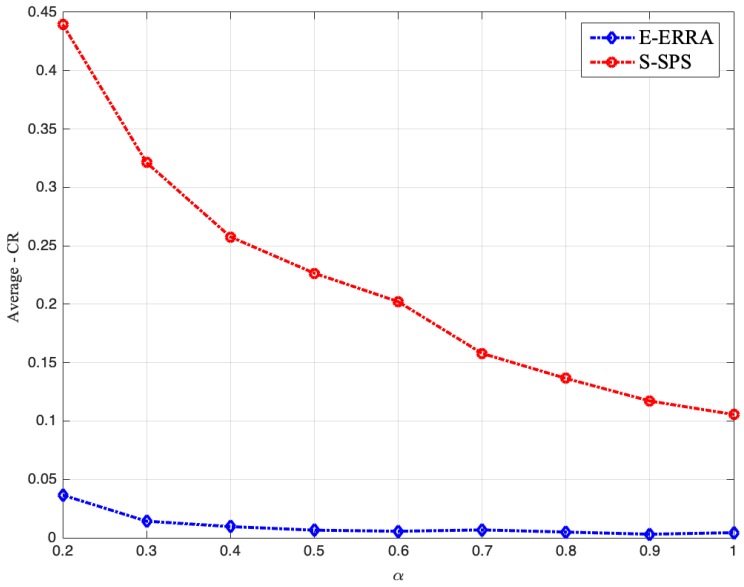

FIGURE 3.9: The average collision ratio vs. the vehicle density factor.

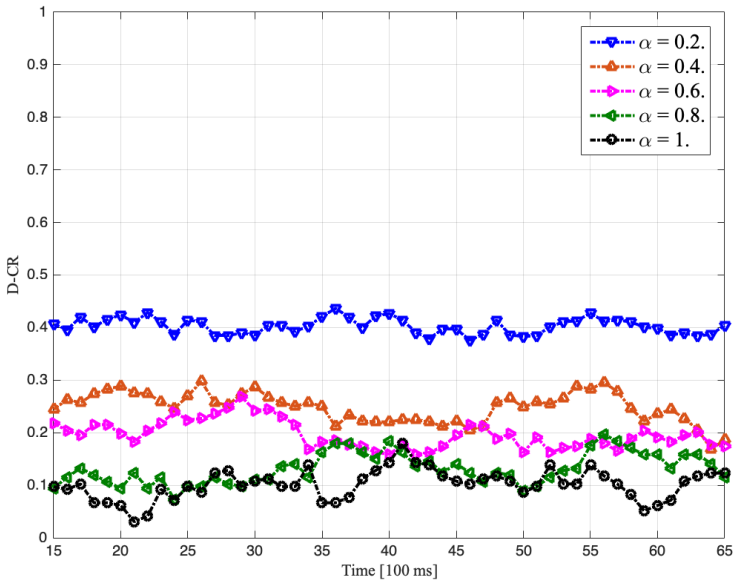

FIGURE 3.10: The performance difference in collision ratio between S-SPS and E-ERRA algorithms.

The S-SPS result in Scenario 3 is the worst case in this simulation because the highest number of vehicles leads to a higher probability of packet collision. Furthermore, the extended estimation and reservation of the resource allocation (E-ERRA) algorithm has been introduced in this chapter.

Subsequently, the E-ERRA algorithm was developed to improve the performance of resource allocation in C-V2X Mode 4 to solve the drawback of the lack of tracking of the reserved resources in the ERRA algorithm. As we have noticed, this problem is caused by the departure of vehicles with reserved resources from the awareness area or the entry of new vehicles into this area. These vehicles can cause a resource collision with already reserved resources.

The system performance of the E-ERRA algorithm is compared with the S-SPS algorithm for different vehicle densities. The simulation results obtained show a significant improvement in terms of PRR, D-CR, and average CR of the proposed E-ERRA algorithm compared to the S-SPS algorithm. The performance in terms of PRR of E-ERRA is higher than that of S-SPS, and we observe that CR is very low when E-ERRA is applied. The impressive performance in the average CR for different vehicle densities also results in high stability and reliability in solving the problem of dropped resources in the E-ERRA algorithm compared to S-SPS. In contrast, the latter is highly affected by the number of vehicles on the network.

Chapter 4

Resource Reselection with Adaptive Modulation Algorithms

4.1 Motivation

This chapter describes the results of investigations of autonomous resource re-selection for C-V2X Mode 4 applied in LTE when the S-SPS algorithm is applied, despite its drawbacks analyzed in Chapter 3. The system-level performance of the S-SPS algorithm is studied for some specific modifications proposed by the author. The S-SPS with Adaptive Modulation (AM) and Adaptive Modulation and Collision Detection (AMCD) resource re-selection algorithms are the algorithms newly proposed to improve the packet reception ratio and reduce resource collision ratio. It is known that S-SPS faces failures in resource re-selection and causes collision problems when multiple transmitters re-select the same resource at the same time or when channel load is increased for the given transmission range. In the literature, adaptive modulation has previously been introduced to solve this collision problem in IEEE 802.11p by managing Distributed Congestion Control (DCC). The AM and AMCD algorithms proposed in this chapter for C-V2X Mode 4 take into account the Channel Busy Ratio (CBR) and the probability of resource re-selection P to solve the channel load collision and resource collision problems by broadcasting the collided resource locations to announce the source of these collisions. It is shown that

AMCD is a promising method of maintaining efficient and reliable vehicular communications by re-selecting resources with proper modulation when RC counter applied in the MAC layer reaches zero and when the current resource is assigned as a collided resource by surrounding vehicles. The AMCD algorithm shows better performance than the AM algorithm in resource reselection, and is more reliable in broadcasting awareness messages.

This chapter is based on the published article [105].

4.2 Challenges and Contributions

As mentioned earlier, the S-SPS method uses a sensing strategy to avoid resource collision in the same broadcast range. However, the sensing strategy has shown limited efficiency when the density of vehicles increases or when two or more vehicles choose the same resource simultaneously. When the traffic density in the broadcasting range exceeds the established threshold of available resources in Mode 4, DCC has been suggested to balance the channel load. This balance can be achieved using one of the following options: dropped packet retransmission, dropped packet transmission, adaptation of the Modulation and Coding Scheme (MCS) or adaptation of transmission power [37].

As already mentioned, this chapter focuses on autonomous scheduling of resource allocation and resource collision avoidance in Mode 4 with varying channel load. We propose adaptive power broadcasting with AM and AMCD as resource reselection algorithms taking into account CBR and probability of resource reselection P with the range of awareness under control. Furthermore, vehicles using AMCD detect conflicting resources and announce the collided resource to surrounding vehicles. AM and AMCD algorithms are proposed to avoid overloading the channel above its capacity when high CBR has been observed and when resource collision in the same awareness range has been detected.

The main contributions in this chapter help to avoid channel capacity overloading when the CBR is high and to avoid resource collisions in the same

awareness range. A highway scenario with five different vehicle density zones has been set to evaluate system performance in terms of PRR and CR for Mode 4 in AM and AMCD resource reselection algorithms.

Many research groups have investigated solutions to the collision problem. In [107], Bazzi investigated Distributed Congestion Control (DCC) in IEEE 802.11p and Sidelink C-V2X. In [108], DCC algorithms were proposed for the 802.11p standard to avoid resource collisions and keep the level of traffic density below the specified threshold based on the Channel Busy Ratio (CBR). These algorithms apply adaptation to Transmission Power Control (TPC-DCC), Transmit Rate Control (TRC-DCC), and Transmit Data rate Control (TDC-DCC). In TPC-DCC, the output power is changed to adjust the current channel load. The consequence of this is that vehicles further away from the broadcaster will experience a reduced CBR [109]. TRC-DCC increases the time interval between two packets for a vehicle to avoid channel overload [110]. TDC-DCC is a mechanism that can reduce CBR by increasing the MCS order. This mechanism can increase the number of resources and therefore reduce the channel transmission range and CBR [111].

4.3 Assumptions and Background

As we have already presented in Chapter 2, C-V2X features SC-FDMA as a modulation technique to support the 10 and 20 MHz bandwidth channels. As mentioned in Section (3.3), the channel is divided into groups of Resource Blocks (RBs) to form subchannels. Each RB contains 12 subcarriers that span 180 kHz. Two slots (0.5 ms each) form a subframe as the smallest time unit for resource assignment. Four subsequent OFDM symbols contain DMRSs, enabling the estimation of the channel and Doppler effect at high speeds of vehicles. Furthermore, the last subframe symbol is used as a guard symbol for timing adjustments (see Fig. 4.1).

CBR is found using the calculation of the busy subchannel plus the number of subchannels in the same subframe, divided by the maximum number of

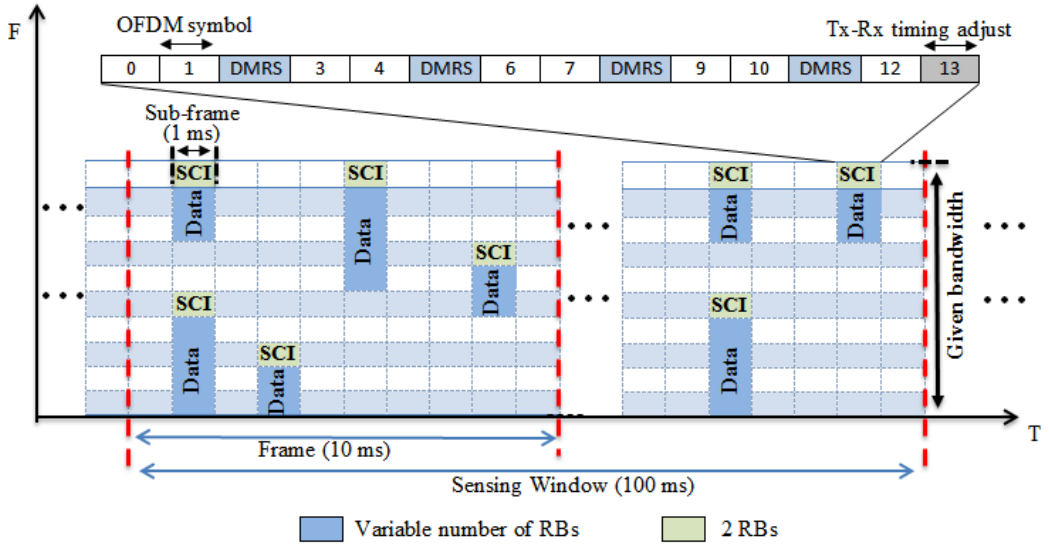

FIGURE 4.1: Resource grid and sensing window for C-V2X Mode 4 for non-fixed sub-channel size

vehicles in the same broadcasting range V_{max}. CBR calculation is given by the following expression:

$$CBR = \frac{S_{busy} + S_{sf}}{V_{max}} \tag{4.1}$$

where S_{busy} is the number of resources that experience a signal-to-interference plus noise ratio γ higher than the minimum allowed signal-to-interference plus noise ratio $\gamma_{\min}$, and S_{sf} is the number of all subchannels in the same subframe, respectively.

It is worth mentioning that the smallest number of RBs in one subchannel is assumed in this work to calculate CBR. The broadcasting range can be estimated by the following steps:

Step 1: Calculate the coding rate C_{rate} for the desired amount of data N_{Bits} as follows:

$$C_{rate} = \frac{N_{Bits}}{2RB_{SCH}N_{symbols}N_{SC}N_{element}} \tag{4.2}$$

where $N_{symbols}$, N_{SC}, and $N_{element}$ are the number of symbols carrying the desired information that is equal to 9, the number of subcarriers in an RB that is equal to 12, and the number of bits per symbol, respectively.

Step 2: Calculate the spectrum efficiency ζ [b/s/Hz]

$$\zeta = \frac{N_{Total} N_{SC} N_{element} C_{rate}}{T_{Subf} RB_{band}} \tag{4.3}$$

where N_{Total}, T_{Subf}, and RB_{band} are the total number of symbols in a subframe equal to 14, the time duration of a subframe equal 1 ms, and the bandwidth of an RB equal 180 kHz, respectively.

Step 3: Calculate the minimum signal-to-interference plus noise ratio $\gamma_{\min}$

$$\gamma_{\min} = 2^{\frac{\zeta}{1-\Gamma}} - 1 \tag{4.4}$$

where Γ is the expected implementation loss that is assumed to be 0.6 [106].

Step 4: Calculate the maximum awareness range D_{max} as

$$D_{\max} = \left[\frac{P_{tx} G_r}{\gamma_{\min} P_{ref} PL_{loss}} \right]^{\frac{1}{\alpha}} \tag{4.5}$$

where P_{tx}, G_r, P_{ref}, and PL_{loss} are the broadcast power, receiver antenna gain, reference path loss for 1 m, and the noise power for one subchannel, respectively. The path loss exponent is denoted by α.

The interference in the received signals is used to calculate γ, which is a combination of two types of signals. These interference signals differ in transmitted power and in the number of resource blocks. γ_i should be greater than $\gamma_{\min}$ to allow decoding in the ith receiver $(i = 1, ..., N)$, where N is the total number of vehicles in the awareness range. The value of γ_i can be calculated using the following expression:

$$\gamma_{min} < \gamma_i = \frac{P_{r,i}}{\sum\limits_{x \in N \setminus i} P_{r,x} + \sum\limits_{y \in N \setminus i} P_{r,y} + N_0} \tag{4.6}$$

where $P_{r,i}$, and $P_{r,x}$ are the received power of the desired signal with index i and the interference signal with index x with the same transmission power and the number of RBs as the desired signal, respectively, while $P_{r,y}$ is the

interference signal with index y with different power and different number of RBs compared to the desired signal. The power of the received signal in dB $P_{r,dB}$ can be found by the following equation:

$$P_{r,dB} = P_{tx,dB} - (PL_{dB}(D) + SH) \tag{4.7}$$

where $P_{tx,dB}$, $PL_{dB}(D)$, and SH are the transmitted power, the path loss when the distance between the broadcaster and receiver is equal to D, and the shadowing in dB, respectively.

4.4 AM Resource Reselection Algorithm

The algorithm, presented in detail in the form of a pseudo-code in Algorithm 1, can be described as follows. When the RC value reaches zero and $1 - P$ is higher than P, the new selected resource address will be the location of the resource that has the lowest $S\text{-}RSSI_{avg}$ and an appropriate number of RBs in the list $List_B$. Otherwise, the same subframe and subchannel are considered for the next transmission cycles. The decision about the applied modulation size will be made when RC reaches zero and the CBR is higher or lower than the upper or lower threshold boundaries. Furthermore, when a vehicle enters a different density zone with a higher or lower threshold boundary than the current one, the modulation order and the higher/lower threshold boundaries will be changed according to the new calculated CBR (see Fig. 4.1). Transmission power will be increased simultaneously with modulation size to keep the same broadcasting range when the CBR is increased to a higher value than the upper threshold, and vice versa. The value of P has been assumed to change with the CBR change, respectively. In other words, when the CBR increases, P decreases and vice versa. A new RC value will then be generated randomly according to the upper and lower value ranges $R1$ and $R2$, respectively. The time point of the last broadcast, the subframe, and the subchannel that should be used in the broadcast are indicated by t_{last}, $txSub_f$, and $txSub_{ch}$, respectively.

Algorithm 1: AM re-selection of resources.

Input: $RC, CBR, MCS_i, t_{last}, txSub_f, txSub_{ch}, R1, R2$
Output: $txSub_f, txSub_{ch}, RC, MCS, P_{tx}$

while $TRUE$ **do**
  if $t == t_{last} + T_{step}$ **then**
    $txSub_f(txSub_{ch})$
    $txSub_{ch} \leftarrow txPacket$
    $RC = RC - 1$
    if $RC == 0$ AND $1 - P > P$ **then**
      if $CBR >= thr_{upper}$ **then**
        $MCS = MCS_{i,+order}$
        $P_{tx} = P_{+tx}$
      else if $CBR < thr_{lower}$ **then**
        $MCS = MCS_{i,-order}$
        $P_{tx} = P_{-tx}$
      else
        $MCS = MCS_i$
        $P_{tx} = P_{tx}$
      end if
      Call Resource ($List_B$)
      if $MCS \neq MCS_i$ **then**
        $txSub_f = List_B(Sub_f)$
        $txSub_{ch} = List_B(Sub_f(Sub_{ch}))$
        $RC = random(R1, R2)$
      end if
    end if
  else if $RC == 0$ AND $1 - P <= P$ **then**
    $txSub_f = txSub_f$
    $txSub_{ch} = txSub_f(txSub_{ch})$
    $RC = random(R1, R2)$
  end if
end while

4.5 AMCD Resource Reselection Algorithm

The adaptive modulation size and collision detection algorithm is a new resource reselection algorithm that is proposed to avoid or eliminate resource collision in C-V2X Mode 4. The AMCD algorithm is applied when the RC value reaches zero or the location of the used resource has been marked as a collided resource ($Col = True$) by the surrounding vehicles. In Algorithm 2, the instantaneous time of the last CAM broadcast, modulation size, transmission power, and the upper and lower range of RC values applied during generation are denoted as t_{last}, MSC_i, $P_{i,tx}$, $R1$, and $R2$ respectively. The proposed subframe and subchannel are denoted by $txSub_f$, and $txSub_{ch}$, respectively, as before.

The algorithm, presented in detail as a pseudocode in Algorithm 2, can be described as follows. New resource reselection can occur calling the candidate with the lowest $S\text{-}RSSI_{avg}$ in the list $List_B$ with the appropriate number of RBs when the RC value reaches zero and $P - 1$ is higher than P, or when the used resource has been assigned by the surrounding vehicles as a collided resource. Furthermore, it is assumed that the value of P changes appropriately with the CBR change. Otherwise, the transmission will take place using the current resource location. The MCS order and the transmission power could be specified depending on the CBR value. If the CBR moves to values higher or lower than the boundary thresholds, it is necessary to consider increasing or decreasing the order of the MCS and the transmission power (see Fig. 4.1). Furthermore, if the used resource is marked as a collided resource before the RC reaches zero, the resource reselection will be performed without a new RC value.

Algorithm 2: AMCD re-selection of resources

Input: $RC, CBR, t_{last}, MCS_i, Col, MSC_i, P_{i,tx}, R1, R2$
Output: $txSub_f, txSub_{ch}, RC, MCS, P_{tx}$

while $TRUE$ **do**
  if $t == t_{last} + T_{step}$ AND $Col == False$ **then**
    $txSub_f(txSub_{ch})$
    $txSub_{ch} \leftarrow txPacket$
    $RC = RC - 1$
    if $RC == 0$ AND $1 - P > P$ **then**
      if $CBR >= thr_{upper}$ **then**
        $MCS = MCS_{i,+order}$
        $P_{tx} = P_{+tx}$
      else if $CBR < thr_{lower}$ **then**
        $MCS = MCS_{i,-order}$
        $P_{tx} = P_{-tx}$
      else
        $MCS = MCS_i$
        $P_{tx} = P_{tx}$
      end if
      if $MCS \neq MCS_i$ **then**
        $txSub_f = List_B(Sub_f)$
        $txSub_{ch} = List_B(Sub_f(Sub_{ch}))$
        $RC = random(R1, R2)$
      end if
    end if
  else if $RC == 0$ AND $1 - P <= P$ **then**
    $txSub_f = txSub_f$
    $txSub_{ch} = txSub_f(txSub_{ch})$
    $RC = random(R1, R2)$
  else if $Col == True$ **then**
    Call Resource ($List_B$)
    $txSub_f = List_B(Sub_f)$
    $txSub_{ch} = List_B(Sub_f(Sub_{ch}))$
  end if
end while

4.6 System Scenario and Setting

A system-level simulation has been run for a highway scenario with different vehicle density zones (see Fig. 4.2) in order to test and compare S-SPS with AM and AMCD resource reselection algorithms. Six lanes, three in each direction, with a fixed width for each lane, have been modeled using the MATLAB® platform. Poisson distribution is used to distribute vehicles on the highway. In this work, similarly as in Chapter 3, Section 3.6.1, the Poisson distribution rate parameter λ has been defined as the ensemble average of the number of vehicles on a fixed highway length in a given period according to (3.10) and (3.11).

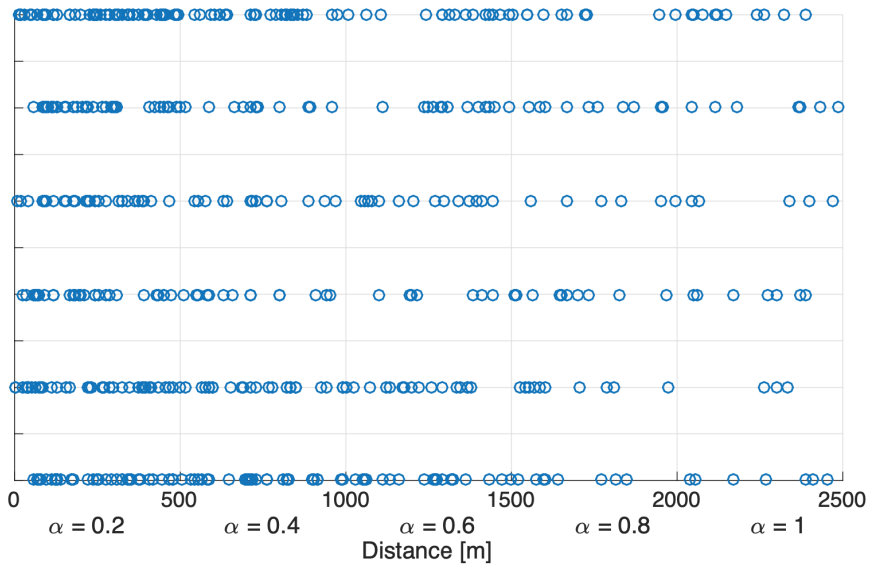

FIGURE 4.2: Highway environment with different vehicle density zones.

Throughout the simulation time, in each T_{step}, each vehicle continuously calculates CBR to decide the next location of the resources and transmission parameters. The main setting of the simulation is summarized in Table 4.1. CBR, $\gamma_{\min}$, D_{max}, $P_{tx,dB}$, and γ are calculated according to equations (4.1), (4.4), (4.5), (4.6), and (4.7), respectively. The WINNER+ B1 channel model [103] has been applied as the propagation model.

TABLE 4.1: Main simulation settings.

Common Parameters and Settings	**Values**
Carrier frequency	5.9 GHz
Bandwidth	10 MHz
Broadcast power	23 dBm, and 30 dBm
MCS order	8, and 14
No. of subchannels per subframe	Variable
No. of PRB in each subchannel	6, and 12
Road length $\times$ Road width (in each lane)	2500 m $\times$ 4 m
No. of lanes in each direction	3
Vehicle density factor in each zone	0.2, 0.4, 0.6, 0.8, and 1
Subframe duration	1 ms
Shadowing	Log-normal
Standard deviation	3
Absolute vehicle speed	70,100,140kmph
Antenna gain at receiver side	3 dB
Loss exponent	4
Reference path loss for 1 m	41.34 dB
Noise power over 10 MHz	-95 dBm
Periodicity of CAM message	100 ms
CAM packet size.	190 bytes

4.7 Simulation Results

System level simulations have been performed to investigate the proposed algorithms in terms of PRR, and CR that were described previously in Section 3.5.2.

The simulation results, comparison, and performance differences between AM and AMCD resource reselection algorithms are shown in this section. The same simulation scenario is applied to broadcast CAM packets by vehicles in two MCS orders depending on probability P and CBR. Fig. 4.3 shows the PRR for these vehicles that used the MCS order equal to 8 or 14. The AMCD resource reselection algorithm shows better results in receiving packets than the AM algorithm. 97-99% of all broadcast packets were correctly received in the AMCD algorithm when the distance between transmitters and receivers was shorter than 200 m. However, 90-98% of all broadcast packets were correctly received when the AM algorithm was applied for the same distance. The AMCD algorithm with an MCS order equal to 8 achieved PRR performance

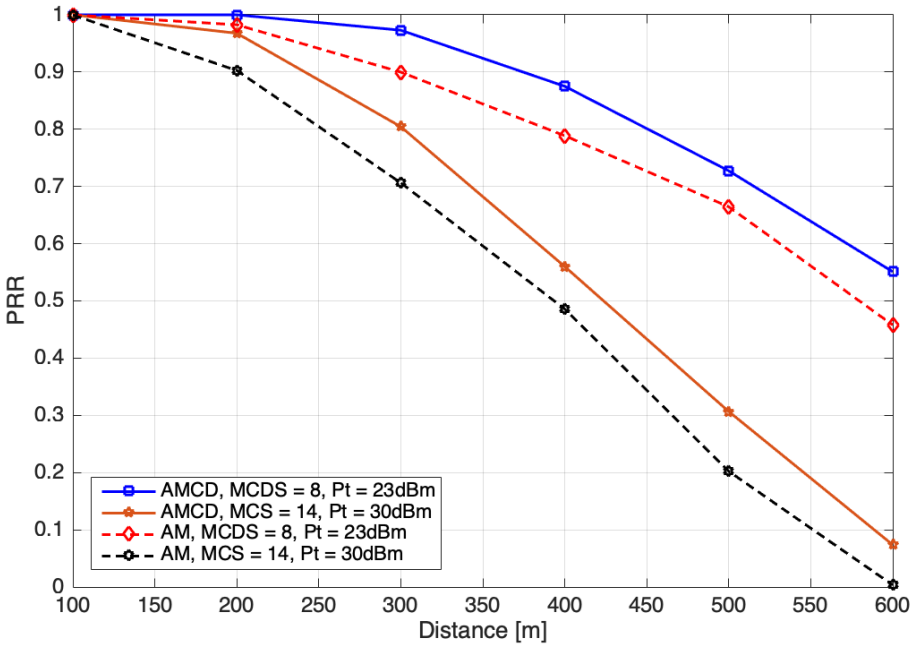

FIGURE 4.3: The packet reception ratio with MCS equal to 8 and 14 when the AM and AMCD algorithms are applied.

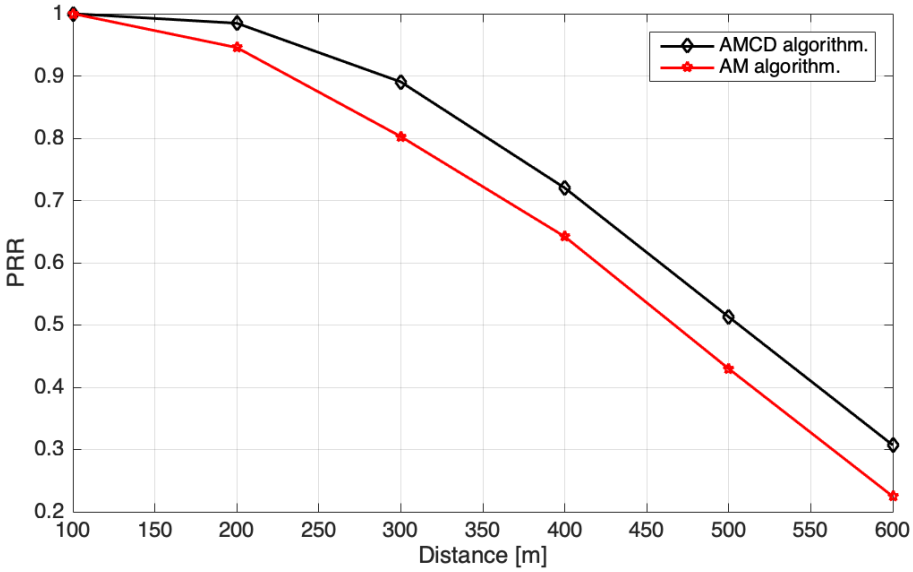

FIGURE 4.4: System packet reception ratio when AM and AMCD algorithms are applied.

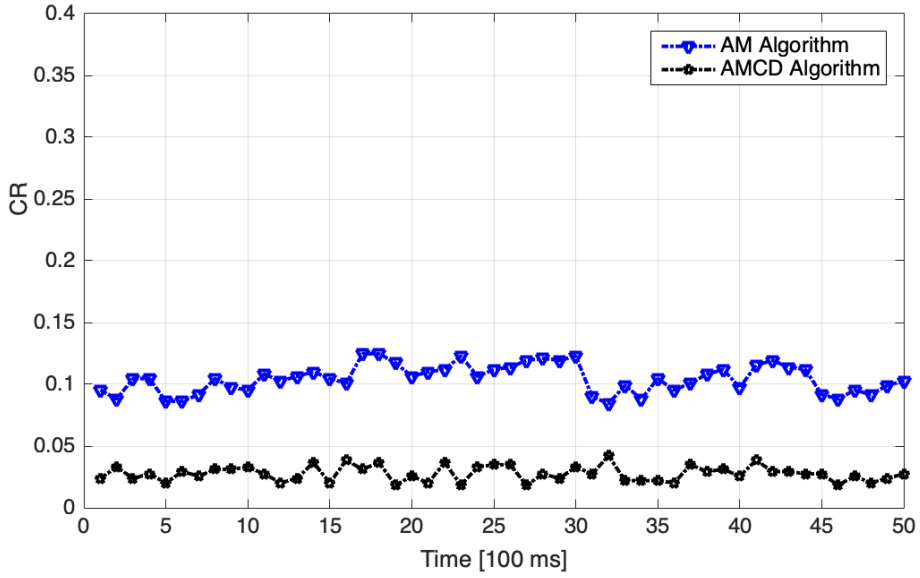

FIGURE 4.5: Resource collision ratio for AM and AMCD algorithms.

greater than 90% when the distance was shorter than 380 m, where it dropped to 80% for the AM algorithm. For both algorithms, the PRR curves sloped down when the MCS order was equal to 14 compared to the MCS order equal to 8, ending with a 50% difference when the distance was equal to 600 m. The PRR curves of AMCD maintain a PRR performance of about 10% higher than that of AM when the same MCS order was applied. The PRR performance of the system of both algorithms is shown in Fig. 4.4. The AMCD algorithm starts with a performance of 4% higher when the distance between transmitters and receivers is 200 m, as compared with the AM algorithm, and retains a 10% difference when the distance is in the range 300 - 600 m.

In Fig. 4.5, the AMCD algorithm shows a lower collision ratio compared to the AM algorithm. During the simulation time interval, the system that applied AMCD detected a collision ratio lower than that with AM by approximately 8-15%. The AMCD resource reselection algorithm shows promising performance results with an error less than 5% during the simulation time.

4.8 Summary

In this chapter we reported on the application of Adaptive Modulation (AM) and Adaptive Modulation and Collision Detection (AMCD) resource reselection algorithms to improve the Sensing-based Semi-Persistent Scheduling (S-SPS) resource reselection in C-V2X Mode 4 to solve the resource collision problem for autonomous resource reselection. The resource collision problem is created when two or more vehicles in the same awareness area choose the same resource simultaneously or when the channel load becomes higher than the maximum allowed threshold. We compared the performance of both algorithms in a highway scenario consisting of five different density zones of vehicles. Choosing the appropriate MCS order depends on the CBR in the AMCD algorithm and the collided resources that are announced by the surrounding nodes to warn the transmitter that uses this collided resource. The AMCD algorithm has a higher resource reselection reliability than the AM algorithm, which adapts the MCS order depending on P and CBR. The simulation results obtained show a better improvement in the Packet Reception Ratio (PRR) and excellent Collision Ratio (CR) of the proposed AMCD algorithm compared to the AM algorithm.

Chapter 5

Congestion Control in C-V2X Autonomous Resource Selection

5.1 Motivation

In this chapter, the author suggests a decentralized congestion control and transmission power control mechanism (TPC-DCC) with an adaptive threshold for the received signal as a combination method to decrease channel load in the network. Furthermore, in this chapter, a novel channel load adjustment is introduced. The new adjusting algorithm is based on a constant difference between the upper and lower boundaries of channel load at each level to handle channel overload and provide greater flexibility using DCC mechanisms. The interactions of the proposed algorithm with the S-SPS and E-ERRA algorithms that were previously proposed in Section 3.6 are investigated. The results indicate that the performance of the system can be substantially improved when transmission power and the reception threshold are adaptively matched to the proposed channel load adjustment.

This chapter is based on the paper (A.3, [1]) which at the time of preparing this dissertation was during the review process.

5.2 Challenges and Contributions

As mentioned in Section 4.1, an increase in channel load in the given band in a vehicle broadcast range can cause resource collisions and hidden nodes, especially when the number of broadcasters is higher than the limited number of resources. The restricted number of resources depends on several factors, such as the data rate and the amount of data related to the number of resource blocks in each subchannel [112], the transmission rate and the coverage area resulting from the transmission power.

In [108], DCC mechanisms for VANET communication are proposed to handle the increased channel load problem by adapting the parameters of the physical layer through multiple levels of channel load. However, the technical report [108] did not clearly explain the mechanism for selecting the resources for packet transmission when the channel load is high and changes rapidly. Generally, little attention is paid in the literature to investigating interactions between DCC and scheduling methods of C-V2X communication. The DCC mechanisms feature three parameters that adjust the mechanisms to regulate the channel load. These mechanisms can adjust the transmission power, the data rate, or transmission rate based on CBR. Furthermore, the DCC mechanism is characterized by three states: relaxed, active, and restrictive states. The active state also contains one or more active levels that differ in physical parameters. In this chapter, an adjustment algorithm is proposed to support several levels of CBR. A fixed relative difference between the upper and lower boundaries of CBR levels provides more flexibility and excellent immunity against high channel overload. The levels of transmission power adaptation using the transmission power mechanism are synchronized with the signal reception sensitivity thresholds to adjust the channel load for the LTE-V2X Mode 4 vehicular communication system. Furthermore, this work investigates the interaction of the proposed method with the S-SPS and E-ERRA radio resource scheduling methods in terms of packet reception ratio and packet collision ratio. The proposed algorithms are verified by simulation. To provide more

realistic environments, the simulation considers two highway scenarios and MCS orders for fixed and varying vehicle densities.

Several research groups paid attention to the DCC mechanisms applied in C-V2X. In [37] Mansouri et al. carried out one of the first investigations on the DCC mechanisms that enable C-V2X Mode 4. Based on the table of the fixed number of channel load adjustments proposed in the 3GPP report[??????????????], Mansouri investigated the mechanism of dropped packets when applying the S-SPS scheduling method for a fixed number of vehicles. Furthermore, in [37] Mansouri highlighted the S-SPS problem of resource selection when channel load increases and proposed a packet drop technique to reduce the busy channel ratio.

In [113], the authors analyzed the efficiency of the packet drop technique to improve QoS in the application layer and tested the proposed method for several vehicle speeds. Consequently, the authors found that dropping packets as a congestion control harms performance at the application layer. In [114], interactions of DCC mechanisms with the LTE-V2X Mode 4 resource allocation algorithm were investigated by changing the resource reservation interval (RRI) within the S-SPS with the measured CBR or the channel occupancy. Bazzi et al. in [115] recommended further investigation when increasing the frequency of awareness message transmissions without influencing vehicle awareness. Adaptive resource (re)selection with the resource collision detection algorithm was proposed in [105]. In [121], the author of this dissertation introduced with his coauthors a spectrum partitioning technique to avoid the overlap area of the broadcast in C-V2X Mode 3. Some studies focus on the comparison between the Cellular-V2X Mode 4 and IEEE 802.11p standards, such as DSRC or ITS-G5 [99], [116], [117], and [119]. The multihop clustering algorithm was investigated using a hybrid architecture with infrastructure support [120]. An analytical model for autonomous Cellular-V2X Mode 4 was investigated using the Veins software platform [94] to compare performance at different vehicle densities.

5.3 Assumptions and Background

5.3.1 Congestion Control

In [56], the application of congestion control in LTE-V2X Mode 4 has been specified. The standard does not describe a precise algorithm for controlling channel congestion but presents the corresponding metrics and possible mechanisms to decrease the channel load that leads to resource congestion. In each packet (re)transmission, the vehicle has to measure SL's CBR and Channel Occupancy Ratio (COR). Measurements should be performed on the subframe $\tau - 4$ when packet transmission will be broadcast on the subframe τ. The CBR indicates the level of channel load, which can be defined as the number of subchannels in the last 100 ms (100 subframes) that feature an average of RSSI higher than a pre-established threshold. On the other hand, the COR quantifies the channel occupancy caused by vehicle broadcast packets. It defines the number of subchannels that the vehicle utilizes to transmit during an interval of 1000 ms (1000 subframes). Each vehicle can divide this time period into two intervals, the past and future intervals, and can decide how many past and future subframes for COR are used for measurement. However, the number of past subframes should be equal to or greater than 500. Moreover, only the subframes already used by broadcasting vehicles can be considered to measure COR. The standard specifies that up to 16 CBR levels can be defined [118]. Vehicles cannot overpass COR_{limit} that increases as the CBR decreases in each level. The value of COR_{limit} is a function of the priority of the TB and the absolute speed of the vehicle. Each vehicle needs to measure the CBR and quantifies its COR before (re)transmission of the packets. If the measured COR is higher than the configured COR_{limit} established for the current CBR level, the vehicle must reduce this COR to below COR_{limit} by adjusting the transmission parameters [118]. However, to achieve this reduction in COR, the standard [108] indicates several potential mechanisms:

- **Transmit power control (TPC):** In TPC, the transmission power changes to adjust the current channel load. For example, a vehicle decreases its

transmission power when a high channel load is observed, reducing the interference range and reducing the CBR.

- **Transmit rate control (TRC):** This mechanism works by adjusting the time between two consecutive transmission packets sent by a vehicle.
- **Transmit data rate control (TDC):** This mechanism can be used by a vehicle that can transfer data in several rate options. During high channel load time periods and depending on the application, a car can adjust the SL transmission data rate to be appropriate to the current channel condition.

It is essential to mention that the standard [108] does not specify the ranges of CBR levels and the weights of COR_{limit} for each level. However, 3GPP introduced a working document on CBR ranges. In this context, our work proposes a new algorithm to assign CBR to each level, compared to the solutions presented in the literature such as [37] and [114].

5.3.2 C-V2X Communication Assumptions

Section 3.4, generally describes the assumptions of the communication system of C-V2X Mode 4. However, the number of subchannels in one subframe of 1 ms, the total number of subchannels in T_{step}, and CBR can be obtained through (3.1), (3.2), and (4.1), respectively. The distance D for the successful reception of a signal should be equal or lower than the maximum transmission range $D_{\max}$ and the minimum signal-to-interference plus noise ratio $\gamma_{\min}$ can be obtained by the predefined equations (4.5) and (4.2) - (4.4), respectively.

Also, assume that the received power and the transmitted power are denoted P_r and P_t, respectively. Let the path loss exponent be denoted as α, and let the path loss coefficient (on the linear scale) at the reference distance 1 m be PL_{loss}. Then the received power can be written as follows:

$$P_r = \frac{P_t G_r}{PL_{loss} D^{\alpha}} \tag{5.1}$$

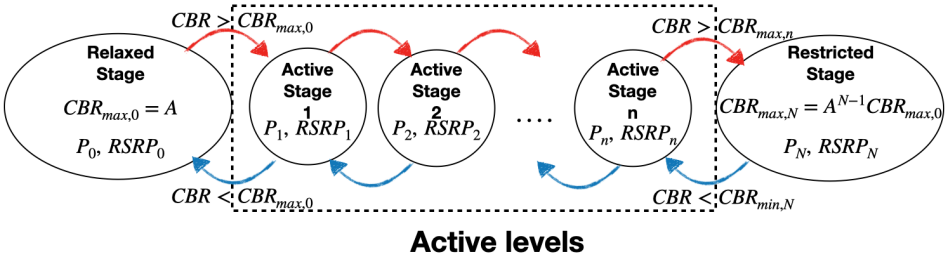

FIGURE 5.1: DCC access state machine with n active sub-stages.

In our work, two modulation and coding schemes are applied; thus, two values of $\gamma_{\min}$ are calculated to obtain different $D_{\max}$ according to the transmission power for each of them.

5.4 System Model

The proposed algorithm aims to generate multilevel CBR according to the concept of the DCC mechanism. The reaction of the system to adjust CBR is represented by three factors at each level; maximum and minimum CBR, transmission power and the established S-RSSI threshold. The relaxed state is characterized by a minimum threshold for signal reception sensitivity represented by $S\text{-}RSSI_{thr,\min}$, the maximum transmission power $P_{t,\max}$, and the acceptable maximum CBR (denoted as $CBR_{\max,0}$). $CBR_{\max,0}$ is equal to the difference between unity and a specific fraction of the CBR denoted as $\triangle CBR$ ($0 < \triangle CBR < 1$) set by the operator. The active state consists of N active levels ($n = 1, ..., N$). Each level n features a maximum and minimum CBR, transmission power $P_{t,n}$, and $S\text{-}RSSI_{thr,n}$. In the restrictive state, it is proposed that the lower limit of CBR reaches 0.1 of $CBR_{\max,0}$ or less, while the transmission power reaches its lowest level.

The maximum CBR in the relaxed state can be expressed as follows.

$$A = 1 - \triangle CBR \tag{5.2}$$

$$CBR_{\max,0} = A \tag{5.3}$$

where A is the maximum CBR in the relaxed state. The maximum and minimum CBRs in the active state n are assumed to be given by the formulae:

$$CBR_{\max,n} = A^n \, CBR_{\max,0} \tag{5.4}$$

$$CBR_{\min,n} = A^{n+1} \, CBR_{\max,0} \tag{5.5}$$

According to the above equations, the value of CBR for a given level is in the range between the highest and lowest CBR of this level. These boundaries have the following relationship with $CBR_{\max,0}$ of the relaxed state:

$$A^{n+1} CBR_{\max,0} \leq CBR_n < A^n CBR_{\max,0} \tag{5.6}$$

The maximum and minimum CBR that can be applied in the restrictive state can be found as follows.

$$CBR_{\max,N} = A^N \, CBR_{\max,0} \tag{5.7}$$

$$CBR_{\min,N} = A^{N+1} \, CBR_{\max,0} \tag{5.8}$$

According to (5.4) and (5.5), the number of levels of CBR is inversely proportional to the value $\triangle CBR$ (that is, when the value of $\triangle CBR$ increases, the number of levels decreases).

The procedure of the proposed algorithm is presented in the form of a pseudocode in Algorithm 3.

In the algorithm input, n represents the current TPC-DCC level that a vehicle has used in the last T_{step} of the resource life cycle (when the RC reaches zero) before obtaining a new resource. CBR_{cur}, and $S\text{-}RSSI_{thr,n}$ are the current CBR and the threshold of $S\text{-}RSSI$ at the level n. A vehicle obtains CBR_{cur} using (4.3), and the subchannels are indicated as busy if $S\text{-}RSSI$ is greater than $S\text{-}RSSI_{thr,n}$ of the current level. $S\text{-}RSSI_{thr,n}$ will continuously increase its threshold by 3 dB until it reaches the appropriate level of CBR. Furthermore, the number of the increase steps also indicates the number of increased levels. If the achieved number is greater than the number of levels, the next level of the resource life

Algorithm 3: Proposed adjustment algorithm.

Input: $n, N, CBR_{cur}, S\text{-}RSSI_{thr,n}, CBR_{\max,0}, A, RC$
Output: $CBR_{\max,n}, CBR_{\min,n}, P_t, S\text{-}RSSI_{thr,n}, RC$

while $RC = 0$ **do**
  if $CBR_{cur} > A^n\ CBR_{\max,0}$ **then**
    for i = 1 to N-n **do**
      $n = n + 1$
      $S\text{-}SRRI_{thr,n} = S\text{-}SRRI_{thr,n} + 3$ dB
      $CBR \leftarrow$ **Calculate a new CBR using (4.1)**
      if $CBR < A^n\ CBR_{\max,0}$ **then**
        break for loop
      end if
    end for
  else if $CBR_{cur} < A^{n+1}\ CBR_{\max,0}$ **then**
    for i = 1 to n **do**
      if $i \neq n$ **then**
        $S\text{-}SRRI_{thr,n} = S\text{-}SRRI_{thr,n} - 3$ dB
        $CBR \leftarrow$ **Calculate a new CBR using (4.1)**
        if $CBR > A^{n+1-i} CBR_{\max,0}$ **and** $CBR \leq A^{n-i} CBR_{\max,0}$ **then**
          $n \leftarrow n - i$
          break for loop
        end if
      else
        $n \leftarrow 0$
      end if
    end for
  end if
  $CBR_{\max,n} \leftarrow A^n\ CBR_{\max,0}$
  $CBR_{\min,n} \leftarrow A^{n+1}\ CBR_{\max,0}$
  $P_t \leftarrow P_{t,n}$ (P_t **assigned to level n (see Fig.5.1))**
  $S\text{-}SRRI_{thr} \leftarrow S\text{-}SRRI_{thr,n}$
  $RC \leftarrow$ new RC
end while

cycle will be the restrictive state. Furthermore, when CBR_{cur} is less than the minimum CBR of this level, $S\text{-}RSSI_{thr,n}$ will continuously decrease its threshold by 3 dB until it achieves a compatible CBR with the current maximum and minimum CBR. Suppose that the zero level is achieved, then the state machine achieves the relaxed state. The number of decreasing steps will also be the decreasing number of levels. According to the new level, a new transmission power $P_{t,n}$, maximum and minimum CBR of the new level and a new $S\text{-}RSSI_{thr,n}$ will be established.

Recall that the S-SPS and E-ERRA resource allocation algorithms have been explained in Sections 3.4 and 3.6, respectively.

5.5 Simulation Scenarios and Assumptions

5.5.1 System Assumptions

The simulation at the system level was developed to test and compare the interaction of the E-ERRA and S-SPS performance scheduling algorithms with the proposed multilevel adjustment of CBR in C-V2X Mode 4. The evaluation of the system model can be summarized in the following steps:

1. Each vehicle in the network will evaluate the channel load at the last T_{step} of its resource life cycle before resource reselection.

2. Two separate simulations are run with two different MCSs for a constant inter-vehicle distance (the density is constant over time) and for time-varying vehicle density.

3. The system is modeled to calculate the packet reception ratio and the resource collision ratio with both scheduling methods.

4. In (4.5), the maximum transmission distances are calculated for different transmission powers, and the minimum signal-to-interference-plus-noise ratio is calculated for each MCS using (4.2) - (4.4).

It is important to note that the number of vehicles in the awareness range is calculated in each CAM period for each vehicle in the network.

5.5.2 Simulation Scenarios and Settings

Different highway scenarios have been designed using the Matlab platform, as in previous simulations. Matlab was integrated with the open source Simulation of Urban MObility (SUMO) package [102] to model more realistic environments. The scenarios in this work have been classified into two groups: standard network and hybrid network. Each of these groups consists of two scenarios. These scenarios differ in terms of vehicle distribution in the network, transmission power, and signal reception sensitivity as follows:

1. *Standard network*: The performance of the system layer was investigated for fixed inter-vehicle distance and service range. Furthermore, the number of vehicles in each lane of the highway was constant (wrapped network) during the simulation time, as proposed in [103]. As mentioned above, the range of awareness depends on the transmission power. Scenarios 1 and 2 were simulated for different transmission powers and different MCSs (see Table 5.2). The aim of selecting these scenarios is to test the behavior of the system for various transmission powers in the same network.

2. *Hybrid network*: The performance of the system layer was investigated for variable vehicle densities in the network, thus for variable transmission power corresponding to CBR of the resources in the service range of each vehicle. The service range can vary from one vehicle to another on the same network. The number of vehicles moving in each lane was variable during the simulation time. Furthermore, the transmission power should be related to the channel load in the service range according to the proposed multilevel adjustment of CBR. Scenarios 3 and 4 were evaluated for different transmission powers and different MCS schemes, and are parameterized in Table 5.2. The aim of these scenarios is to test the

TABLE 5.1: Common settings.

Common Parameters and settings	**Values**
Carrier frequency	5.9 GHz
Bandwidth	10 MHz
Shadowing	log-normal
Std. dev.	3
Road length $\times$ road width	2000 m $\times$ 4 m
No. of lanes in each direction	3
Frame duration	10 ms
Subframes duration	1 ms
Subcarrier space	15 KHz
No. of subcarriers in each RB	12
No. of symbols in a subframe	14
No. of effective symbols in a subframe	9
Vehicles speed in each direction	70, 100, 140 Kmph
Antenna gain	3 dB
Path loss at 1 meter	37.02 dB
Loss exponent	4
Noise power over 10 MHz	-95 dBm
CAM frequency	10 Hz
CAM period	100 ms
Packet size	190 bytes
Lowest RSRP	-92.5 dB
The maximum ratio difference $\triangle CBR$	0.2
The maximum CBR in the relaxed state	0.8

performance of the proposed congestion control algorithm in different vehicle densities in the same network and the interaction between the resource allocation methods and the proposed algorithm in more realistic environments.

In each simulation in this investigation, the positions and distances of all vehicles in the network were updated and calculated in each CAM interval (assuming that they were equal to 100 ms). Furthermore, the scheduling algorithms were investigated and evaluated in all vehicles in the network for each CAM period.

The common parameters for all scenarios are presented in Table 5.1. We assumed that the given channel bandwidth is 10 MHz. In our simulations, the Winner II B1 propagation model was applied. The maximum distances

TABLE 5.2: Parameters and settings of the main scenarios.

Parameters	**Scenario 1**	**Scenario 2**	**Scenario 3**	**Scenario 4**
Min-Gap between vehicles for 70, 100, 140 km/h speed	12, 18, and 21 m	3, 7, and 10 m	variable	variable
No. of vehicles in the network	622	1375	See Fig.8	See Fig.9
The number of vehicles in the awareness range	constant	constant	variable	variable
PRB/subchannel RB_{SCH}	12	6	12	6
Subchannels/Subframe N_{TSCH_sf}	4	8	4	8
Transmission power	16, 18, 20, and 22 dBm	24, 26, 28, and 30 dBm	16, 18, and 20	26, 28, 30 dBm
MSC Index	8	15	8	15
Coding rate C_{rate}	0.645	0.67	0.645	0.67
Min. SINR $\gamma_{\min}$	8.49 dB	18.76 dB	8.49 dB	18.76 dB
Max. Distances $D_{\max}$	503.7, 595.5, 704.1, and 832.5 m	513.9, 607.5, 718.3, and 849.30 m	503.7, 595.5, and 704.1 m	513.9, 607.5, 718.3, and 849.30 m
No. of simulations	8	8	2	2
Simulations time	5 sec.	6 sec.	6 sec.	5 sec.

of the service ranges for specific transmission powers have been calculated according to (4.5). Four highway scenarios were applied in several simulations that differed in selected parameters to obtain different results in the packet reception ratio and packet collision ratio for different vehicle densities.

5.6 Simulation Performance and Results

In our simulations, we estimated, as previously, two basic measures of packet transmission quality, namely, the packet reception ratio PRR and the collision ratio CR. PRR is the ratio of the number of successfully decoded packets to the number of transmitted packets. CR is the ratio of the number of detected packets that collided with other packets in transmission messages to the total number of transmitted packets. PRR and CR have been calculated for all vehicles in the simulated network for each period of the CAM cycle for both resource scheduling algorithms in each scenario. PRR, and CR were previously described in Subsection 3.5.2.

This subsection shows the system layer performance for two scheduling algorithms with the proposed algorithm of adjustment of the CBR levels. The E-ERRA and S-SPS scheduling algorithms have been tested, evaluated, and compared in two types of environment for two scenarios. The E-ERRA and S-SPS scheduling algorithms have been run with a combination of TPC-DCC and adaptation of signal reception thresholds according to the calculation of the proposed levels. The performance of E-ERRA in terms of PRR in Fig. 5.2 for Scenario 1 (see Table 5.2) shows promising results compared to S-SPS. PRR values increased from 11% at a distance of 100 m for all transmission powers to approximately 30-35% at 250 m and 2-20 % at 450 m for several transmission powers (see the legend in Fig. 5.2).

In Scenario 2 (Fig. 5.4), the performance of PRR increases by approximately 18% for all transmission powers in a 100 m distance to 25-30% at 250 m, and to 11-30% at 450 m. The highest performance improvement for E-ERRA is observed when the highest transmission power is applied (in the relaxed state).

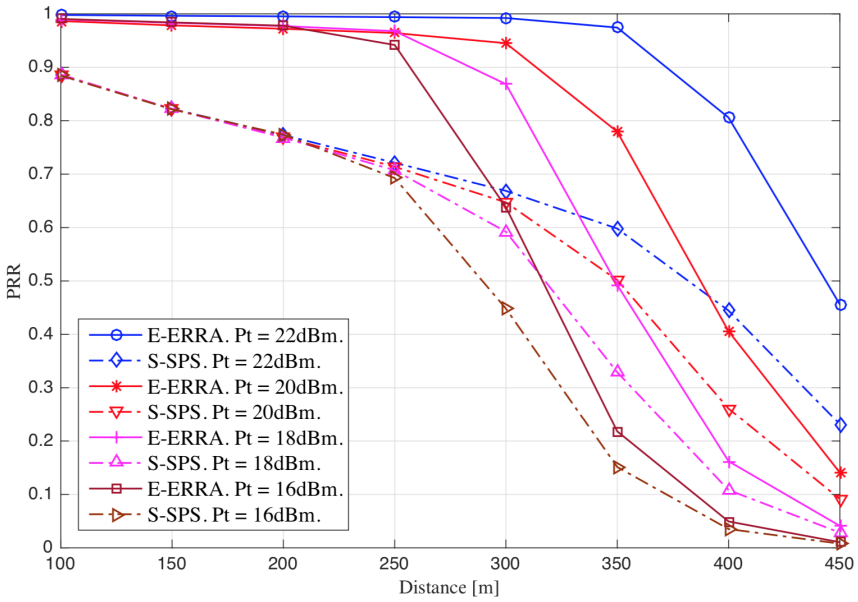

FIGURE 5.2: Performance comparison for E-ERRA and S-SPS algorithms in the form of *PRR* vs. distance *D* in a standard network, in Scenario 1 with different broadcasting powers.

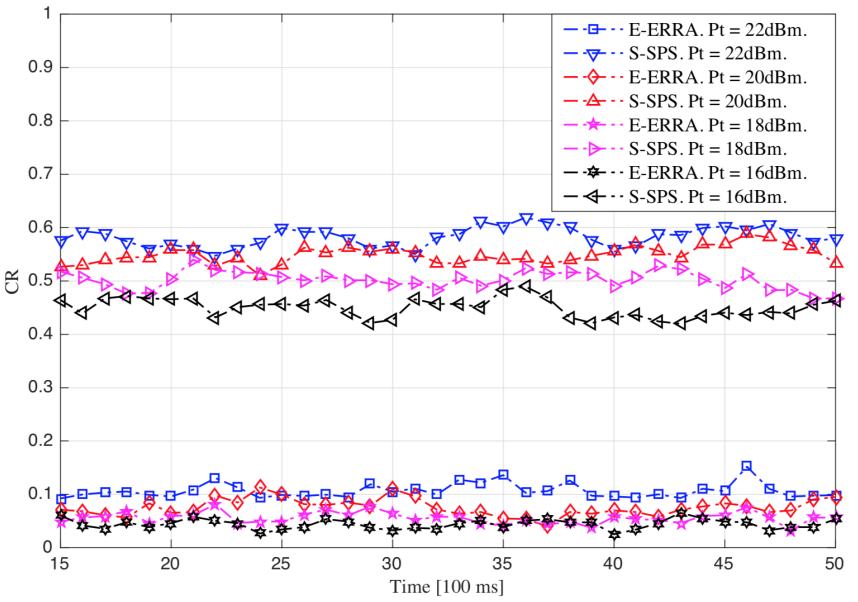

FIGURE 5.3: Performance comparison for E-ERRA and S-SPS algorithms in the form of packet Collision Ratio *CR* vs. simulation time in a standard network with different broadcasting powers in Scenario 1.

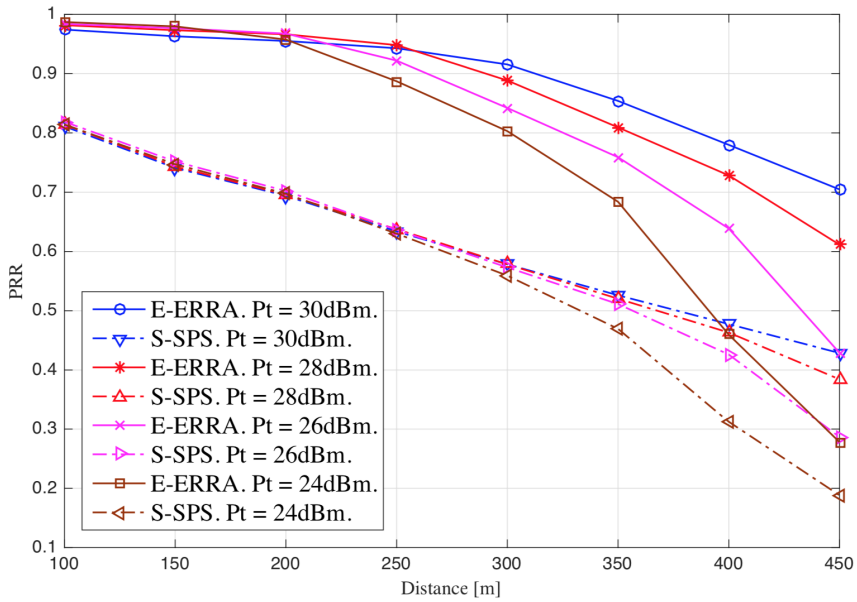

FIGURE 5.4: Performance comparison for E-ERRA and S-SPS algorithms in the form of *PRR* vs. distance *D* in a standard network, in Scenario 2 with different broadcasting powers.

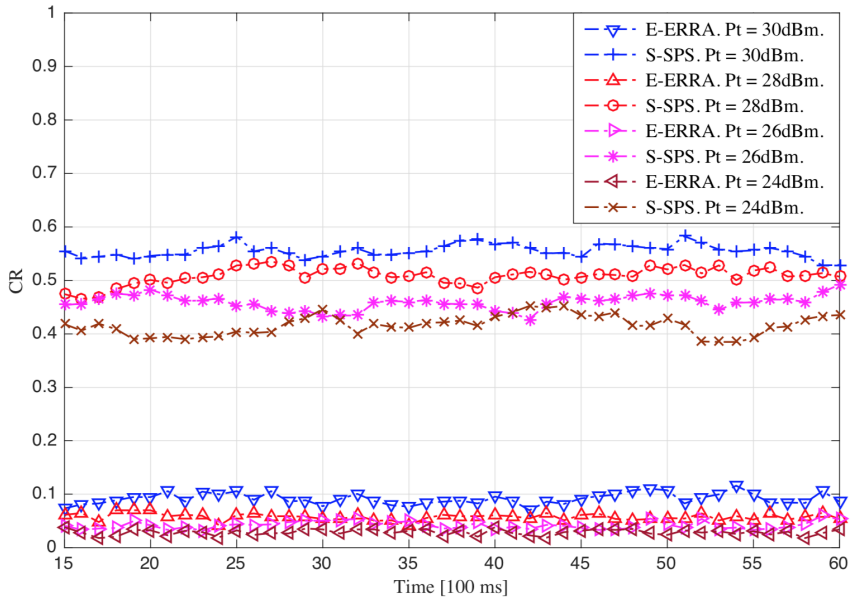

FIGURE 5.5: Performance comparison for E-ERRA and S-SPS algorithms in the form of packet Collision Ratio *CR* vs. simulation time in a standard network with different broadcasting powers in Scenario 2.

Furthermore, high capability with the E-ERRA algorithm is observed when the proposed CBR levels are applied with the proposed adjustment method using TPC-DCC and adaptation of the sensitivity to reception signals. Increasing CBR levels provides greater precision in resource selection. However, Figs. 5.3 of Scenario 1 and 5.5 of Scenario 2 show an exceptionally significant improvement in the packet collision ratio CR when the E-ERRA algorithm is applied. Reservation of resources by the E-ERRA algorithm and tracking them reduces packet collisions significantly. The results show a 50-60% improvement for E-ERRA compared to S-SPS for all transmission powers. It is worth stressing once again that the E-ERRA algorithm has very high performance stability, high reliability in selection resources, and low complexity in processing and implementation.

The numbers of vehicles in Scenarios 3 and 4 vary over time during simulation time. The proposed methods for adjusting the parameters motivated the prevention of resource collision by continuously calculating CBR and selecting the appropriate level of parameters of the physical layer. Transmission power changes appropriately with the channel load of the vehicles in the transmission area. Thus, in the same network, there are different service ranges. Fig. 5.6 of Scenario 3, and Fig. 5.7 of Scenario 4, present the variability of the number of vehicles in the network. These vehicles broadcast packets with different transmission powers but apply the same MCS in each scenario.

Figs. 5.8 and 5.9 show the performance of the system in the form of PRR for vehicles that use different transmission power for broadcasting. Fig. 5.8 shows the performance of the E-ERRA algorithm, which is about 13-18% higher than the performance of S-SPS.

In QPSK applications (Scenario 3), the effects of limited resources, inconstant service ranges of vehicles in the same network, and interference effects appear strongly by partially affecting the packet reception ratio in general, as compared to the standard network. Furthermore, the efficiency of the proposed method of adjusting physical parameters is limited by limited resources.

On the other hand, as seen in Fig. 5.9, in 16QAM applications (Scenario

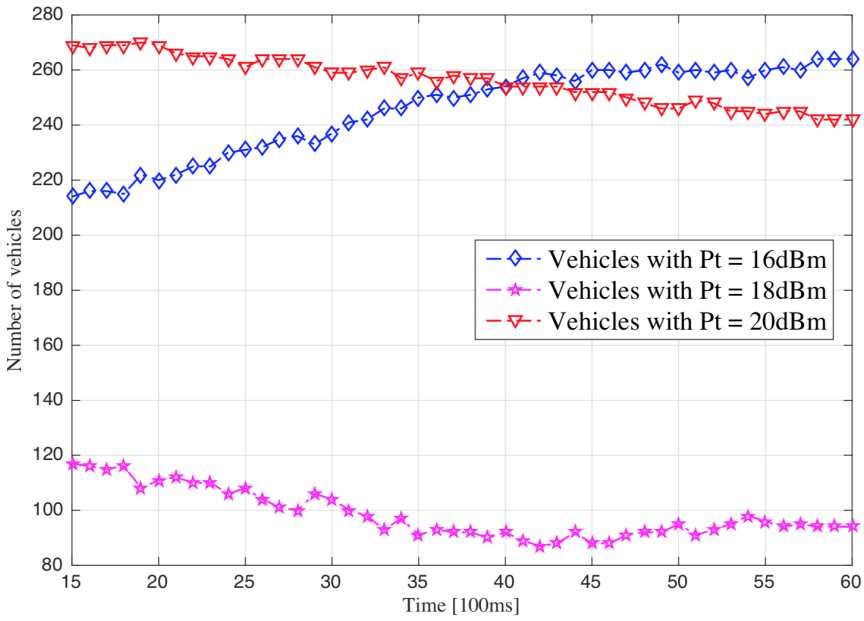

FIGURE 5.6: Number of vehicles in the network along simulation time in Scenario 3.

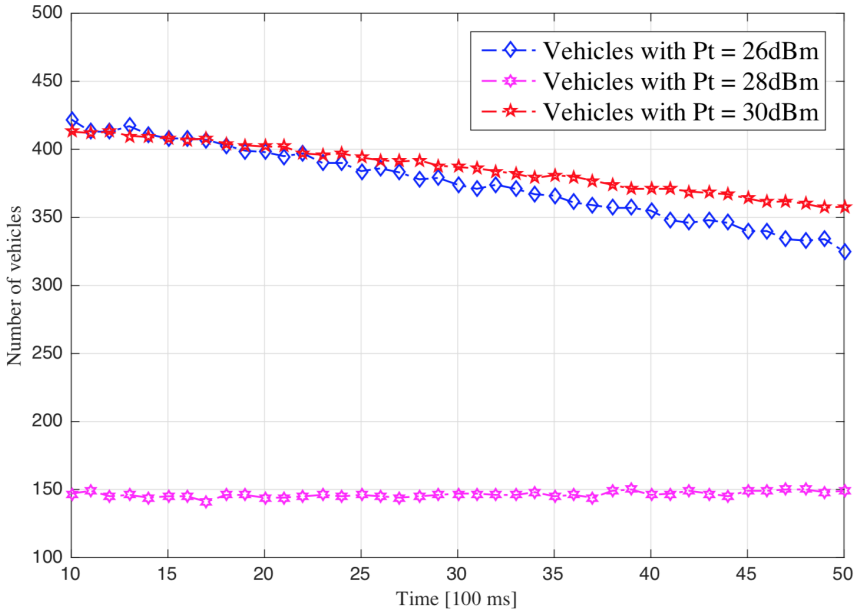

FIGURE 5.7: Variable number of vehicles in the network along simulation time in Scenario 4.

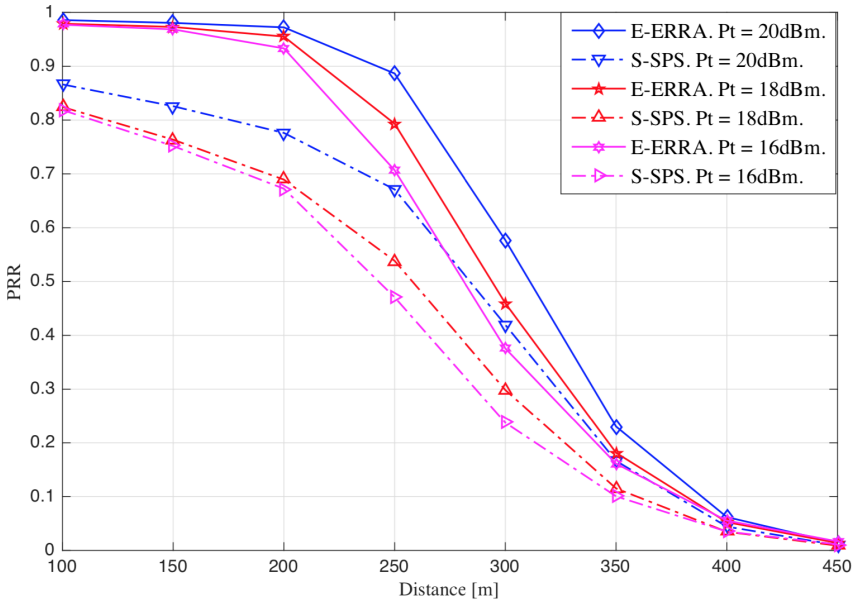

FIGURE 5.8: Performance comparison of E-ERRA and S-SPS algorithms in the form of *PRR* vs. *Distance* in a hybrid network in Scenario 3 with different broadcasting powers.

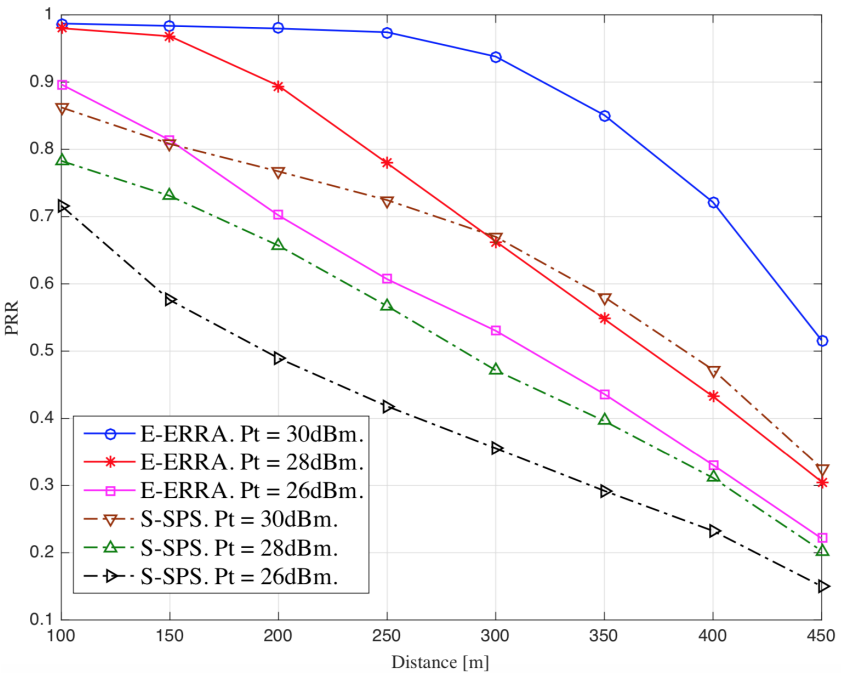

FIGURE 5.9: Performance comparison of E-ERRA and S-SPS algorithms in the form of *PRR* vs. *Distance* in a hybrid network in Scenario 3 with different broadcasting powers.

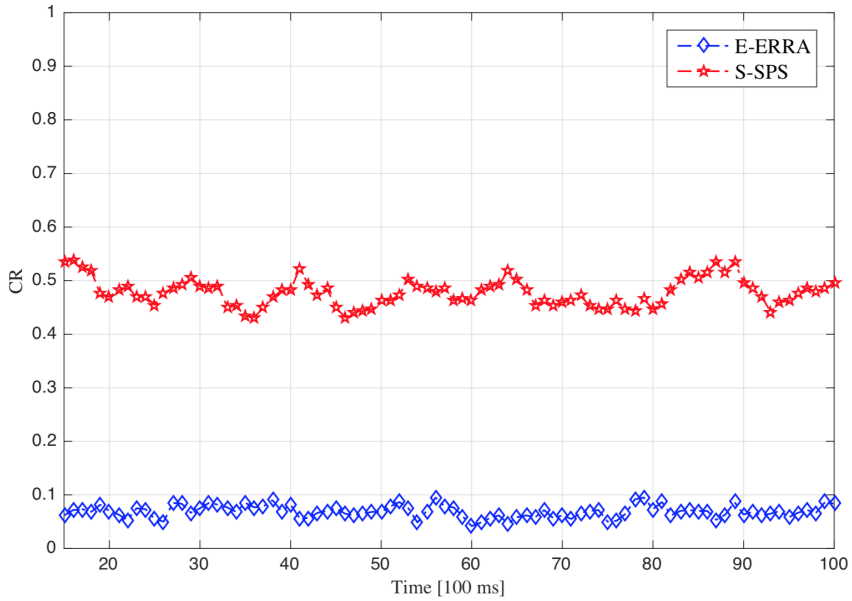

FIGURE 5.10: Collision ratio CR vs. simulation time in Scenario 3.

4), the resources have a higher level of channel load than in Scenario 3, and more flexibility is possible in the selection between these resources (the high number of resources provides more flexibility in the selection between several levels of the proposed CBR levels). Furthermore, these features are strongly supported by using the queue $ListB$ in the E-ERRA algorithm to avoid collision in resource selection and compensate for the losses in reserved resources that can appear when owners of reserved resources have left the awareness range. E-ERRA in this scenario shows a gradual enhancement compared to S-SPS by up to 27% when the distance is 300 m. The packet collision ratio in Figs. 5.10 and 5.11 in E-ERRA shows about 40% higher efficiency compared to S-SPS by avoiding packet collision. Consequently, E-ERRA is more convenient than S-SPS broadcasting in the hybrid network environment. Increasing CBR levels with TPC-DCC and adaptive signal reception sensitivity shows high compatibility with the E-ERRA algorithm compared to S-SPS.

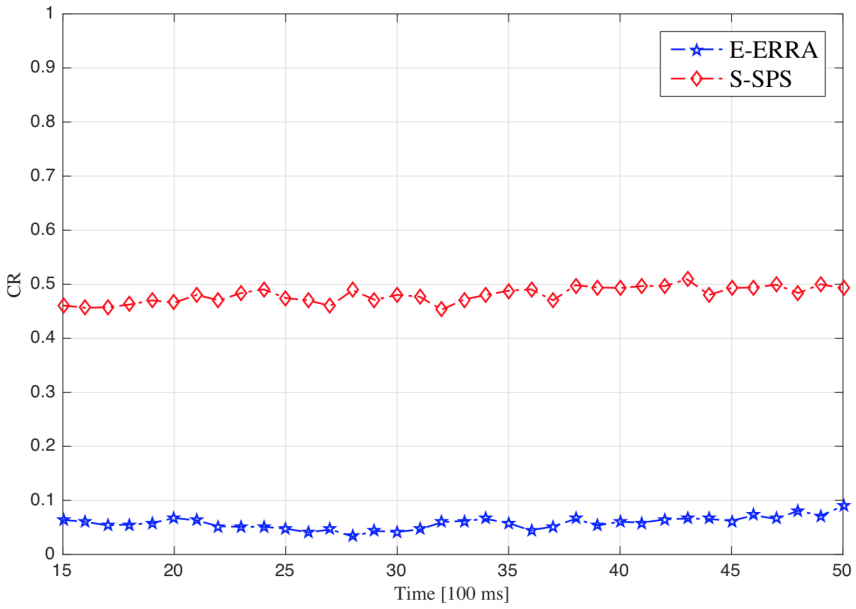

FIGURE 5.11: Collision ratio *CR* vs. simulation time in Scenario 4.

5.7 Summary

The proposed TPC-DCC method with the proposed multilevel channel busy ratio adjustment algorithm for Cellular V2X in a fixed and variable number of vehicle densities has been considered and examined for two scheduling algorithms. These algorithms are Sensing-based Semi-Persistent Scheduling (S-SPS), and the author's previously proposed method called Extended-Estimation and Reservation Resource Allocation (E-ERRA). Both scheduling algorithms have been investigated and compared in terms of packet reception ratio (PRR) and collision ratio (CR) in system layer simulations. Recall that in this research, the Matlab platform has been integrated with SUMO (vehicle traffic software generator) for four vehicle traffic density scenarios to simulate both scheduling algorithms with TPC-DCC. Traffic density scenarios have been classified into two categories: standard and hybrid networks (with two scenarios in each category).

The simulation results of standard networks with E-ERRA supported by TPC-DCC have shown higher PRR, reliability in radio resource selection, and lower CR than S-SPS for all levels of physical parameters.

The E-ERRA algorithm is applied with TPC-DCC, adaptive signal sensitivity in receiving, the proposed multilevel channel busy ratio algorithm in a hybrid network, and a variable number of vehicles in the same broadcast range. These networks feature higher performance stability, PRR and improved immunity against packet losses and CR compared to those applying S-SPS.

Chapter 6

Spectrum Re-partitioning for C-V2X

6.1 Motivation

In the case of C-V2X Mode 3 transmission, 3GPP has standardized dynamic and semi-persistent resource scheduling algorithms as resource allocation and scheduling techniques. Both techniques result in a signalling cost problem between vehicles and infrastructure. Therefore, in this chapter, a means to reduce it is proposed. We propose the Reselection Counter (RC) in centralized resource allocation to be used as a decremental counter of new resource requests. Furthermore, two new spectrum re-partitioning and frequency reuse techniques in Roadside Units (RSUs) are considered to avoid resource collisions and diminish high interference impact via increasing the frequency reuse distance. The spectrum partitioning techniques are proposed to be managed by the cellular station (i.e. eNB in 4G or gNB in 5G). The two techniques, full and partial frequency reuse, partition the bandwidth into two sub-bands. Two adjacent RSUs apply these sub-bands with the Full Frequency Reuse (FFR) technique. In the Partial Frequency Reuse (PFR) technique, the subbands are further re-partitioned among vehicles located in the central and edge parts of the RSU coverage area. The assignment of subbands in the nearest RSUs using the same subbands is inverted with respect to the current RSU to increase the frequency reuse distance. It is worth mentioning that both spectrum techniques can be employed in vehicular communication with centralized resource allocation using LTE or/and NR.

This chapter is based on the article [121] published by the author of this dissertation and its co-authors.

6.2 Challenges and Contributions

In C-V2X Mode 3, the infrastructure selects the resources for all vehicles in the network, and therefore, high reliability is achieved in packet transmission [122], [123]. Dedicated signals between the cellular infrastructure and vehicles improve transmission reliability. Unlike Mode 4, 3GPP did not specify a resource allocation algorithm for Mode 3. Each operator can implement its own algorithm, which should fall into one of two categories [124]: Dynamic Scheduling (DS) and Semi-Persistent Scheduling (SPS). In DS, vehicles request subchannels from the cellular infrastructure prior to each transmission, which increases the cost of control signaling and lengthens the delay in the transmission of CAM messages. On the other hand, the cellular infrastructure reserves resources for periodic broadcasting by vehicles in SPS. However, the cellular infrastructure is responsible for deciding how long the reservation should last (that is, 3GPP did not define RC in Mode 3). Furthermore, only the cellular infrastructure can activate, deactivate, or modify the resources or the reservation time interval of the subchannels. Vehicles in Mode 3 should inform the infrastructure about the type, size and transmission cycle of the CAM to reserve the fitting subchannels.

The probability of correct reception of messages with properly selected receiving parameters and the required C-V2X communication range that ensures high reliability communication are the 3GPP use cases [56] discussed in this chapter. The main objective of the research reported in this chapter is to avoid the drawbacks in C-V2X Mode 3 observed for such reasons as: overlapping in CAM's broadcast area, high signalling cost and signal latency between cellular infrastructure, mitigating the interference signals that can negatively impact the packet reception ratio of vehicles in C-V2X Mode 3. In this chapter, cooperation among Road Side Units (RSUs), a part of the cellular infrastructure

and managed by eNB, is proposed. We have investigated the application of the RC in the centralized reselection of resources of C-V2X Mode 3. RC values generated in an RSU can provide the ability to advance knowledge when vehicles need new resources. In this way, assuming stationary subchannels and transmission power, vehicles do not need to send requests to the RSU for new resources. Thus, a reduction in signaling costs can be achieved. Furthermore, we propose the concepts of fractional frequency reuse and soft frequency reuse [125] that an RSU can use to specify vehicle broadcast resources. In other words, frequency partitioning is used to grant vehicles with resource allocations needed to broadcast CAM messages. The given bandwidth is divided into two bands that are used by two adjacent RSUs. In our proposal, the full frequency reuse technique (FFR) partitions the bandwidth into two separate bands for two adjacent RSUs to guarantee that the vehicles' broadcasts do not overlap. In this case, the frequency reuse distance means that another single RSU coverage area is located between two RSUs that use the same band. Moreover, in the partial frequency reuse technique (PFR), further repartitioning of the band into two subbands (inner and outer bands) takes place for central and edge users, respectively, and the subbands are distributed inversely with respect to the nearby RSUs that use the same band. As a result, the partial frequency reuse technique promises encouraging results compared with the full frequency reuse technique. Moreover, both techniques provide performance advantages over the system in which a regular single band (SB) is applied for all RSUs.

As we have already mentioned, during the last few years, many research groups have investigated and evaluated the performance of C-V2X, focusing on the packet reception ratio (PRR), packet collision ratio (CR), and resource allocation algorithms. In [126], the authors proposed a "look ahead" technique to reduce resource collisions by identifying the next resource location. The authors of [127] introduced a comprehensive analysis related to the interaction between transmission power and the performance of scheduling radio

resources in C-V2X Mode 4. In addition, they have proposed adaptive transmit power control to achieve a higher quality of service in different traffic scenarios. Based on the predefined positions of vehicles in the network, the network-controlled resource management and frequency reuse distances of vehicles active in Mode 3 could be improved, as shown in [128]. The fuzzy logic-based algorithm and the OpenFlow algorithm have been proposed in [129] as an SDN-based multi-access edge computing for vehicular networks. In [130], interference signals and quality of service in a highway scenario have been investigated by simulations at the system level. In [131] a distributed estimation mechanism has been proposed to improve the scalability and robustness of vehicle connectivity in an RSU coverage area. PRR and latency are the terms used in [132] to evaluate the proposed solution to maximize the scheduling of the reuse distance for C-V2X Mode 3.

6.3 Assumptions and Problem Formulation

6.3.1 C-V2X Assumptions

As mentioned above, SC-FDMA is utilized in SL communication with physical parameters such as in Section 4.3. The number of subchannels in each subframe and the total number of subchannels in a CAM message cycle can be found through (3.1) and (3.2), respectively.

The number of remaining resource blocks RB_{free} in a given bandwidth that can be used later can be obtained as follows.

$$RB_{free} = (RB_{TRB_sf} - \eta RB_{SCH}) V_{Total} \tag{6.1}$$

where RB_{TRB_sf}, η, RB_{SCH}, and V_{Total} are the total number of resource blocks in a subframe, the number of subchannels in a subframe, the number of resource blocks in a subchannel and the total number of subchannels in the CAM transmission period, respectively.

The Poisson distribution is applied again to model the arrival rate parameter λ, where λ has the same meaning as in the previous chapters and is described by (3.10 and 3.11).

To calculate the received power of the broadcast signal and calculate the maximum distance between the transmitter and receiver, equations (5.1) and (4.5) must be applied, respectively.

6.3.2 Problem Formulation

In C-V2X several packet sizes can be applied. In this chapter, it is assumed that all vehicles apply the same packet size, the same number of resource blocks in each subchannel, and the same broadcast power. However, the analysis shown in the following can also be extended to other resource configurations. The set of subchannel indexes for the given resource subchannels is denoted as $Q = \{1, 2, ..., SCH_T\}$, while $C = \{1, 2, ..., c\}$ is the set of indexes denoting RSUs in the network. Let i be the index of a vehicle located within the coverage area of RSU x, and K_x be the number of all vehicles located within the coverage area of RSU x where $x \in C$. Furthermore, j is the index for users who use the same resource r in RSU y where $y \in C \backslash x$ and $r \in Q$. K_y represents all vehicles located in RSU y. Thus, the signal-to-interference plus noise ratio $\gamma^r_{i,x}$ experienced by the vehicle i belonging to the RSU x can be represented as follows:

$$\gamma^r_{i,x} = \frac{\frac{P_{tx} G_r}{PL_{loss}(D^r_{i,x})^\beta}}{\rho + \sum_{y \neq x, y \in C} \sum_{j \in K_y} \frac{P_{tx} G_r}{PL_{loss}(D^r_{j,y})^\beta}} \tag{6.2}$$

where $D^r_{i,x}$ and $D^r_{j,y}$ are the distances between the receiver and vehicle i and vehicle j, respectively. The desired signal is the one transmitted by vehicle i using resources r and the signals transmitted by vehicle j are interference signals. This research aims to reduce the interference experienced at the receiver by increasing the frequency reuse distance. As a consequence, $\gamma^r_{i,x}$ will increase. For this purpose, the minimum frequency reuse allowed distance h_{reuse} should be

determined as the minimum acceptable distance between two vehicles using the same channel frequency. The worst case of h_{reuse} can be calculated by assuming that the receiver is located on the edge of two maximum broadcasting ranges of vehicles along a horizontal line. In other words, the distances $D^r_{i,x}$ and $D^r_{j,y}$ in (6.2) are equal to the maximum broadcast range $D_{\max}$. According to this assumption, h_{reuse} can be obtained by rewriting equation (6.2) as follows:

$$\gamma^r_{i,x} = \frac{\frac{P_{tx}G_r}{PL_{loss}(D^r_{i,x})^\beta}}{\rho + \sum_{y\neq x, y\in C}\sum_{j\in K_y}\frac{P_{tx}G_r}{PL_{loss}(h_{reuse}-D^r_{i,x})^\beta}} \tag{6.3}$$

$$\text{subject to :} \qquad D^r_{j,y}, D^r_{i,x} = D_{\max}, \tag{6.3.1}$$

$$D^r_{j,y} = h_{reuse} - D^r_{i,x}, \qquad h_{reuse} = 2D_{\max} \tag{6.3.2}$$

$$\forall x \in C, \forall i \in K_x, \forall r \in Q$$

Another case of h_{reuse} occurs when $D^r_{j,y} \neq D^r_{i,x}$ and $D^r_{j,y} > D^r_{i,x}$. If a single interfering vehicle is assumed, then in formula (6.3) the sum in the denominator can be omitted and then from this simplified version of (6.3) the minimum allowed frequency reuse distance can be derived as:

$$h_{reuse} = \left[\frac{1}{\gamma^r_{i,x}(D^r_{i,x})^\beta} - \frac{\rho PL_{loss}}{P_{tx}G_r}\right]^{\frac{-1}{\beta}} + D^r_{i,x} \tag{6.4}$$

$$\text{subject to :} \qquad D^r_{j,y} \neq D^r_{i,x}, \tag{6.4.1}$$

$$D^r_{j,y} > D_{\max}, \qquad D^r_{j,y} = h_{reuse} - D^r_{i,x} \tag{6.4.2}$$

$$\forall x \in C, \forall i \in K_x, \forall r \in Q$$

Let I^r_x denote the interference in subchannel r used by a vehicle located in the coverage area of RSU x, and thus the objective function can be written as follows:

$$\min_{a\in A} \sum_{x\in C}\sum_{r\in Q} I^r_x \tag{6.5}$$

where A is a set of possible strategies of band partitioning between the RSUs, with a particular strategy a referring to a split, e.g., according to FFR, PFR or full reuse (but other strategies can also be considered). By applying the interference component of (6.2) in (6.5) the objective function can be rewritten as follows:

$$\min_{a \in A} \sum_{r \in Q} \sum_{y \neq x, y \in C} \sum_{j \in K_y} \frac{P_{tx} G_r}{PL_{loss}(D^r_{j,y})^{\beta}} \tag{6.6}$$

$$\text{subject to :} \qquad \gamma^r_{i,x} \geq \gamma_{\min}, \quad D^r_{j,y} > D_{\max} \tag{6.6.1}$$

where (6.6.1) are the constraints that are set to achieve the required quality of broadcasting with the minimum frequency reuse distance h_{reuse}. The constraint (6.6.1) can be more precisely formulated as

$$\frac{\dfrac{P_{tx} G_r}{PL_{loss}(D^r_{i,x})^{\beta}}}{\rho + \displaystyle\sum_{y \neq x, y \in C} \sum_{j \in K_y} \frac{P_{tx} G_r}{PL_{loss}(h_{reuse} - D^r_{i,x})^{\beta}}} \geq \gamma_{\min} \tag{6.7}$$

$$\text{subject to :} \quad h_{reuse} - D^r_{i,x} > D_{\max} \tag{6.7.1}$$

$$\forall x \in C, \forall i \in K_x, \forall r \in Q$$

The above conditions ensure that only one vehicle can occupy a non-collided subchannel in its CAM broadcasting range.

6.3.3 Broadcast Collision Zone

Overlapping of coverage of two broadcast signals using the same resource allocation in different RSUs can cause packet collision for receivers in this zone. The broadcast collision zone (BCZ) can arise when the frequency reuse distance between two broadcasters is lower than the minimum frequency reuse distance, that is, $h < h_{reuse}$. Furthermore, BCZ can decrease as the distance h increases, or vice versa as it decreases, as shown in Fig. 6.1. In this figure,

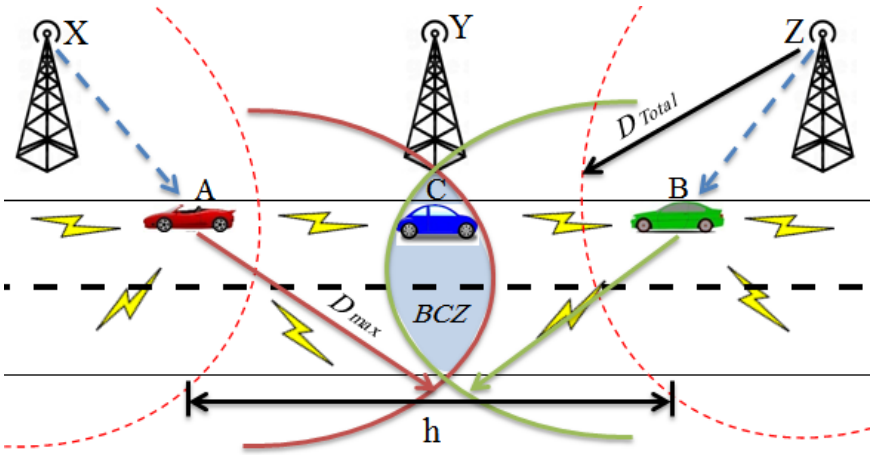

FIGURE 6.1: BCZ_{area} of two vehicles located in different RSUs coverage areas.

the two broadcasting vehicles A and B are located in the coverage areas of different RSUs. Both vehicles broadcast CAMs with the same resource location in the time and frequency domains. Thus, vehicle C is located in BCZ of the overlapped coverage area of vehicles A and B. This area can be expressed as follows:

$$BCZ_{area} = \begin{cases} 0 & h \geq h_{reuse} \\ A_A \cap A_B & h < h_{reuse} \end{cases} \tag{6.8}$$

where A_A and A_B are the coverage areas of transmitters A and B, respectively. Vehicles in BCZ (e.g. vehicle C in Fig. 6.1) receive signals with γ lower than $\gamma_{\min}$ due to interference. Thus, the BCZ area depends on the values of D_{max} and h and can be calculated as [133]:

$$BCZ_{area} = D_{\max}^2 \left(\theta(D_{\max}, h) - \sin\theta(D_{\max}, h)\right), \tag{6.9}$$

where $\theta(.)$ can easily be expressed in terms of $D_{\max}$ and h_{reuse} using the Carnot theorem as:

$$\theta(D_{\max}, h) = 2\arccos\left(\frac{h}{2D_{\max}}\right). \tag{6.10}$$

In this chapter, we focus on the distribution of resources among vehicles in the network to reduce or eliminate the BCZ of the broadcasting vehicles, assuming that the broadcasting power is fixed and the same for all vehicles.

6.4 Techniques of Bandwidth Repartitioning among RSUs

Bandwidth repartitioning techniques are necessary to reduce or eliminate BCZ. This reduction or elimination can be achieved by increasing the frequency reuse distance for each pair of transmitters. Therefore, in this section two techniques are proposed based on fractional and soft frequency reuse methods [125] from the perspective of centralized vehicular communication: Full Frequency Reuse (FFR) and Partial Frequency Reuse (PFR). The cooperating RSUs have been assumed in a highway scenario to support resource allocation for vehicular communication, focusing on increasing the minimum frequency reuse distances and selection and reselection of radio resources for high-reliability broadcasting. We assume that cooperating RSUs are connected through the X2 interface using a fiber optic backhaul network to exchange information related to the used and free resources, making RSUs ready when new vehicles just enter or exit their coverage area. Each vehicle in the network broadcasts CAM messages to surrounding vehicles through radio resources selected by RSU using the SPS method with some proposed modifications. CAMs are periodically transmitted in current subchannels until the RC value reaches zero in the RSU and vehicle. When RC equals 0, the RSU generates a new RC value in a specific range, depending on the CAM interval used. When a new vehicle has just entered a new RSU coverage area, the new RSU should wait until this vehicle's RC reaches zero to be notified about the new reselected resource. Furthermore, when a vehicle broadcasts the last packet (RC reaches zero) at the time instant T, the RSU must know in advance when the RC would reach zero and must prepare the new resources for broadcasting and generate the new RC value. At $T + T_{cycle}$, the RSU must send one message that contains the new address of the resource and the new RC value that will be decreased by one in both the RSU and the vehicle in each broadcast.

It should be mentioned that the remaining resource blocks RB_{free} given in (6.1) are assumed to facilitate the necessary signaling of vehicles to RSUs.

These signals are used to exchange control information when a vehicle enters a new RSU coverage area and in unexpected situations.

6.4.1 Full Frequency Reuse Technique (FFR)

The FFR technique protects the packets broadcast in the network from interference signals. Each RSU deployed along the highway uses partially a given frequency band. In other words, the given band is divided into two subbands dedicated to vehicles located in the two adjacent RSU coverage areas. Each subband is applied again by the RSU which is adjacent to the RSU neighboring to the current one. In this technique, the distance between the nearest two RSUs using the same subband $h_{s\text{-}band}$ is equal to the diameter $RSU_{diameter}$ of the coverage area of the center RSU.

$$h_{s\text{-}band} = RSU_{diameter} \tag{6.11}$$

h_{reuse} will be lower than h (see Fig. 6.1) if $RSU_{diameter}$ is higher than the vehicle broadcast range. Otherwise, if two vehicles use the same frequency resource and are located at the edge of their RSU coverage (that is, RSUs X and Z in Fig. 6.1) adjacent to their common RSU (that is, RSU Y), BCZ will be observed in the middle of the RSU Y coverage area. Vehicles in this area will not be able to decode packets from transmitter A or transmitter B. The failure to increase the RSU coverage area is the limitation of resources in each RSU_{band} for the number of vehicles. Decreasing the number of vehicles in an RSU coverage area is disadvantageous and unacceptable. Therefore, to eliminate this possibility, the PFR technique is proposed to solve this drawback.

6.4.2 Partial Frequency Reuse Technique (PFR)

In the PFR technique, a given band is partitioned between two adjacent RSUs (see Fig. 6.2a) with each part denoted as RSU_{band}. Furthermore, RSU_{band} is divided into two adjacent bands, named the Center (inner) Frequency Band

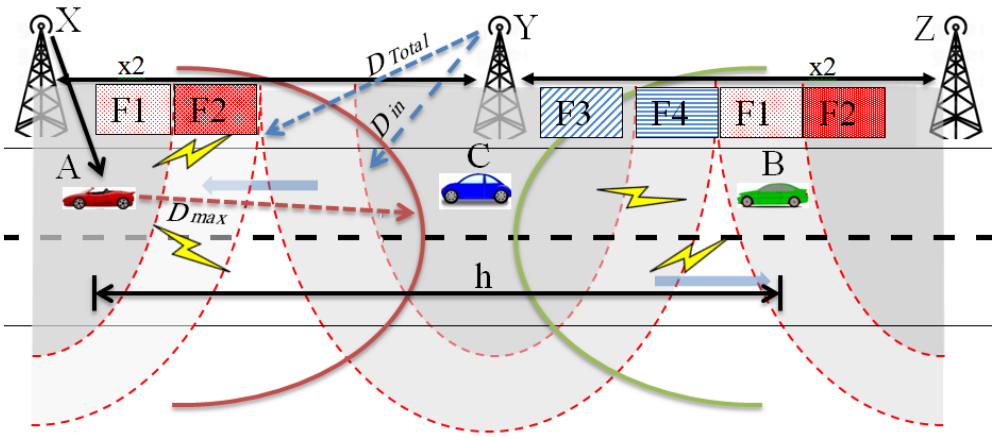

(A) Example of PFR with three RSUs.

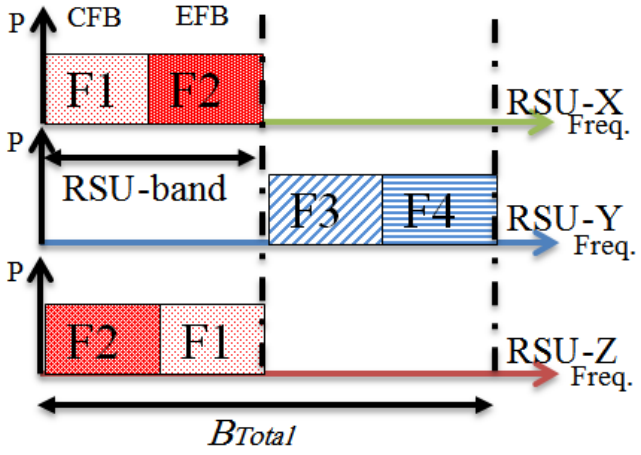

(B) PFR bandwidth partitioning among three RSUs.

FIGURE 6.2: Example of PFR for three RSUs.

(CFB) with the maximum distance from RSU to vehicles equal to D_{in} to serve Center Users (CU) and the Edge (outer) Frequency Band (EFB) with the maximum distance from RSU to vehicles equal to D_{Total} to serve Edge Users (EU) located in the distance between D_{in} and D_{Total}. Let us call the RSUs that use the same RSU_{band} twin RSUs. The distribution and usage of these bands can be illustrated by the example shown in Fig. 6.2b. The CFB of an RSU is the EFB of the nearest twin RSUs using the same RSU_{band} and vice versa. The next resource location will be a free resource in the current and nearest twin RSUs. For example, if we assume vehicle A (in Fig. 6.2a) to be a central user in RSU X that needs a new resource to allocate, the RSU denoted by X will compare

the resource grid of its CUs with the resource grid of edge users in the RSU denoted by Z (a twin RSU with X) to identify unused resources in both RSUs to avoid high interference. Moreover, if the unused resources in both RSUs cannot be found, then the next allocated resource will be a free one in the RSU X CU resource grid.

In this technique, h_{reuse} is undoubtedly increased. In the current case, $h_{s\text{-}band}$ is calculated as follows:

$$h_{s\text{-}band} = RSU_{diameter} + D_{Total} - D_{in} \tag{6.12}$$

As a result of increasing the distance between zones using the same resources, the signal-to-interference plus noise ratio is increased compared to the FFR technique.

As mentioned above, the partition of radio resources in the RSU has been divided into two subbands denoted as RSU_{band} as follows:

$$RSU_{band} = \frac{B_{Total}}{2} \tag{6.13}$$

where B_{Total} is the bandwidth of the system.

Let us assume that the partition of resources between CUs and EUs in an RSU is proportional to the ratio of the inner radius D_{in} to the radius of the RSU D_{Total}. Thus, RSU_{band} is divided into two subbands: CFB to be allocated to CUs, and the band adjacent to EFB reserved for EUs. Subbands received due to bandwidth repartitioning are given by the formulas:

$$CFB = RSU_{band}\frac{D_{in}}{D_{Total}} \tag{6.14}$$

$$EFB = RSU_{band}\frac{D_{Total} - D_{in}}{D_{Total}} \tag{6.15}$$

The main achievement of this method is that h_{reuse} increases compared to that of the FFR technique. Consequently, the probability of the existence of BCZ is decreased compared to the FFR technique.

6.5 System Model and Settings

The author has developed a system-level MATLAB simulator to run, test and compare the performance of FFR, PFR with the centralized resource allocation of C-V2X and the system with conventional SB operation. The bandwidth is divided between RSUs with the FFR technique and further between inner and outer vehicles, as assumed in the PFR technique. The Poisson distribution (see Subsection 3.6.1) is assumed to distribute vehicles along the highway with three lanes in each direction, different vehicle speeds, and distances in each lane according to [48].

A 100 ms interval with the RC range [5, 15] is proposed as the simulation time step (CAM interval) and the RC range. Each vehicle in the network receives packets from all vehicles before specifying which are located within its coverage area. Each vehicle transmits its packet to all vehicles. In other words, all vehicles transmit/receive packets to/from all vehicles in each CAM interval (that is, if the number of vehicles is equal to 150 and the simulation step is equal to 100 ms, each vehicle will test 150 packets from all vehicles in the network in each simulation step). Vehicle positions are updated according to their direction and speed in each simulation time step.

For each technique, γ_{min} has been tested with different densities of vehicles in the network (determined by the variable scalar factor) to investigate the impact of the number of vehicles on the performance of these techniques. Each simulation run spans a 5-second time interval to test the packet reception ratio for all vehicles, the minimum frequency reuse distance, the average frequency reuse distance, and the impact of interference on the network in every T_{cycle} period.

Five connected RSUs that are managed by eNB have been placed within an equal distance from each other to cover five kilometers along the highway. The main parameters of the simulations for both FFR and PFR are the same and are described in Table 6.1. The WINNER+B1 model has been assumed as

a propagation model [103]. To show the gains obtained thanks to both bandwidth partitioning methods, we compare their performance with the system applying the conventional single band (SB) transmission.

TABLE 6.1: Common Settings

Common parameters and settings	**Values**
Carrier frequency	5.9 GHz
MCS	8
Broadcasting power by vehicles	23 dBm
Bandwidth	10 MHz
Shadowing	log-normal
Std. dev.	3 dB
Road length $\times$ road width	5000 m $\times$ 4 m
No. of lanes in each direction	3
Number of RSUs	5
Radius of RSU coverage	500 m
Distance between RSUs	1000 m
Radius of vehicle broadcasting coverage area	600 m
Radius of inner RSU coverage	250 m
Distance of RSUs to the highway	3 m
Vehicles speed in each direction	70, 100, 140 kmph
Antenna gain	3 dBi
Path loss at 1 meter	37.02 dB
Loss exponent	4
Noise power over 10 MHz	-95 dBm
CAM interval	100 ms
Packet size	190 bytes
Simulation time	5 sec
Simulation time step	100 ms
Vehicle density factor	[0.6 - 1]
Number of subchannels in a subframe	4
Number of RBs in a subchannel	12

6.5.1 System Performance

Simulations were performed for different vehicle densities. This comparison was made with the following metrics:

- *Packet Reception Ratio (PRR)*: As already defined previously, it is a ratio of the number of successfully received packets to the total number of

broadcast packets in a CAM message interval. Additional PRR values have been calculated as a reference PRR without interference impact for all vehicles with different vehicle densities and have been denoted by REF_{val}. The purpose of REF_{val} is to analyze the performance with and without interference effects.

- *Difference of the packet reception ratio (D-PRR)*: It is the difference between the PFR and FFR packet reception ratios for each density of the vehicles.

- *Minimum Frequency Reuse Distance* $(MFRD)$: It is the smallest distance between two broadcasters that use the same resources when in the coverage of different RSUs. $MFRD$ can be described as follows:

$$MFRD = \min[D_{reused}] \tag{6.16}$$

where $[D_{reused}]$ is a vector of all distances between vehicles reusing the same frequencies expressed in meters.

- *Average Frequency Reuse Distance (AFRD)*: It is the average of all frequency reused distances applied for a specific scalar factor α determining the number of vehicles in the modeled network. $AFRD$ is calculated by collecting all frequency reuse distances throughout the simulation time for each vehicle density and then dividing them by their number. The following formula expresses $AFRD$:

$$AFRD = \frac{\sum D_{reused}}{Number\ of\ D_{reused}} \tag{6.17}$$

- The percentage of vehicles located within BCZ areas to the total number of vehicles in the network $Coll_{perc}$ is the percentage of the total number of receivers receiving two or more non-decodable packets $Pack_{col}$ from transmitters using the same resource allocation to the number of

TABLE 6.2: Percentage of vehicles located within BCZ for the FFR technique.

α	0.6	0.7	0.8	0.9	1
$Coll_{perc}$	1.32%	1.02%	0.80%	0.78%	0.72%

TABLE 6.3: Percentage of total vehicles located within BCZ for the SB technique.

α	0.6	0.7	0.8	0.9	1
$Coll_{perc}$	35.5%	33.4%	31.8%	29.5%	26.7%

all broadcast packets $Pack_{Total}$. $Coll_{perc}$ can be calculated as follows:

$$Coll_{perc} = \frac{Pack_{col}}{Pack_{Total}} 100\% \tag{6.18}$$

Because in the PFR technique the distance h between two frequency reuse bands is larger than h_{reuse}, $Coll_{perc}$ is equal to zero. Furthermore, in the FFR technique, some of the frequency reuse distances are lower than h_{reuse}, creating BCZ. Table 6.2 shows the percentage of vehicles that are located within the BCZ zone $BCZ_{vehicles}$ with the FFR technique.

- *Interference Ratio (IR)*: The impact of interference on the system has been defined as the difference between the performance of the PRR system without interference effects (defined as the reference values REF_{val}) and the observed PRR with interference.

6.6 Simulation Results

The performance of the system in terms of the PRR packet reception ratio for the FFR technique and the IR interference ratio for different vehicle densities is shown in Fig. 6.4 and Fig. 6.3a, respectively. The reference curve in Fig. 6.4 (and Fig. 6.5) indicates the PRR for a system without interference effects - REF_{val}. We observe excellent performance with more than 95% of the packets correctly

delivered to vehicles in the distance range from 100 to 300 m and good performance for those vehicles which are within 300 to 400 m range between the broadcasters and receivers. This distance usually corresponds to the transmission carried out in the inner part of the RSU coverage area, so the impact of interference or collisions in BCZ is minimal, as shown also in Fig. 6.3a.

According to the FFR technique, the repetition of *RSU-bands* has been defined for the distance equal to the doubled radius of the RSU coverage area (effectively specifying the frequency reuse factor of 2). Despite excellent performance at low distances, when the spacing between the transmitter and receiver increases above 400 m, the probability that BCZ appears is high when two or more vehicles are using the same resources and the distances between them are smaller than the minimum allowed frequency reuse distance h_{reuse}. We observed rapid degradation in PRR, with unacceptable values of around 65 - 73% and a steep slope in IR between 18% and 27% for all vehicle densities and for the distance of 600 m.

With the PFR technique, the possibility of a receiver being in the BCZ zone, which is a common case with FFR, does not exist because the re-partitioning band distance is higher than h_{reuse}. Furthermore, the interfering devices are located at a greater distance than in the cases where the FFR technique is applied. Thus, for the PRR of PFR and IR shown in Fig. 6.5 and Fig. 6.3b, we observe higher performance and lower interference impact with inter-vehicle distances below 400 m for all vehicles densities. Furthermore, the PRR and IR observed at 600 m vary between 72% and 89%, and between 3% and 18%, respectively. Therefore, an improvement can be observed compared to the FFR case, especially with the lower number of vehicles served.

The gains resulting from the use of frequency domain partitioning are clearly highlighted when we compare the PRR obtained with FFR and PFR, shown in Figs. 6.4 and 6.5, with the results of the evaluation of the system performance with SB operation without any split of resources, presented in Fig. 6.6. It can be clearly seen that the successful reception ratio increases with partitioning, compared to the SB case, and at the distance of 400 m is about 15%. Moreover,

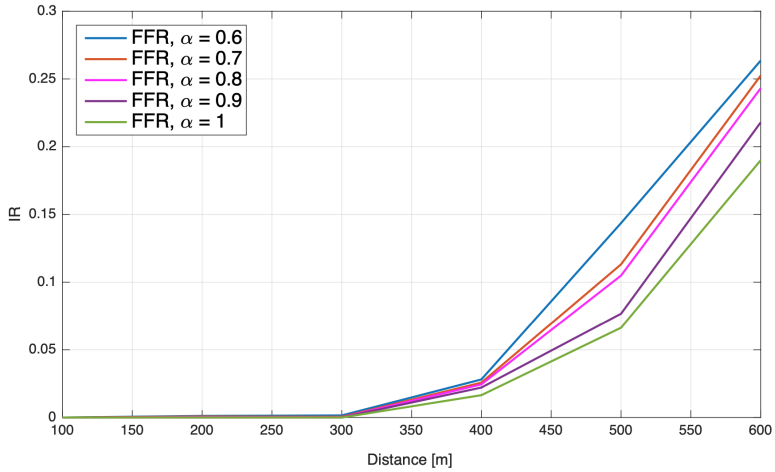

(A)

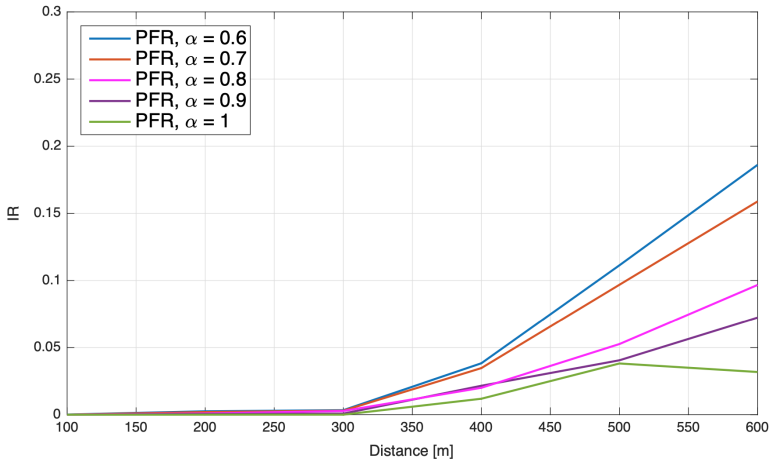

(B)

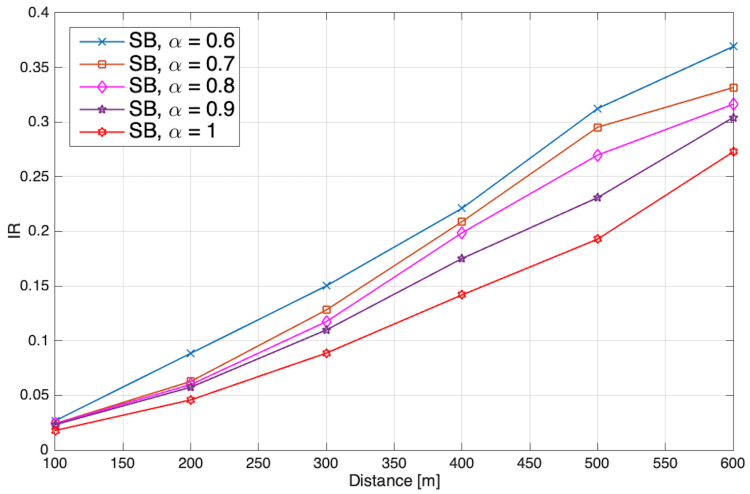

(C)

FIGURE 6.3: The interference impact of the system in partitioning techniques:(A) FRR, and (B) PRR. (C) SB (the system without any partitioning technique).

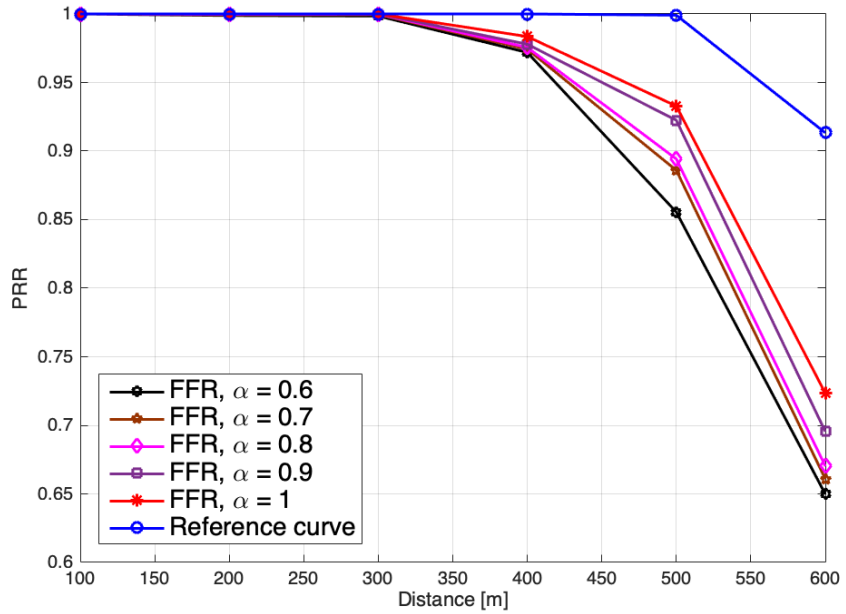

FIGURE 6.4: The packet reception ratio (PRR) of vehicles' CAM messages broadcast for different vehicle density factors with bandwidth partitioning using the Full Frequency Reuse (FFR) technique.

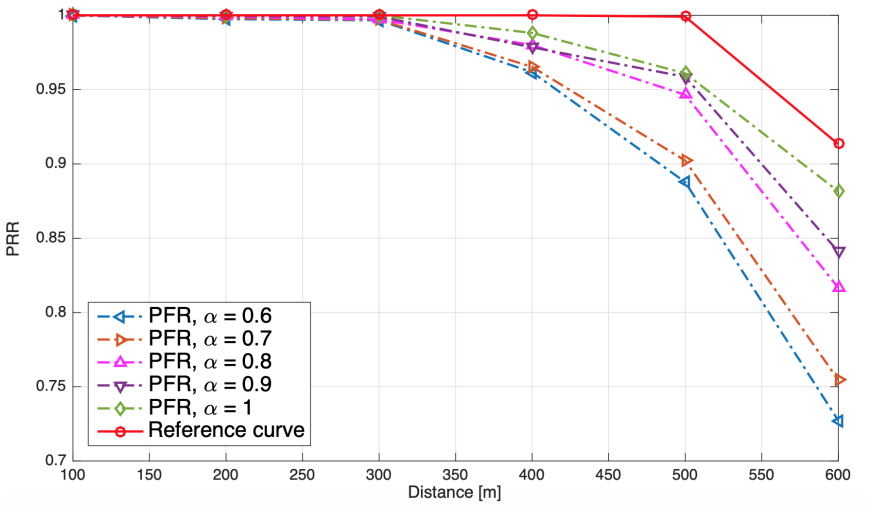

FIGURE 6.5: The packet reception ratio (PRR) of CAM messages broadcast for different vehicle density factors bandwidth partitioning using the Partial Frequency Reuse (PFR) technique.

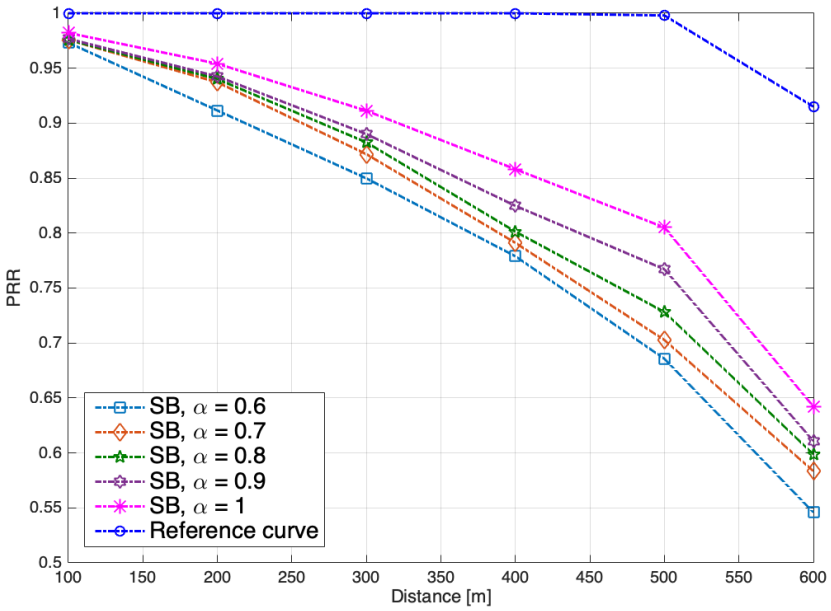

FIGURE 6.6: The packet reception ratio (PRR) of vehicles CAM messages broadcast for different vehicle density factors for the single band (SB) frequency reuse.

for the short-distance links we observe the successful reception probability of almost 1 with frequency partitioning, while for the SB configuration the impact of interference, presented in Fig. 6.3c, significantly affects the transmission success rate.

In Fig. 6.7, the differential PRR (D-PRR=$\text{PRR}_{PFR} - \text{PRR}_{FRR}$) values obtained comparing PFR with FFR techniques are visualized, to show the difference between them for the vehicle densities considered. The results show almost the same system performance for all vehicle densities (D-PRR is equal to or close to zero) when the distance between the transmitters and the receiver is about 100 to 300 m. Furthermore, the performance of PFR starts to be higher than for FFR resulting in D-PRR being around 1% when the distance between the transmitter and the receiver is around 400 m for vehicle densities $\alpha = 0.6$ and 0.7. A rapid increase in PFR over FFR (rising D-PRR) is observed for all vehicle densities when the distance is around 500 to 600 m.

MFRD has been obtained for two vehicles using the same frequency resources that were located within the smallest distance from each other. The

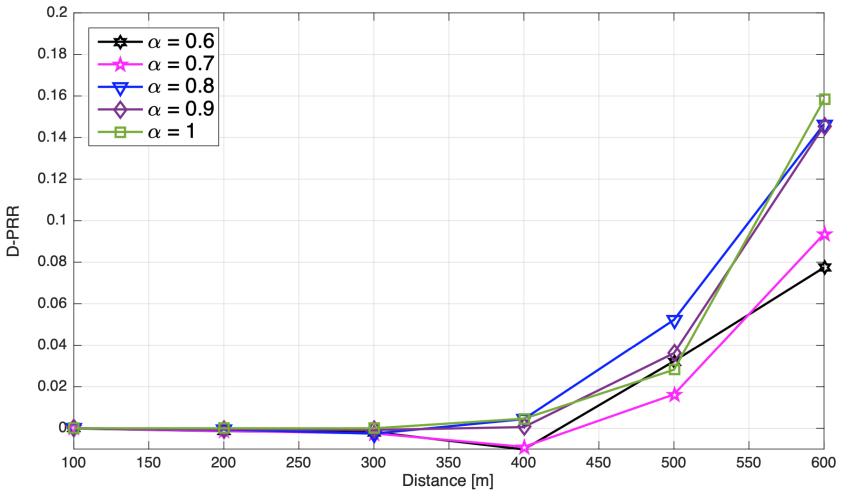

FIGURE 6.7: Difference in packet reception ratio (D-PRR=$PRR_{PFR}-PRR_{FRR}$) between both FFR and PFR bandwidth partitioning techniques versus distance for different vehicle densities.

MFRD versus the vehicle density factor, presented in Fig. 6.8, shows a perfectly rational result, with the minimum frequency reuse distance being higher than the relevant h_{reuse} (that is equal to 1200 m) for the PFR technique. With the applied FFR technique, the observed minimum frequency reuse distance is in all cases shorter than the specified h_{reuse}, the largest difference being observed especially when the number of vehicles in the network is high. One can also note the much lower MFRD level when SB without frequency-domain partitioning is considered. According to the observation above, one can conclude that BCZs appear in the networks without partitioning or when the FFR technique is applied. Furthermore, the percentages of vehicles (referenced to the total number of vehicles) located in BCZs are given in Tables 6.2 for FFR and 6.3 for SB, with respect to different vehicle densities.

AFRD is calculated by averaging the distances between all vehicles that use the same frequency resources in the nearest *RSU-twins*. *AFRD* vs. the vehicle density factor, presented in Fig. 6.9, shows a significant improvement in the average frequency reuse distance for PFR compared to FFR, especially when the number of vehicles in the network is high. The impact of increasing *AFRD* has a positive effect on PRR (see Fig. 6.5) due to the increase in the observed

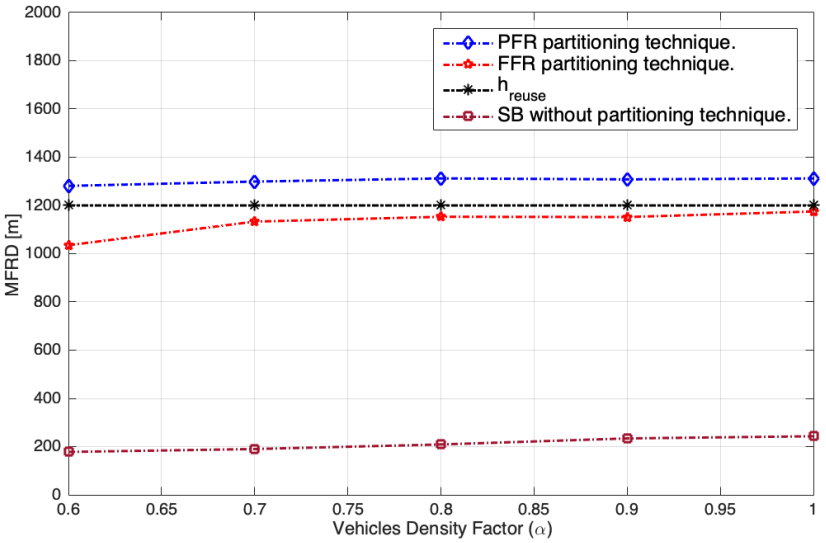

FIGURE 6.8: The minimum frequency reuse distance of CAM broadcasting messages in different vehicle density factors for both Bandwidth partitioning techniques: full frequency reuse (FFR) and partial frequency reuse (PFR).

signal-to-interference plus noise ratio, and thus a higher probability of correct reception of broadcast packets.

In conclusion, the proposed partitioning of resources in the frequency domain based on the geographical location of the vehicles provides a significant improvement in terms of reduced interference. Thus, it positively improves the likelihood of successful delivery of CAM packets broadcast to neighboring vehicles. Both the proposed FFR and PFR techniques ensure significant gains compared to the conventional single-band configuration, where all vehicles share the same resources without applying any interference mitigation.

The main purpose of FFR and PFR techniques is to mitigate the impact of interference for C-V2X communications with the support of a dedicated infrastructure, such as RSUs. Although the proposed techniques are unable to fully mitigate the impact of interference, which is possible with centralized resource allocation in Mode 3, they can be utilized to employ autonomous resource allocation of the RC features (Mode 4 operation) to reduce the need to control signalling between the RSUs and the vehicles. With the geographical areas specified based on RSUs coverage, especially in the case of PFR where the inner

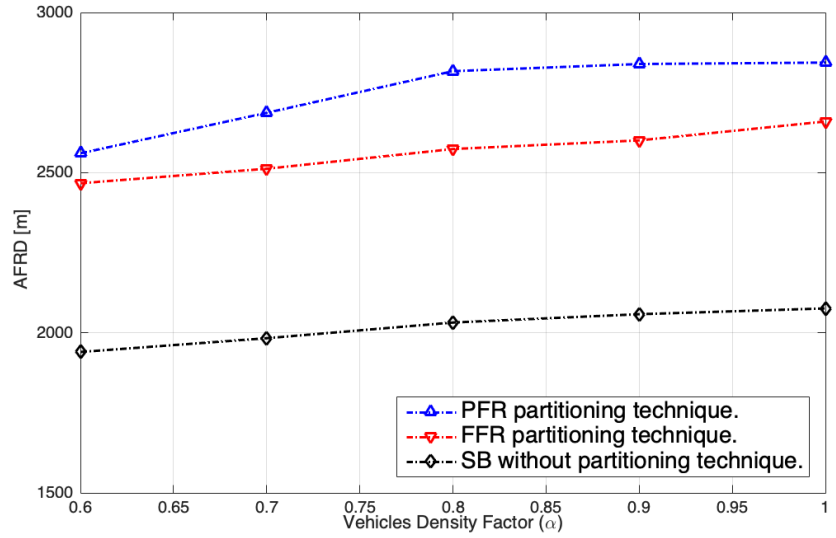

FIGURE 6.9: The average frequency reuse distance of CAM broadcasting messages by vehicles for different vehicle density factors for both bandwidth partitioning techniques: full frequency reuse (FFR) and partial frequency reuse (PFR).

and outer zones are considered, communicating cars can use different resource pools with the aim of reducing the impact of interference. Such an approach allows for reducing the need for control signalling compared to Mode 3 operation while maintaining a significantly higher likelihood of successful reception than the standard Mode 4 operation in dense traffic scenarios. Certainly, the effectiveness of these methods depends on the accuracy of vehicle location estimation, as significant errors (which are possible, e.g., with low-quality GPS receivers) can result in incorrect association with a geographical area.

6.7 Summary

In this chapter, we have investigated 3GPP C-V2X Mode 3 communications, employing bandwidth partitioning to reduce the number of packet collisions in broadcast transmission. In order to reduce the need for signalling between vehicles and RSUs, we have considered the use of Reselection Counter to perform the resource allocation in infrastructure nodes. With the investigated

scheme, the RSU can send the resource allocation grant without the need to receive a vehicle request, resulting in a decrease in signaling.

Two novel applications of bandwidth partitioning techniques have been suggested, namely Full Frequency Reuse and Partial Frequency Reuse, with the aim of reducing the interference from simultaneously broadcasting vehicles. If vehicle broadcast areas overlap, the use of bandwidth partitioning reduces the likelihood of using the same resources by these vehicles, which should avoid packet collisions experienced by some receivers. Moreover, a Broadcast Collision Zone has been formulated that can arise when the frequency reuse distance is lower than the minimum required distance. Both techniques have been evaluated in system-level simulations with respect to different densities of vehicles in terms of the Packet Reception Ratio, Minimum Frequency Reuse Distance, and Average Frequency Reuse Distance. The simulation results show promising performance for PFR, compared to FFR. It has turned out that the repartitioning of the frequency band into two subbands for central and edge users performs better than a fixed split of the available band into two non-overlapping subbands for neighboring RSUs. It is worth stressing that both proposed band partitioning methods result in higher system performance than when no band partitioning is applied.

Chapter 7

Centralized NR V2X Resource Allocation Latency

7.1 Motivation

In this chapter, latency of centralized resource allocation in the New Radio Vehicle-to-Everything (NR V2X) Mode 1 is investigated. The chapter presents a new resource partitioning technique among Road Side Units (RSUs) supervised by a cellular base station. This technique is called Partial Time Reuse (PTR). In this technique, the vehicle transmission period is divided into two intervals for two adjacent RSUs. Each RSU divides its time interval duration into two shorter intervals used by vehicles located in central and edge RSU coverage areas to increase the frequency reuse distance and decrease the resource reallocation delays. Furthermore, we propose the Centralized-Estimation and Reservation Resource Allocation (C-ERRA) algorithm as an alternative resource allocation method to the Configured Grant (CG) method proposed by 3GPP.

C-ERRA works by listing all addresses of resources that will be accessible in an estimated period using a decremental RC. The cellular base station (gNB) generates RC value in each resource (re)allocation. PTR performance is compared with the performance of PFR (see Section 6.4.2), in which the spectrum is divided instead of time as it is in the technique considered in this chapter.

The content of this chapter is based on the paper written by the author

of this dissertation and presented in the 4th International Workshop on Intelligent Communication Network Technologies (ICNET-4) accompanying 2022 IEEE 96th Vehicular Technology Conference - VTC 2022-Fall (see A.1, [4]).

7.2 Challenges and Contribution

The main challenges in NR V2X Mode 1 are the high signalling cost, distribution of resources, and high resource (re)allocation delay that can cause high processing cost in resource selection [53].

In this chapter we investigate Configured Grant (CG) resource allocation of NR V2X Mode 1 in gNB and partitioning of resources between vehicles in a highway scenario when vehicles periodically broadcast awareness messages to the surrounding nodes. The following items summarize the contribution of this chapter:

- Maximizing the frequency reuse distances between vehicles using a new resource partitioning technique among RSUs managed by centralized gNB resource allocation in the highway scenario. In the proposed approach the time slots are divided between two consecutive messages broadcast among vehicles located in contiguous RSUs. The proposed PTR technique is compared to the PFR resource partitioning technique.
- Proposal of a novel resource allocation algorithm called Centralized-Estimation and C-ERRA to minimize the delay of resource (re)allocation/selection in gNB for vehicles.

Both C-ERRA and PTR are compared to and tested with the CG resource allocation algorithm standardized by 3GPP and PFR in terms of packet reception ratio, average reallocation delay, and frequency reuse distance.

The literature has paid little attention to investigating resource partitioning in the cellular infrastructure and the (re)allocation delay of the vehicle's broadcast coverage area in Mode 1 to avoid broadcast overlapping zones. However, many recent works have concentrated on V2X resource allocation. Interference

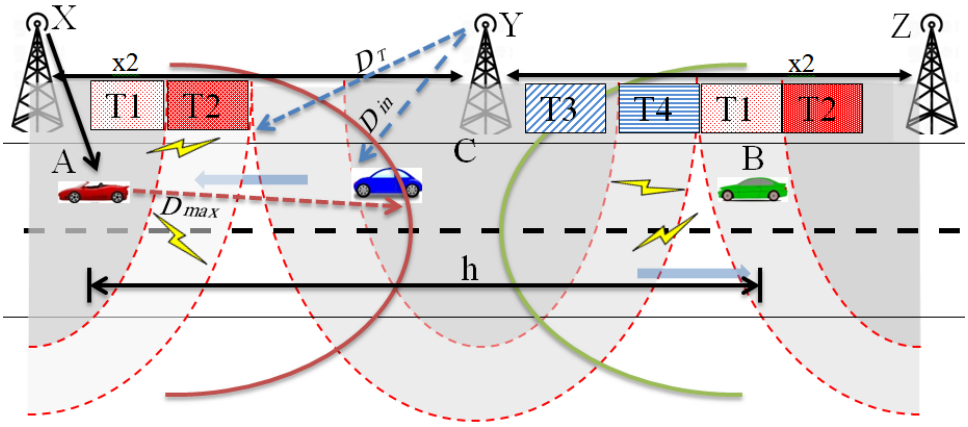

FIGURE 7.1: PTR technique in a highway scenario.

graph-based resource sharing methods are proposed in [134] for throughput improvement. In [135], the authors propose a resource allocation algorithm based on latency limitations under a one-tier cellular network of LTE-V2V. In [121] and Chapter 6 of this dissertation, two frequency reuse techniques are investigated based on fractional and soft frequency reuse methods called FFR and PFR, respectively, to decrease the resource collision probability and increase the reliability of the packet reception. In [136], the authors investigate a capacity improvement without considering the delay. A semi-persistent resource allocation method is suggested in [138] based on a two-tier heterogeneous cellular network to avoid traffic congestion and reduce signalling delay.

7.3 Assumptions and Problem Formulation

In this chapter, three layers of communication infrastructure are considered. The gNB base station is responsible for the centralized resource allocation of vehicular communication at the first layer. In the second layer, five RSUs are connected with their gNBs. Each RSU schedules radio resources for SideLink (SL) communications of vehicles inside its coverage area using pre-allocated (granted by its gNB) resources. In the third layer, vehicles in each RSU coverage area use the provided radio resource for periodic broadcast awareness messages within a specific transmission range. The vehicles ask upper layers for new radio resources when the provided resources are already used.

According to the bandwidth part (BWP) concept, all UEs (vehicles) in the network use the same portion of the bandwidth and the same numerology [62], [63]. Therefore, each subchannel consists of a fixed number of resource blocks (RBs) with subcarrier spacing equal to 15 kHz. The time slot lasts for 1 ms, and each UE broadcasts messages periodically every T_{step}.

Increasing the signal-to-interference plus noise ratio $SINR$ during vehicles' broadcasting can positively maximize the frequency reuse distance h to avoid overlapping between the broadcasting vehicles that use the same frequency band in the network. Let us assume a vehicle receives signals from another vehicle x (the desired one) from distance D_x using subchannel frequency r. The $SINR$ value γ must to be equal or higher than the minimum γ_{min} as shown in (6.7) and (6.7.1).

To obtain the minimum allowed frequency reuse distance h_{reuse}, let us assume that a vehicle receives two packets broadcast from two transmitters located along the same horizontal line in different RSU coverage areas. Both transmitters use the same subchannel address and have the same distance to the receiver. Thus, h_{reuse} can be obtained via (6.4) subject to (6.4.1) and (6.4.2).

In this chapter we consider the means to minimize the interference signals that can negatively affect the receiving packets (see Section 6.3.3) and make the bandwidth usage efficient without resource allocation delay. The interference power signals are represented by (6.5). The objective function is expressed by (6.6) subject to (6.6.1).

One of the challenges faced by centralized resource allocation of vehicular communication is the delay between two consecutive resource selections that are denoted by $\tau^r_{D,M}$. Let us assume that $\tau^r_{j,M}$ is the time slot of the last selected subchannel r by a vehicle. This vehicle is located in the coverage area of RSU M, where $r \in SCH_T$, SCH_T is the number of selected resources in the time period T_{step} and $M \in RSU_{tot}$, RSU_{tot} is the set of all RSUs in the network.

Thus, the subsequent transmission is supposed to be at time slot $\tau^r_{i,M}$, where $\tau^r_{i,M}$ is equal to $\tau^r_{j,M} + T_{step}$. However, sometimes the supposed time takes more

than what it should be. According to the above, the objective function is formulated as follows:

$$\begin{aligned} \underset{\tau^r_{i,M}}{\text{minimize}} \quad & \tau^r_{D,M}, \forall\, SCH_T; \\ \text{subject to} \quad & \tau^r_{D,M} = (\tau^r_{i,M} - \tau^r_{j,M}) - T_{step}, \\ & \tau^r_{i,M} \geq \tau^r_{j,M} + T_{step}, \\ & \tau^r_{D,M} \ll T_{step} \end{aligned} \tag{7.1}$$

Our objective is to find optimal resource locations for the next broadcast message with the lowest delay to minimize $\tau^r_{i,M}$.

7.4 Partial Time Reuse (PTR) Technique

PTR is a resource partitioning technique aimed to provide high immunity against resource collision and overlapping of vehicle broadcasting areas. PTR technique divides the broadcast period T_{step} into two intervals denoted as T_{RSU} for two adjacent RSUs. Furthermore, each RSU further divides T_{RSU} into two intervals T_{center} and T_{edge} for those vehicles located in the center and edge RSU coverage areas. Moreover, T_{center} and T_{edge} are repeated alternately to the RSUs adjacent to the neighboring RSUs.

The example in Fig. 7.1 illustrates the PTR technique. The vehicles in the T1, T3, and T2 zones of RSUs denoted by X, Y, and Z use the T_{center} interval. Meanwhile, vehicles in the T2, T4, and T1 zones of the same RSUs utilize the T_{edge} interval. T1 uses T_{edge} interval of RSU X, which is repeated alternately for T_{center} in RSU Z, and so on. Furthermore, vehicles A and B in Fig. 7.1 are two vehicles for which we would wish their distance between each other to be larger. These vehicles broadcast messages using the same subchannel (the same time slot and frequency) in different RSUs. The minimum distance between two RSU coverage areas that manage the same time periods D_{repeat} is

given as follows:

$$D_{repeat} = RSU_{diameter} + D_T - D_{in} \tag{7.2}$$

where $RSU_{diameter}$, D_T, and D_{in} are the RSU coverage diameter, the radius of RSU coverage area, and the radius of RSU center coverage area, respectively (see Fig. 7.1). Furthermore, T_{center} and T_{edge} can be obtained by the following expressions:

$$T_{center} = T_{RSU}\frac{D_{in}}{D_{Total}} \tag{7.3}$$

$$T_{edge} = T_{RSU}\frac{D_T - D_{in}}{D_T} \tag{7.4}$$

where:

$$T_{RSU} = \frac{T_{step}}{2} \tag{7.5}$$

7.4.1 Centralized-Estimation and Reservation Resource Allocation (C-ERRA) Algorithm

This subsection describes the proposed resource allocation algorithm to support the selection/reselection of resources for vehicle broadcast messages. The algorithm is presented in detail in the form of a pseudo-code in Algorithm 4.

A gNB base station provides centralized resource management for RSUs, and each RSU is directly responsible for passing the granted resources to the vehicles. gNB grants each UE in its coverage area a decremental Random Number (RC) that is decreased by one in each broadcast. For each RSU coverage area, gNB will create the lists for all resources used by the vehicles located in the same RSU coverage area V_{RSU} and have the same RC value. Moreover, D_x, *C-list*, and *E-list* indicate the maximum broadcast coverage area of a vehicle, and lists of all UEs requesting new resources that are located in the central and edge locations (have the same RC value in the central and edge coverage areas), respectively. Furthermore, C_{free} and E_{free} are the lists of free resources

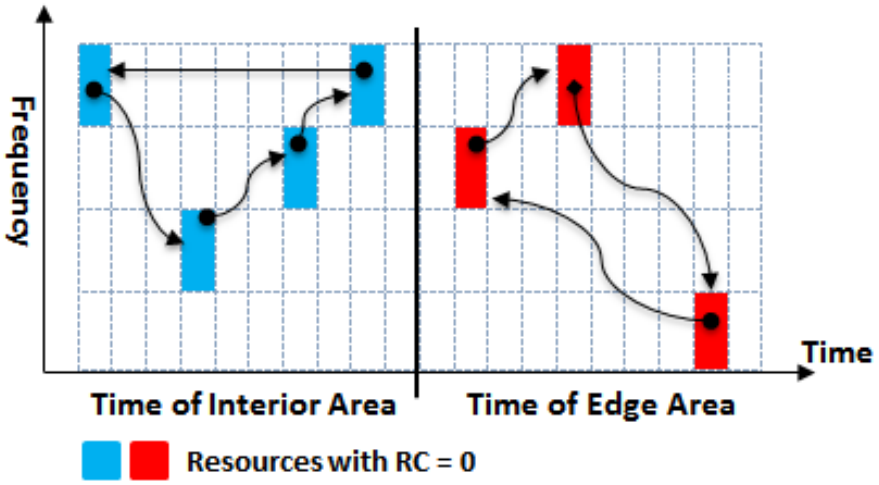

(A) Example of C-EERA when there are no arrivals.

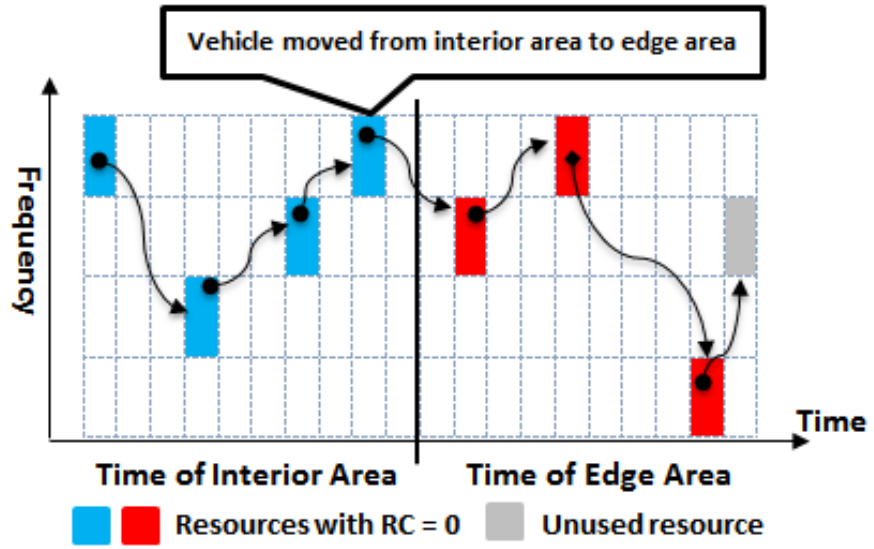

(B) Example of C-EERA when there is one arrival.

FIGURE 7.2: C-ERRA algorithm cases.

Algorithm 4: C-ERRA algorithm.

Input: $V_{RSU}, D_{in}, C\text{-}list, E\text{-}list, C_{free}, E_{free}$
Output: $V_{RSU}, C\text{-}list, E\text{-}list, C_{free}, E_{free}$

1: **while** $TRUE$ **do**
2: **if** $V_{RSU}(i).RC == 0$ **then**
3: **if** $V_{RSU}(i).D_x < D_{in}$ **then**
4: $list = C\text{-}list$
5: **else**
6: $list = E\text{-}list$
7: **end if**
8: **if** $list.length \neq 0$ **then**
9: $SF_x = list(1).SF$
10: $SCH_x = list(1).SCH$
11: $list.length = list.length - 1$
12: $C\text{-}list$ **or** $E\text{-}list = list$ (**depends on the condition in line 3**)
13: **else**
14: **if** $V_{RSU}(i).D_x < D_{in}$ **then**
15: $list = C_{free}$
16: **else**
17: $list = E_{free}$
18: **end if**
19: $temp = Random(list)$
20: $SF_x = list(temp).SF$
21: $SCH_x = list(temp).SCH$
22: C_{free} **or** $E_{free} = list$ (**depends on the condition in line 14**)
23: **end if**
24: $V_{RSU}(i).SF = SF_x$
25: $V_{RSU}(i).SCH = SCH_x$
26: $SF_{list} \leftarrow$ **all vehicles** V_{RSU} **that have** $SF = V_{RSU}(i).SF$
27: $RC\text{-}list \leftarrow$ [**RCs of** SF_{list}]
28: $RC_{range} = [R_{\min} R_{\max}]$
29: $RC_{dif} =$ **set difference**$(RC_{range}, RC\text{-}list)$
30: $V_{RSU}(i).RC = random(RC_{dif})$
31: **else**
32: $V_{RSU}(i).RC = RC_i + 1$
33: **end if**
34: **end while**

within a specified broadcast time portion for the central and edge coverage areas of the RSU. *C-list* and *E-list* are the queues arranged in time. The vehicle of the first resource address in the queue will use the next one, and so on. If there is no new arrival(s) from other coverage areas, the last candidate in the queue will use the first resource address in the queue (see Fig. 7.2a). Otherwise, when the RC value of the new arrival reaches zero, the vehicle that uses the last resource in the resource queue will randomly select a resource address from the free resource lists C_{free} or E_{free} (see Fig. 7.2b).

The new RC value should be set differently from the vehicles' RCs using the same time slot. This helps RSUs avoid conflicts in selecting the same resource by two vehicles simultaneously. As a result of this algorithm, the time of resource selection or reselection is reduced.

TABLE 7.1: Main simulation settings.

Common Parameters and Settings	**Values**
Carrier frequency	5.9 GHz
Bandwidth	10 MHz
Broadcast power	23 dBm
MCS order	8
No. of subchannels per time slot	4
Highway length $\times Roadwidth(ineachlane)$	5000 m $\times 4m$
No. of lanes in each direction	3
Vehicle density factor in each zone	0.6, 0.8, and 1
The random number RC range	$[5, 15]$
Time slot	1 ms
Propagation model	WINNER+B1
Absolute vehicle speed	70, 100, and 140 kmph
Antenna gain at receiver side	3 dB
Loss exponent	4
Reference path loss for 1 m	20.06
Noise power over 10 MHz	-95 dBm
Periodicity of awareness message T_{step}	100 ms
Diameter of RSU coverage area	1 km
Diameter of center RSU coverage area	500 m
CAM packet size	190 bytes

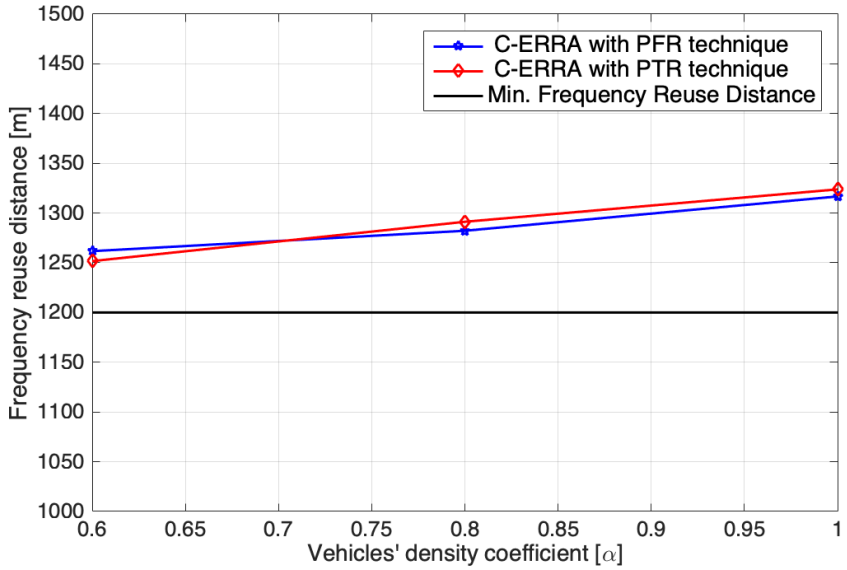

FIGURE 7.3: Frequency reuse distances.

7.5 Scenario and Simulation Setting

System-level simulations are implemented using MATLAB® for a highway scenario to test and investigate the proposed resource allocation algorithm C-ERRA with PTR and PFR resource partitioning techniques. Poisson distribution is applied to distribute vehicles along a highway in different distance densities (see 3.10 and 3.11). Table 7.1 shows additional simulation settings and parameters.

The system performance is evaluated through the frequency reuse distance and the average of reallocation delay τ_{avg} [ms]. τ_{avg} can be defined by the following expression.

$$\tau_{avg} = \frac{\sum_{r \in SCH, M \in RSU_T} \tau^{r}_{D,M}}{SCH_T} \tag{7.6}$$

The third evaluation element is the Packet Reception Ratio (PPR) which refers, as previously, to the ratio of correctly received packets to the total packets sent.

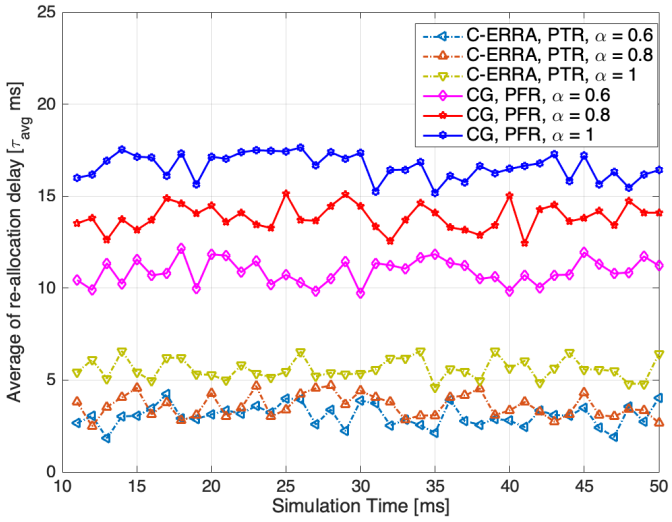

FIGURE 7.4: Average re-allocation time delay.

7.6 Simulation Results

This section shows the simulation results of the C-ERRA and CG resource allocation algorithms with respect to resource selection (scheduling) time and the proposed PTR resource partitioning technique compared to the case where PFR is applied. The algorithms and methods considered above are tested for different distances between vehicles.

In Fig. 7.3, the PTR and PFR techniques are applied to the C-ERRA algorithm. The results of both approaches show nearly exactly the same and promising frequency reuse distances h_{reuse}, with a minor improvement in the performance of the PTR compared to the PFR when the vehicle density factors are equal to 0.8 and 1. This similarity in performance occurs because the distribution of resources is the same between RSUs.

Comparisons between C-ERRA with PTR and CG with PFR methods in terms of τ_{avg} are shown in Fig. Fig. 7.4. The resource tracking method in C-ERRA shows promising results compared to CG in decreasing the delay in reallocation of radio resources. When the vehicle density factor is equal to 1, C-ERRA results in a shorter τ_{avg} compared to CG by about 15 ms and about 13 ms when the density factor is equal to 0.8. Furthermore, C-ERRA achieves the shortest τ_{avg} of about 3 ms and differs from CG by about 7 ms when the

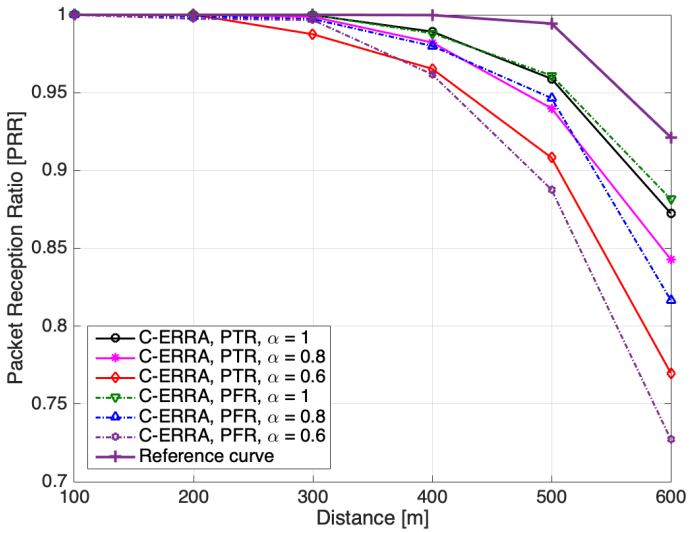

FIGURE 7.5: Packet reception ratio of C-ERRA

density factor is equal to 0.8.

Fig. 7.6 shows the packet reception ratio when C-ERRA is applied with PTR and PFR resource partitioning techniques. The results generally show excellent performance with minor differences because h_{reuse} is almost the same. The reference PRR curve is shown without the interference effects of both the PTR and PFR techniques. Both techniques have the same partitioning concept that leads to the same h_{reuse}. When the distance between transmitters and receivers is less than or equal to 200 m, the system performance of both methods is the same. C-ERRA with PTR shows better results when the distance between transmitters and receivers exceeds 400 m. About 5%, 3% and 1% are the performance differences between PTR and PFR when α is equal to 0.6, 0.8, and 1, respectively.

7.7 Summary

In this chapter, NR V2X centralized resource (re)allocation techniques for vehicles in highway scenarios have been investigated. The C-ERRA algorithm is proposed and compared with the CG resource allocation method proposed by 3GPP. The C-ERRA algorithm aims to reduce reallocation delay by creating a

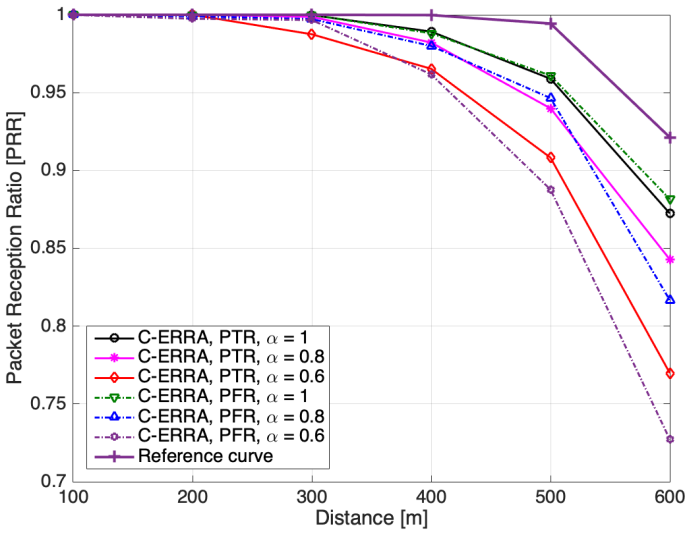

FIGURE 7.6: Packet reception ratio of C-ERRA

time queue for resources with the same RC. When the RC reaches zero, the allocation moves to the next subframe in the timeline. Both algorithms are tested and compared with two resource partitioning techniques, PFR and PTR. PTR divides the broadcast period among two adjacent RSUs, and each RSU divides its period between the vehicles located in the center and edge of the RSU coverage area. The results show encouraging results in the proposed C-ERRA and PTR compared to the CG and PFR methods.

Chapter 8

Conclusion and Future Works

8.1 Conclusion

C-V2X communication systems have faced many challenges since they were proposed as a solution for direct communication between vehicles and vehicles with surrounding nodes.

Section 1.3 of this dissertation presents general concepts of the challenges of C-V2X resource management, the problems highlighted and investigated, and proposed solutions to address issues related to resource scheduling and allocation algorithms.

In Chapter 3, two resource allocation algorithms, ERRA and E-ERRA, are proposed to solve the radio resource collision and hidden node problems that occur in LTE-V2X Mode 4 when the SB-SPS radio resource allocation algorithm standardized by 3GPP is applied. The ERRA algorithm focuses on decreasing the packet collision ratio by tracking busy resources. Thus, unlike the SB-SPS algorithm, the ERRA algorithm does not depend on sensing the free resources and then selecting new resources among them. The ERRA algorithm has been extended to the E-ERRA algorithm to solve the problem of untraceable resources that the tracker has previously reserved. Both algorithms (ERRA and E-ERRA) show excellent packet reception ratio (PRR) results and immunity against the packet collision ratio (CR).

In Chapter 4, the author of this dissertation has proposed two algorithms that can be integrated with the SB-SPS algorithm and are based on adaptive

modulation (AM) and adaptive modulation and collision detection (AMCD). These algorithms aim to reduce resource scheduling and allocation errors in areas with high vehicular density and high channel loads. In the reported system-level simulations, the AMCD algorithm shows promising results in collision detection compared to the AM algorithm.

The application of TPC-DCC and an adaptive power threshold of the received signal are investigated with a proposed algorithm of channel load adjustment in **Chapter 5**. This adjustment is based on the channel-busy ratio to reduce the collisions in packets/resources and the interference effect. For this purpose, the E-ERRA and SB-SPS algorithms are considered. The interactions of the suggested solutions with SB-SPS and E-ERRA are discussed for scenarios with static and flexible inter-vehicle distances. The simulations have been run in standard and hybrid networks for fixed and varying inter-vehicle distances. E-ERRA with TPC-DCC support has shown higher PRR, reliability in radio resource selection, and lower CR than SB-SPS with the same transmission parameters.

In Chapter 6, two novel bandwidth partitioning techniques have been suggested for C-V2X Mode 3 communications, namely full frequency reuse (FFR) and partial frequency reuse (PFR), to reduce interference of simultaneous broadcasts of messages by vehicles located in coverage areas of different radio side units (RSUs) and minimize the broadcast collision zones. Both techniques have been evaluated for different vehicle densities in system-level simulations estimating the PRR, the Minimum Frequency Reuse Distance, and Average Frequency Reuse Distance. The simulation results show promising performance for PFR compared to FFR.

Furthermore, NR V2X centralized resource selection / reselection techniques are investigated for vehicle communications in highway scenarios in **Chapter 7**. In our research, five RSUs are responsible for delivering the recommended resources from a cellular base station to vehicles found within its coverage area. The proposed C-ERRA algorithm is compared with the configured grant

(CG) resource allocation method proposed by 3GPP. The C-ERRA aims to reduce the re-allocation delay by forming the ERRA algorithm in a centralized method. Both algorithms are tested and compared with two resource partitioning techniques, PFR and partial time reuse (PTR).

Summarizing, analysis of several proposals for improving transmission reliability, maximization of packet reception ratio, minimization of collision ratio, and ensuring minimization of realocation latency fully justifies the validity of the thesis of this dissertation stated in Chapter 1.

8.2 Future Works and Perspectives

There are many additional challenges to face in V2X cellular communication, which extend many new research avenues to develop proposals or suggest more complementary developments. On the basis of research and deep considerations, in the opinion of the author of this dissertation, possible challenges are as follows.

1. Spectrum usage needs further investigation to become more reliable for higher data rates. Using machine learning algorithms in C-V2X with autonomous resource selection to estimate suitable radio resources appears to be one of the most promising future solutions.

2. The reduction of signalling cost in centralized resource selection in C-V2X systems needs further improvements and investigation. Signalling costs can cause SideLink transmission to be delayed. Even with the configured grant method proposed by 3GPP, this issue still needs to be a subject of improvement, and pre-reserved resources need to be increased.

3. In contrast to the IEEE 801.11p standard, which relies on the DC mechanism to solve the problem of high resource congestion in a high vehicle density network, the C-V2C standard does not indicate any new mechanism or method that helps solve this problem. In this goal, we have given

some ideas to consider for future work that needs further research and improvement.

Appendices

Appendix A

A list of Publications

A.1 International Conference Articles

[1] S. Sabeeh, P. Sroka and K. Wesołowski, "Estimation and Reservation for Autonomous Resource Selection in C-V2X Mode 4" 2019 IEEE 30th Annual International Symposium on Personal, Indoor and Mobile Radio Communications (PIMRC), 2019, pp. 1-6, doi: 10.1109/PIMRC.2019.8904095.

[2] S. Sabeeh and K. Wesołowski, "C-V2X Mode 4 Resource Allocation in High Mobility Vehicle Communication" 2020 IEEE 31st Annual International Symposium on Personal, Indoor and Mobile Radio Communications (PIMRC), 2020, pp. 1-6, doi: 10.1109/PIMRC.48278.2020.9217297.

[3] S. Sabeeh and K. Wesołowski, "Resource Re-Selection with Adaptive Modulation and Collision Detection in LTE V2X Mode 4" 2021 IEEE 32nd Annual International Symposium on Personal, Indoor and Mobile Radio Communications (PIMRC), 2021, pp. 1005-1010, doi: 10.1109/PIMRC.50174.2021.9569449.

[4] S. Sabeeh, "Centralized Resource Allocation Latency of SideLink Communication in NR V2X" 2022 IEEE 96th Vehicular Technology Conference (VTC-Fall), accepted.

A.2 Published Journal Articles

[1] S. Sabeeh, K. Wesołowski. and P. Sroka. "C-V2X Centralized Resource Allocation with Spectrum Re-Partitioning in Highway Scenario," Electronics, 11(2), p.279., 2022.

A.3 Articles Under Reviewing Process

[1] S. Sabeeh and K. Wesołowski, "Congestion Control in Autonomous Resource Selection of Cellular-V2X" Submitted to IEEE Access journal.

Bibliography

[1] D. Q. Xi Zhang, *Quality, reliability, security and robustness in heterogeneous networks.* Springer International Publishing, Berlin, Heidelberg, 2010.

[2] X. Cheng, L. Yang, and X. Shen, "D2D for intelligent transportation systems : A feasibility study," *IEEE Transactions on Intelligent Transportation System*, vol. 16, no. 4, pp. 1784–1793, Aug. 2015.

[3] *CAMP vehicle safety communications consortium, vehicle safety communications project: Task 3 Final Report: Identify intelligent vehicle safety applications enabled by DSRC*, Nat. Highway Traffic Safety Admin., US Dept. Transp., Washington DC, 2005

[4] S. Chen *et al.*, "Vehicle-to-everything (V2X) services supported by LTE-based systems and 5G," *IEEE Communications Standard Magazine*, vol. 1, no. 2, pp. 70–76, Jul. 2017.

[5] J. B. Kenney, "Dedicated short-range communications (DSRC) standards in the united states," *Proc. IEEE*, vol. 99, no. 7, pp. 1162–1182, Jul. 2011.

[6] G. Araniti, C. Campolo, M. Condoluci, A. Iera, and A. Molinaro, "LTE for vehicular networking: A survey," *IEEE Communications Mag.*, vol. 51, no. 5, pp. 148–157, May 2013.

[7] W. Chen (Ed.), *Vehicular communications and networks: Architectures, protocols, operation and deployment*, Elsevier Ltd, Amsterdam, 2015.

[8] H. Hartenstein and K.P. Laberteaux, "A tutorial survey on vehicular Ad Hoc networks," *IEEE Comm. Magazine*, vol. 46, no. 6, pp. 164-171, June 2008.

[9] A. Vinel, “3GPP LTE versus IEEE 802.11 p/WAVE: Which technology is able to support cooperative vehicular safety applications?” *IEEE Wireless Communications Letters*, vol. 1, no. 2, pp. 125–128, April 2012.

[10] H. J. Qiu, I. W. H. Ho, C. K. Tse, and Y. Xie, “A methodology for studying 802.11 p VANET broadcasting performance with practical vehicle distribution,” *IEEE Transactions on Vehicular Technology*, vol. 64, no. 10, pp. 4756-4769, Oct. 2015.

[11] J. B. Kenney, “Dedicated short-range communications (DSRC) standards in the United States”, *Proc. IEEE*, vol. 99, no. 7, pp. 1162–1182, Jul. 2011.

[12] Y. Morgan, “Notes on DSRC and WAVE standards suite: Its architecture, design, and characteristics,” *IEEE J. Commun. Surv. Tutorials*, vol. 12, no. 4, pp. 504–518, Sep. 2010.

[13] Z. Xu, X. Li, X. Zhao, M. H. Zhang, and Z. Wang, “DSRC versus 4G-LTE for connected vehicle applications: A study on field experiments of vehicular communication performance,” *Journal of Advanced Transportation*, vol. 2017, pp. 1–10, Aug. 2017.

[14] C. Bettisworth, M. Burt, A. Chachich, R. Harrington, J. Hassol, A. Kim, K. Lamoureux, D. LaFrance-Linden, C. Maloney, D. Perlman, and G. Ritter, "Status of the dedicated short-range communications technology and applications: report to Congress (No. FHWA-JPO-15-218)". *Department of Transportation. Intelligent Transportation Systems Joint Program Office*, United States, 2015.

[15] IEEE 802.11p press release for review [802SEC]. https://grouper.ieee.org/groups/802/secmail/msg12802.html

[16] Z. MacHardy, A. Khan, K. Obana and S. Iwashina, "V2X access technologies: Regulation, research, and remaining challenges", *IEEE Communications Surveys and Tutorials*, vol. 20, no. 3, pp. 1858-1877, Third Quarter 2018, doi: 10.1109/COMST.2018.2808444.

[17] Federal Communication Commission, "Amendment of parts 2 and 90 of the commission's rules to allocate the 5.850–5.925 GHz band to the mobile service for dedicated short range communications of intelligent transportation services," *ET Docket* vol. 14, no. 98-95, Report and Order, 14 FCC Rcd 1822, pp. 98–95, 1999.

[18] ARIB, ARIB STD-T109: 700 MHz band intelligent transport systems. Tokyo, Japan: Association of Radio Industries and Businesses, Feb. 2012. [Online]. Available: https://webstore.arib.or.jp/en/

[19] R. A. Uzcategui, and G. Acosta Marum,"WAVE: a tutorial," *IEEE Communications Magazine*, vol. 47, no. 5, pp. 126 - 133, May 2009. doi: 10.1109/ MCOM.2009.4939288.

[20] O. Urmonov, H. W. Kim, "Highly reliable MAC protocol based on associative acknowledgement for vehicular network", *Electronics*, 10(4), p.382, 2021

[21] Chen, Q., F. Schmidt-Eisenlohr, D. Jiang, M. Torrent-Moreno, L. Delgrossi, and H. Hartenstein, "Overhaul of IEEE 802.11 modeling and simulation in ns-2", in *Proc. of the 10th ACM Symposium on Modeling, analysis, and simulation of wireless and mobile systems (MSWIM '07)*, Chania (Greece), pp. 159–168, 22-26 Oct. 2007.

[22] G. V. Rossi, and K. K. Leung, "Optimised CSMA/CA protocol for safety messages in vehicular ad-hoc networks", Heraklion, Greece, *Proc. IEEE Symposium on Computers and Communications (ISCC)*, Jul. 2017, pp. 689–696.

[23] G. Thandavarayan, M. Sepulcre, and J. Gozalvez,"Analysis of message generation rules for collective perception in connected and automated driving", Paris, France, *Proc. IEEE Intell. Vehicles Symp. (IV)*, 9 -12 Jun. 2019.

[24] M. Hadded, P. Muhlethaler, A. Laouiti, R. Zagrouba and L. A. Saidane, "TDMA-Based MAC Protocols for Vehicular Ad Hoc Networks: A Survey, Qualitative Analysis, and Open Research Issues," *in IEEE Communications Surveys and Tutorials*, vol. 17, no. 4, pp. 2461-2492, Fourthquarter 2015, doi: 10.1109/COMST.2015.2440374.

[25] R. Molina-Masegosa, J. Gozalvez, and M. Sepulcre, "Configuration of the C-V2X mode 4 sidelink PC5 interface for vehicular communication", in *Proc. 14th International Conference on Mobile Ad-Hoc and Sensor Networks (MSN)*, Shenyang, China, 2018, pp. 43-48, doi: 10.1109/MSN.2018.00014.

[26] T. P. Fowdur, P. Jhengree. "Enhanced pulse shaping filters for IEEE 802.11 OFDM WLANs", *Journal of Electrical Engineering, Electronics, Control and Computer Science* vol. 3, no. 1, 2017, pp. 21-28.

[27] F. Arena, G. Pau, and S. Alessandro. "A review on IEEE 802.11p for intelligent transportation systems." *Journal of Sensor and Actuator Networks*, vol. 9, no. 2, 2020, paper no. 22.

[28] X. Lin, J. G. Andrews, A. Ghosh and R. Ratasuk,"An overview of 3GPP device-to-device proximity services," *IEEE Communications Magazine*, vol. 52, no. 4, pp. 40-48, April 2014.

[29] M. Shih, H. Liu, W. Shen, and H. Wei, "UE autonomous resource selection for D2D communications: Explicit vs. implicit approaches," in *Proc. IEEE Conference on Standards for Communications and Networking (CSCN)*, Berlin, Germany, 2016, pp. 1-6, doi: 10.1109/CSCN.2016.7785185.

[30] A. Muthanna, A. A. Ateya, M. A. Balushi, and R. Kirichek, "D2D enabled communication system structure based on software defined networking for 5G network," in *Proc. International Symposium on Consumer Technologies (ISCT)*, 2018, pp. 41-44, doi: 10.1109/ISCE.2018.8408913.

[31] G. Fodor, H. Do, S. A. Ashraf, R. Blasco, W. Sun, M. Belleschi, and L. Hu, "Supporting enhanced vehicle-to-everything services by LTE release

15 systems," *IEEE Communications Standards Magazine*, vol. 3, no. 1, pp. 26–33, Mar. 2019.

[32] 3GPP TS 36 300, "Technical specification group radio access network; Evolved universal terrestrial radio access (E-UTRA and evolved terrestrial radio access Network (E-UTRAN)", Rel-14 v14.4.0. Oct. 2017.

[33] 3GPP TS 136 211, " Evolved universal terrestrial radio access (EUTRA); Physical layer procedures" Rel-14 v14.8.0, Oct. 2018.

[34] J. B. Kenney, "Dedicated short-range communications (DSRC) standards in the united states," *Proc. of the IEEE*, vol. 99, no. 7, pp. 1162-1182, July 2011.

[35] 3GPP TS 36.211, " Evolved universal terrestrial radio access (E- UTRA); Physical channels and modulation", Rel-14 v14.3.0, Aug. 2017.

[36] S. Chen, J. Hu, Y. Shi, Y. Peng, J. Fang, R. Zhao, L. Zhao, "Vehicle-to-everything (V2X) services supported by LTE based systems and 5G", *IEEE Communications Standards Magazine*, vol. 1, no. 2, pp. 70–76, Jun. 2017.

[37] A. Mansouri, V. Martinez, and J. Härri, "A first investigation of congestion control for LTE-V2X mode 4", in *Proc. 15th IEEE Annual Conference on Wireless On-demand Network Systems and Services (WONS)*, Wengen, Switzerland, 22-24 Jan. 2019, pp. 56-63.

[38] N. Lyamin, A. Vinel, M. Jonsson, and B. Bellalta, "Cooperative awareness in VANETs: on ETSI EN 302 637-2 performance," *IEEE Transactions on Vehicular Technology*, vol. 67, no. 1, pp. 17–28, Jan. 2018.

[39] 3GPP TS 36.331, "Evolved universal terrestrial radio access (E-UTRA); radio resource control (RRC); Protocol specification", Rel-14 v14.10.0, May 2019.

[40] A. Bazzi, B. M. Masini, and A. Zanella, "How many vehicles in the LTE-V2V awareness range with half or full duplex radios?," in *Proc. 15th International Conference on ITS Telecommunications (ITST)*, 2017, pp. 1-6, doi: 10.1109/ITST.2017.7972195.

[41] R. Shrestha, S.Y. Nam, R. Bajracharya, and S. Kim, "Evolution of V2X communication and integration of blockchain for security enhancements". *Electronics*, vol. 9, no. 9, p.1338, 2020

[42] M. Boban, A. Kousaridas, K. Manolakis, J. Eichinger, and W. Xu, 2017. "Use cases, requirements, and design considerations for 5G V2X". *arXiv preprint*, arXiv:1712.01754.

[43] A. Bazzi, B. M. Masini, A. Zanella, and I. Thibault, "On the performance of IEEE 802.11 p and LTE-V2V for the cooperative awareness of connected vehicles," *IEEE Transactions on Vehicular Technology*, vol. 66, no. 11, pp. 10419-10432, Nov. 2017, doi: 10.1109/TVT.2017.2750803.

[44] R. Shrestha, S.Y. Nam, R. Bajracharya, and S. Kim, "Evolution of V2X communication and integration of blockchain for security enhancements". *Electronics*, vol. 9, no. 9, p.1338, 2020

[45] 3GPP TS 38.211 “5G; NR; Physical channels and modulation”, Rel-16, v16.2.0, Jul. 2020.

[46] 3rd Generation Partnership Project (3GPP), “RP-170837 New SI proposal: Study on evaluation methodology of new V2X use cases for LTE and NR," *TSG RAN Meeting 75*, Dubrovnik, Croatia, March 2017.

[47] LG Electronics, Huawei, “RP-190766. New WID on 5G V2X with NR sidelink,” *3GPP TSG RAN Meeting 83*, Shenzhen, China, March 2019.

[48] 3GPP TR 36.885, "3rd Generation Partnership Project (3GPP), Study on LTE-based V2X services”, Rel-14 v14.0.0, Jul. 2016.

[49] C. Campolo, A. Molinaro, F. Romeo, A. Bazzi, and A. O. Berthet, "5G NR V2X: On the impact of a flexible numerology on the autonomous sidelink mode," in *Proc. IEEE 2nd 5G World Forum (5GWF)*, Sep. 2019, pp. 102–107.

[50] 3GPP TR 22.886, "3rd Generation Partnership Project (3GPP), Study on enhancement of 3GPP Support for 5G V2X Services " Rel-16 v16.2.0, Dec. 2018.

[51] J. Calabuig, J. F. Monserrat, D. Gozalvez, and O. Klemp, "Safety on the roads: LTE alternatives for sending ITS messages," *IEEE Vehicular Technology Magazine*, vol. 9, no. 4, pp. 61–70, Dec. 2014.

[52] 3GPP TR 22.885, "3rd Generation Partnership Project (3GPP), Study on LTE support for Vehicle to Everything (V2X) services", Rel-14 v14.0.0, Dec. 2015.

[53] M. H. C. Garcia *et al.*, "A tutorial on 5G NR V2X communications," *IEEE Communications Surveys and Tutorials*, vol. 23, no. 3, pp. 1972-2026, third quarter 2021, doi: 10.1109/COMST.2021.3057017.

[54] 3GPP TS 23.501, "System architecture for the 5G system (5GS); Stage 2," Rel-16 v16.6.0, Oct. 2020.

[55] 3GPP TR 22.886, "3rd Generation Partnership Project (3GPP), Study on enhancement of 3GPP support for 5G V2X services," Rel-16 v16.2.0, Dec. 2018.

[56] 3GPP TS 22.186, "Service requirements for enhanced V2X scenarios", Rel-16 v16.2.0, Nov. 2020.

[57] 3GPP TS 22.261, "5G; Service requirements for the 5G system," Rel-16 v16.14.0, Apr. 2021.

[58] 3GPP TS 22.185, "Service requirements for V2X services; Stage 1," Rel-14 v14.3.0, Mar. 2017.

[59] 3GPP TS 22.185, “Service requirements for V2X services; Stage 1,” Rel-15 v15.0.0, June 2018.

[60] LG Electronics, Huawei, “RP-190766. New WID on 5G V2X with NR sidelink,” *3GPP TSG RAN Meeting 83, Shenzhen*, China, March 2019.

[61] 3GPP TS 38.211, "NR; Physical channels and modulation”, Rel-15 v15.2.0, Jul. 2018.

[62] 3GPP TS 38.101-1, "NR; User equipment (UE) radio transmission and reception; Part 1: Range 1 Standalone,” Rel-16 v16.4.0, Jul 2020.

[63] 3GPP TS 38.101-2, "NR; User equipment (UE) radio transmission and reception; Part 2: Range 2 Standalone,” Rel-16 v16.4.0, Jul 2020.

[64] Y. Zou *et al.*, “Impact of major RF impairments on mm-Wave communications using OFDM waveforms,” in *Proc. the 2016 IEEE Global Communications Conference (GLOBECOM) Workshops*, Washington, USA, Dec. 2016, pp. 1-7.

[65] Y. Qi, M. Hunukumbure, H. Nam, H. Yoo, and S. Amuru, "On the phase tracking reference signal (PT-RS) design for 5G new radio (NR)," in *Proc. IEEE VTC 2018-Fall*, Chicago, USA, Aug. 2018, pp. 1-5.

[66] E. Dahlman, S. Parkvall and J. Skold, *5G NR: The next generation wireless access technology*. London, Academic Press, 2018.

[67] 3GPP TS 38.214, "NR; Physical layer procedure for data,” Rel-16 v16.3.0, Nov. 2020.

[68] 3GPP TS 38.211, "NR; Physical channels and modulation,” Rel-15 v15.3.0, Oct. 2018.

[69] LG Electronics, “R1-1913601. Summary of RAN1 agreements/working assumptions in WI 5G V2X with NR sidelink," *3GPP TSG RAN WG1 Meeting 99*, Reno, USA, Nov. 2019.

[70] 3GPP TR 37.985, "3rd Generation Partnership Project (3GPP), Overall description of Radio Access Network (RAN) aspects for Vehicle-to-everything (V2X) based on LTE and NR," Rel-16 v16.0.0, Jul. 2020.

[71] 3rd Generation Partnership Project (3GPP) MCC Support, "Final report of 3GPP TSG RAN WG1 101-e", *TSG RAN WG1 meeting 102-e*, August 2020

[72] 3rd Generation Partnership Project (3GPP) MCC Support, "Final report of 3GPP TSG RAN WG1 100-e v2.0.0", *3GPP TSG RAN WG1 Meeting 100bis-e*, April 2020.

[73] 3GPP TR 37.985, "3rd Generation Partnership Project (3GPP), Overall description of Radio Access Network (RAN) aspects for Vehicle-to-everything (V2X) based on LTE and NR," Rel-16 v16.0.0, Jul. 2020.

[74] 3rd Generation Partnership Project (3GPP) MCC Support, "Final report of 3GPP TSG RAN WG1 100-e v2.0.0," *3GPP TSG RAN WG1 Meeting 100bis-e*, April 2020.

[75] 3rd Generation Partnership Project (3GPP) MCC Support, "Final report of 3GPP TSG RAN WG1 101-e," *3GPP TSG RAN WG1 Meeting 102-e*, August 2020

[76] 3GPP TS 38.214,"TSG RAN; NR; Physical layer procedures for data," Rel-16 v16.4.0, Jan. 2021.

[77] 3GPP TS 38.331, "NR; Radio resource control (RRC); Protocol specification," Rel-16 v16.2.0, Nov. 2020.

[78] 3GPP TS 38.201, "NR; Physical layer; General description," Rel-16 v16.0.0, Sep. 2020.

[79] S. Y. Lien, D. J. Deng, C. C. Lin, H. L. Tsai, T. Chen, C. Guo, and S. M. Cheng, "3GPP NR sidelink transmissions toward 5G V2X", *IEEE Access*, vol. 8, pp. 35368–35382, 2020.

[80] M. Nakamura, Y. Awad, and S. Vadgama, "Adaptive control of link adaptation for high speed downlink packet access (HSDPA) in W-CDMA", in *Proc. International Symposium on Wireless Personal Multimedia Communications*, Honolulu, USA, Dec. 2002, pp. 382-386.

[81] 3rd Generation Partnership Project (3GPP), "RP-170837 New SI proposal: Study on evaluation methodology of new V2X use cases for LTE and NR," 3GPP TSG RAN Meeting 75, Dubrovnik, Croatia, March 2017.

[82] LG Electronics, "R1-1913601. Summary of RAN1 Agreements/Working assumptions in WI 5G V2X with NR sidelink," *3GPP TSG RAN WG1 Meeting 99*, Reno, USA, Nov. 2019.

[83] 3GPP TS 38.214, "NR; Physical layer procedure for data," Rel-16 v16.3.0, Nov. 2020.

[84] M. H. C. Garcia *et al.*, "A tutorial on 5G NR V2X communications," *IEEE Communications Surveys Tutorials*, vol. 23, no. 3, pp. 1972-2026, third quarter 2021, doi: 10.1109/COMST.2021.3057017.

[85] 3GPP TS 38.213, "NR; Physical layer procedures for control," Rel-16 v16.3.0, Nov. 2020.

[86] 3GPP TS 38.321, "NR; Medium access control (MAC) protocol specification," Rel-16 v16.3.0, Jan. 2021.

[87] 3GPP TS 38.321, "NR; Medium access control (MAC) protocol specification," Rel-16 v16.2.1, Nov. 2020.

[88] 3GPP TS 38.214, " NR; Physical layer procedure for data," Rel-16 v16.3.0, Nov. 2020.

[89] 3GPP TR 37.985, "3rd Generation Partnership Project (3GPP), Overall description of Radio Access Network (RAN) aspects for Vehicle-to-everything (V2X) based on LTE and NR," Rel-16 v16.0.0, Jul. 2020.

[90] 3GPP TS 38.331, “NR; Radio resource control (RRC); Protocol specification,” Rel-16 v16.2.0, Nov. 2020.

[91] S. Sabeeh, P. Sroka, and K. Wesołowski, "Estimation and reservation for autonomous resource selection in C-V2X mode 4," in *Proc. IEEE 30th Annual International Symposium on Personal, Indoor and Mobile Radio Communications (PIMRC)*, Istanbul, 8-11 Sept. 2019, pp. 1-6, doi: 10.1109/PIMRC.2019.8904095.

[92] S. Sabeeh, and K. Wesołowski, "C-V2X mode 4 resource allocation in high mobility vehicle communication," in *Proc. IEEE 31st Annual International Symposium on Personal, Indoor and Mobile Radio Communications (PIMRC)*, Sept. 2020, pp. 1-6, doi: 10.1109/PIMRC.48278.2020.9217297.

[93] R. Molina-Masegosa, *et al.*, “System level evaluation of LTE-V2V mode 4 communications and its distributed scheduling,” in *Proc. IEEE 85th Vehicular Technology Conference (VTC Spring)*, Sydney, 4-7 June 2017, pp. 1 - 5.

[94] M. Gonzalez-Martín, M. Sepulcre, R. Molina-Masegosa, J. Gozalvez," Analytical models of the performance of C-V2X mode 4 vehicular communications," *IEEE Transactions on Vehicular Technology*, vol. 68, no. 2, pp. 1155 - 1166, Feb. 2019.

[95] J. He, Z. Tang, Z. Fan, and J. Zhang, "Enhanced collision avoidance for distributed LTE vehicle to vehicle broadcast communications," *IEEE communications Lett.*, vol. 22, no. 3, pp. 630–633, Mar. 2018.

[96] B. Toghi *et al.*, "Multiple access in cellular v2x: Performance analysis in highly congested vehicular networks,” [Online]. (2018). Available: https://arxiv.org/abs/1809.02678.

[97] A. Bazzi, G. Cecchini, A. Zanella, and B. M. Masini, "Study of the impact of PHY and MAC parameters in 3GPP C-V2V mode 4," *IEEE Access*, vol. 6, 2018, pp. 71685-71698.

[98] A. Nabil, V. Marojevic, K. Kaur, C. Dietrich, “Performance analysis of Sensing-Based Semi-Persistent Scheduling in C-V2X networks,” in *Proc. of IEEE VTC 2018-Fall*, , Chicago, USA, pp. 1-5, 27–30 Aug. 2018.

[99] S. Chen, J. Hu, Y. Shi, Y. Peng, J. Fang, R. Zhao, and L. Zhao, "Vehicle-to-everything (V2X) services supported by LTE-based systems and 5G," *IEEE Communications Standards Magazine*, vol. 1 , issue 2, 2017, pp. 70-76.

[100] A. Bazzi, A. Zanella, and B. M. Masini. "Optimizing the resource allocation of periodic messages with different sizes in LTE-V2V," *IEEE Access*, vol. 7, 2019, pp. 43820-43830.

[101] 3GPP TS 36.213, “Evolved universal terrestrial radio access (E-UTRA); Physical layer procedures,” Rel-14 v14.4.0, Oct. 2017.

[102] D. Krajzewicz, G. Hertkorn, Ch. Feld, P. Wagner, “SUMO (Simulation of Urban MObility) an open-source traffic simulation,” in *Proc. 4th Middle East Symposium on Simulation and Modelling (MESM 2002)*, UAE, 2002

[103] P. Kyösti, *et al.*, IST-4-027756 WINNER II "WINNER II Channel models," Deliverable D1.1.2 V1.2, 2007.

[104] D. L. Gerlough, "Use of Poisson distribution in highway traffic. The Probability Theory Applied to Distribution of Vehicles on Two-Lane Highways," The Eno Foundation for Highway Traffic Control, Saugatuck, Conn, USA, 1955, Reprint 2018.

[105] S. Sabeeh, and K. Wesołowski, "Resource re-selection with adaptive modulation and collision detection in LTE V2X mode 4," in *Proc. IEEE 32nd Annual International Symposium on Personal, Indoor and Mobile Radio Communications (PIMRC)*, Helsinki, Sept. 2021, pp. 1005-1010, doi: 10.1109/PIMRC.50174.2021.9569449.

[106] 3GPP TR 36.942, "3rd Generation Partnership Project (3GPP), Evolved universal terrestrial radio access (E-UTRA); Radio frequency (RF) system scenarios,” Rel-14 v14.0.0, Apr. 2017.

[107] A. Bazzi. "Congestion control mechanisms in IEEE 802.11p and sidelink C-V2X," in *Proc. IEEE 53rd Asilomar Conference on Signals, Systems, and Computers*, Pacific Grove, CA, USA, 3-6 Nov. 2019, pp. 1125-1130.

[108] ETSI TS 102 687 V1.1.1, "Intelligent Transport Systems (ITS); De- centralized Congestion Control Mechanisms for Intelligent Transport Systems operating in the 5 GHz range; Access layer part," July 2011.

[109] N. Lyamin, A. Vinel, D. Smely, and B. Bellalta, "ETSI DCC: Decentralized congestion control in C-ITS," *IEEE Communications Magazine*, vol. 56, no. 12, pp. 112-118, Dec. 2018

[110] C. B. Math, H. Li, S. H. de Groot, and I. Niemegeers. "A combined fair decentralized message-rate and data-rate congestion control for V2V communication," in *Proc. of IEEE Vehicular Networking Conference (VNC)*, Torino, 27-29 Nov. 2017, pp. 271-278.

[111] C. B. Math, A. Ozgur, S. H. de Groot, and H. Li. "Data rate based congestion control in V2V communication for traffic safety applications." in *Proc. of IEEE Symposium on Communications and Vehicular Technology in the Benelux (SCVT)*, Luxembourg, November 24, 2015, pp. 1-6.

[112] ETSI, EN 302 637-2, "Intelligent transport systems (ITS) vehicular communications; basic set of applications; Part 2: Specification of cooperative awareness basic service," v1.3.2, Sept. 2014

[113] M. Sepulcre, J. Mira, G. Thandavarayan, and J. Gozalvez, "Is packet dropping a suitable congestion control mechanism for vehicular networks?," in *Proc. IEEE 91st Vehicular Technology Conference (VTC 2020-Spring)*, Antwerp, 25 May - 31 July 2020, pp. 1-5, DOI: 10.1109/VTC2020-Spring48590.2020.912882.

[114] B. McCarthy, and A. O'Driscoll, "Congestion control in the cellular-V2X sidelink," 2021, arXiv:2106.04871. [Online]. Available: http://arxiv.org/abs/2106.04871

[115] A. Bazzi, G. Cecchini, B. M. Masini, and A. Zanella, "Should I really care of that CAM?," in *Proc. IEEE 29th Annual Int. Symp. Pers., Indoor Mobile Radio Communications (PIMRC)*, Bologna, Italy, 9-12 Sep. 2018, pp. 1–6.

[116] A. Bazzi, B. M. Masini, A. Zanella, and I. Thibault, "Beaconing from connected vehicles: IEEE 802.11p vs. LTE-V2V," in *Proc. IEEE 27th Annual International Symposium on Personal, Indoor, and Mobile Radio Communications (PIMRC)*, Valencia, 4-7 Sep. 2016, pp. 1-6.

[117] M. Wang, M. Winbjork, Zh. Zhang, R. Blasco, Hieu Do, S. Sorrentino, M. Belleschi, and Y. Zang. "Comparison of LTE and DSRC-based connectivity for intelligent transportation systems," in *Proc. IEEE 85th Vehicular Technology Conference (VTC 2017 Spring)*, Sydney, 4–7 June 2017, pp. 1-5.

[118] ETSI TS 103 574, "Intelligent transport systems (ITS); congestion control mechanisms for the C-V2X PC5 interface; Access layer part," V1.1.1, Nov, 2018.

[119] D. Smely, S. Rührup, R. Schmidt, J. Kenney, and K. Sjöberg, "Decentralized congestion control techniques for VANETs," in *Vehicular Ad Hoc networks: Standards, solutions and research*, Molinaro, Campoli, Riccardo Scopigno Eds., Springer, Heidelberg, London, 2015.

[120] S. Ucar, S. C. Ergen, and O. Ozkasap. "Multihop cluster-based IEEE 802.11p and LTE hybrid architecture for VANET safety message dissemination," in *IEEE Transactions on Vehicular Technology*, vol. 65, no. 4, 2015, pp. 2621-2636.

[121] S. Sabeeh, K. Wesołowski. and P. Sroka. " C-V2X centralized resource allocation with spectrum re-partitioning in highway scenario," *Electronics*, vol. 11, no. 2, p.279, 2022.

[122] R. Aslani, E. Saberinia, M. Rasti, "Resource allocation for cellular V2X networks mode-3 with underlay approach in LTE-V standard," *IEEE*

Transactions on Vehicular Technology, vol. 69, no. 8, pp. 8601-8612, Aug. 2020.

[123] B. M. Masini, A. Bazzi, A. Zanella, "A survey on the roadmap to mandate on board connectivity and enable V2V-based vehicular sensor networks," *Sensors*, vol. 18, no. 7, 2018.

[124] 3GPP TS 36.331, "Evolved universal terrestrial radio access (EUTRA); Radio resource control (RRC); Protocol specification," Rel-8 v14.8.0, Oct. 2018.

[125] K. Doppler, C. Wijting, K. Valkealahti, "Interference aware scheduling for soft frequency reuse." in *Proc. IEEE 69th Vehicular Technology Conference (VTC 2009 Spring)*, Barcelona, 26-29 April, 2009, pp. 1-5.

[126] Y. Jeon, S. Kuk, H. Kim, "Reducing message collisions in sensing-based semi-persistent scheduling (SPS) by using reselection lookaheads in cellular V2X," *Sensors*, vol. 18, no. 12, 2018.

[127] A. Haider, S. H. Hwang, "Adaptive transmit power control algorithm for sensing-based semi-persistent scheduling in C-V2X mode 4 communication" *Electronics*, 2019, vol. 8, no. 8, p.846.

[128] G. Cecchini, A. Bazzi, B. M. Masini, A. Zanella, "Localization-based resource selection schemes for network-controlled LTE-V2V," in *Proc. IEEE International Symposium on Wireless Communication Systems (ISWCS)*, Bologna, Italy, 16-18 Nov. 2017, pp. 396-401

[129] L. Nkenyereye, S. R. Islam, C. A. Kerrache, M. Abdullah-Al-Wadud, A. Alamri, "Software defined network-based multi-access edge framework for vehicular networks," in *IEEE Access*, vol. 8, pp.4220-4234, 2019.

[130] D. Wang, R. R. Sattiraju, A. Weinand, H. D. Schotten, "System-level simulator of LTE sidelink C-V2X communication for 5G," in *Proc. ITG-Symposium on Mobile Communication Technologies and Applications. 24.*, pp. 1-5. VDE, 2019.

[131] W. Yuan, S. Li, L. Xiang, D. W. K. Ng, "Distributed estimation framework for beyond 5G intelligent vehicular networks," *IEEE Open Journal of Vehicular Technology*, 23 April 2020, pp. 190-214.

[132] G. Cecchini, A. Bazzi, M. Menarini, B. M. Masini, A. Zanella, "Maximum reuse distance scheduling for cellular-V2X sidelink mode 3," in *Proc. IEEE GLOBECOM Workshops*, Abu Dhabi, UAE, 09-13 Dec. 2018, pp. 1-6.

[133] E. Salbaroli, A. Zanella, "Interference analysis in a Poisson field of nodes of finite area" *IEEE Transactions on Vehicular Technology*, vol. 58, no. 4, 2008, pp. 1776-1783.

[134] R. Zhang, X. Cheng, L. Yang, and B. Jiao, "Interference graph-based resource allocation (InGRA) for D2D communications underlaying cellular networks," *IEEE Transactions on Vehicular Technology*, vol. 64, no. 8, pp. 3844-3850, Aug. 2015, doi: 10.1109/TVT.2014.2356198.

[135] J. Mei, K. Zheng, L. Zhao, Y. Teng, and X. Wang, "A latency and reliability guaranteed resource allocation scheme for LTE V2V communication systems," *IEEE Transactions on Wireless Communications*, vol. 17, no. 6, pp. 3850-3860, June 2018, doi: 10.1109/TWC.2018.2816942.

[136] X. Ge, H. Cheng, G. Mao, Y. Yang, and S. Tu, "Vehicular communications for 5G cooperative small-cell networks," *IEEE Transactions on Vehicular Technology*, vol. 65, no. 10, pp. 7882-7894, Oct. 2016, doi: 10.1109/TVT.2016.2539285.

[137] P. Chu, J. A. Zhang, X. Wang, G. Fang and D. Wang, "Semi-persistent V2X resource allocation with traffic prediction in two-tier cellular networks," in *Proc. IEEE 89th Vehicular Technology Conference (VTC 2019-Spring)*, Kuala Lumpur, Malaysia, 28 April – 1 May 2019, pp. 1-6, doi: 10.1109/VTCSpring.2019.8746706.

[138] 3GPP TS 38.101-2, "NR; User equipment (UE) radio transmission and reception; Part 2: Range 2 Standalone," Rel-16 v16.3.1, March 2020.